Drosophila macrophages control systemic cytokine levels in response to oxidative stress via a non-canonical DNA damage repair signaling cascade

Authors: Fabian Hersperger[1,2], Tim Meyring[1], Pia Weber[1], Chintan Chhatbar[1], Gianni Monaco[1,3], Anne-Kathrin Classen[4,5], Marc S. Dionne[6,7], Katrin Paeschke[8], Marco Prinz[1,9,10], Olaf Groß[1,9,10] & Katrin Kierdorf[1,5,9#]

[1] Institute of Neuropathology, Faculty of Medicine, University of Freiburg, Freiburg, Germany

[2] Faculty of Biology, University of Freiburg, Freiburg, Germany

[3] Institute for Transfusion Medicine and Gene Therapy, Medical Center-University of Freiburg, Freiburg, Germany

[4] Center for Biological Systems Analysis, University of Freiburg, Freiburg, Germany

[5] CIBSS-Centre for Integrative Biological Signalling Studies, University of Freiburg, Freiburg, Germany

[6] MRC Centre for Molecular Bacteriology and Infection, Imperial College London, London, United Kingdom

[7] Department of Life Sciences, Imperial College London, London, United Kingdom

[8] Department of Oncology, Haematology and Rheumatology, University Hospital Bonn, Venusberg-Campus 1, Bonn, Germany

[9] Center for Basics in NeuroModulation (NeuroModulBasics), Faculty of Medicine, University of Freiburg, Freiburg, Germany

[10] Signalling Research Centres BIOSS and CIBSS, University of Freiburg, Freiburg, Germany

#corresponding author: katrin.kierdorf@uniklinik-freiburg.de

Summary

Environmental factors, infection, or injury, cause oxidative stress in diverse tissues, resulting in immune activation and loss of tissue homeostasis. Effective stress response cascades, conserved from invertebrates to mammals, ensure reestablishment of homeostasis and tissue repair. Plasmatocytes, the *Drosophila* macrophage-like cells, are thought to respond to oxidative stress by immune activation, however the signaling cascades involved in oxidative stress sensing and subsequent immune activation are yet to be defined. Furthermore, their role in modulating and controlling oxidative stress response to facilitate tissue repair and survival of the organism is not resolved. Here we describe the responses of hemocytes in adult *Drosophila* to oxidative stress and the essential role of non-canonical DNA damage repair activity in direct "responder" hemocytes to control JNK-mediated stress signaling, systemic levels of the cytokine upd3 and subsequently susceptibility to oxidative stress. Our results point to an essential systemic role of hemocytes in controlling systemic oxidative stress response in *Drosophila*, including energy mobilization for potential tissue repair.

Key words: hemocytes; plasmatocytes; *Drosophila* macrophages; oxidative stress; macrophage-derived cytokines; DNA damage; unpaired-3

Introduction

Metazoan organisms must constantly adapt to the surrounding environment. Environmental factors, including radiation, pathogens or toxins, constantly lead to the generation of reactive oxygen species (ROS)[1]. Low levels of ROS support cellular pathways like immune cell differentiation and even immune function such as antimicrobial defense[2,3]. At high concentrations, ROS leads to oxidative stress, a deleterious process that negatively impacts protein synthesis and stability, lipids as well as overall genome stability. ROS mediated cellular damage can further result into degenerative diseases or cancer[4]. Therefore, organisms employ efficient repair and defense mechanisms to circumvent high levels of oxidative stress and subsequent organ damage. Hence, keeping the balance between the production and the antioxidant-dependent clearance of ROS is essential for the survival and well-being of the affected organism[5]. Oxidative stress induced tissue damage is most often followed by a strong local immune response. These molecular processes are conserved across vertebrates and invertebrates such as the fruit fly *Drosophila melanogaster*[6].

Hemocytes, the *Drosophila* blood cells, are essential cellular components of the immune and stress response machinery. They consist of three different subtypes: crystal cells, lamellocytes and plasmatocytes[7]. Plasmatocytes are considered to be macrophage equivalents in *Drosophila* and comprise up to 95 % of all hemocytes in the adult fly[8]. They share many functions as well as the multilayered ontogeny with vertebrate tissue macrophages[9,10]. Adult plasmatocytes are actively involved in many immune functions such as pathogen recognition, defense and phagocytosis but also chronic immune activation upon metabolic stress by dietary lipids[11,12]. Recent studies highlighted the essential role of adult plasmatocytes as key players in regulation of tissue homeostasis, including the gut by regulating the intestinal stem cell niche or in muscles by controlling glucose homeostasis[13,14].

Similar to higher eukaryotes, levels of ROS are used as a central antimicrobial defense mechanisms of hemocytes against invading pathogens[15]. Moreover, larval hemocytes respond differentially to ROS, with two cell subsets mounting a biphasic immune reaction to invading bacteria by controlling hemocyte spreading and adhesion as well as crystal cell rupture[15]. Larval hemocytes have been also attributed to respond to increased oxidative stress of other tissues, as seen in response to oxidative stress in the eye-antenna imaginal disc[16]. Similarly, by regulating the intestinal stem cell (ISC) proliferation in the damaged midgut during infection-induced or chemical-induced oxidative stress[14], adult hemocytes were described to release the bone morphogenetic protein (BMP) homologue

69 *decapentaplegic* (*dpp*) to facilitate tissue repair[14]. Other studies pointed to an essential role of
70 hemocyte-derived *unpaired-3* (*upd3*), which is the invertebrate orthologue of Interleukin-6, in the
71 regulation of ISC proliferation during septic injury[17], as well as wound healing during sterile injury[18]. In
72 line with these findings, hemocytes have been implicated in organ-to-organ immune signaling for
73 example upon infection-induced injury in the gut and antimicrobial peptide (AMP) production in the
74 fat body[19]. Hemocyte activation is thus a hallmark of oxidative stress in defined tissues, though their
75 role in modulating and controlling oxidative stress response to facilitate tissue repair and survival of
76 the organism remains undefined.
77 Here, we demonstrate an essential role of hemocytes to control susceptibility to oxidative stress,
78 where hemocytes orchestrate systemic oxidative stress response by defined cellular states identified
79 by unbiased transcriptomic profiling. Plasmatocytes, which make up 95% of all hemocytes, segregate
80 in oxidative stress responder subclusters characterized by immune activation and cellular stress
81 response and potential bystander subsets more associated with metabolic gene regulations.
82 Mechanistically, we unravel that the direct immune response to oxidative stress by plasmatocytes
83 seems to be essentially controlled by non-canonical DNA damage signaling which subsequently
84 regulates Jun kinase (JNK) activation and induction of the pro-inflammatory cytokine *upd3*. We further
85 describe that plasmatocytes are a major cellular source of *upd3* and that regulation of *upd3* levels in
86 the adult fly determine the organism's susceptibility to oxidative stress, most likely by orchestrating
87 systemic stress responses in other tissues, such as energy mobilization in the fat body.
88
89 **Results**
90
91 **Hemocytes control susceptibility to oxidative stress**
92
93 In vertebrates and invertebrates, prolonged oxidative stress can cause severe tissue damage, hence
94 controlled activation of stress signaling cascades are essential for the survival of the organism and the
95 resolution of oxidative stress with subsequent tissue repair. Yet the precise role of macrophages in the
96 initiation and control of oxidative stress signaling needs to be determined.
97 To analyze the role of macrophages in signaling cascades to oxidative stress, we took advantage of the
98 well-established Paraquat (PQ)-feeding model in adult *Drosophila melanogaster* to induce systemic
99 oxidative stress[20]. Feeding of 7-days old *w;Hml-Gal4,UAS-2xeGFP/+* (*Hml/+*) flies with PQ-
100 supplemented sucrose solution led to an increased lethality of adult *Drosophila* after 18 hours in a
101 dose dependent manner (0mM: 1.25 ± 1.25 %, 2mM: 2.5 ± 1.6 4%, 15mM: 27.78 ± 5.47 %, and 30mM:
102 38.75 ± 6.67 %) (Figure S1A). In agreement with previous studies[20], 15mM PQ was chosen for further
103 experiments (Figure 1A). First, we determined which systemic changes are associated with
104 susceptibility to oxidative stress. Infection induced damage in enterocytes can result in gut leakage and

105 subsequent death[17]. We tested if the death of flies after 18 hours on 15mM PQ food was associated
106 with PQ-induced damage of gut enterocytes and resulting gut leakage, but we found no indication of
107 gut leakage on 15mM PQ food (Figure S1B). Only very few flies on control food and PQ indicated gut
108 leakage of the food color to thorax and abdomen which was unrelated to the treatment and not altered
109 between the groups (control: 3.75%, 2mM PQ: 2.53 %, 15mM PQ: 1.11 % and 30mM PQ: 3.75 %)
110 (Figure S1B). We investigated if aberrant systemic induction of immune signaling cascades are seen
111 upon PQ-mediated oxidative stress. For this gene expression levels of different known immune
112 activated genes were analyzed by qPCR such as *unpaired* (*upd*) cytokines (*upd1*, *upd2*, *upd3*), *Jak/STAT*
113 down-stream targets (*Turandot-A* (*TotA*), *suppressor of cytokine signaling at 36E* (*Socs36E*)), stress
114 induced JNK activation (*puckered* (*puc*)) (Figure 1B), as well as expression of *nuclear factor 'kappa-light-*
115 *chain-enhancer' of activated B-cells* (*Nfkb)*-induced antimicrobial peptides (AMP) and further cytokines
116 such as *eiger*, *dpp* and *dawdle* (*daw*) (Figure S1C-D). These analyses did not reveal significant
117 differences for these gene groups on a systemic level. In contrast, genes associated with carbohydrate
118 metabolism such as *insulin receptor* (*InR*), *phosphoenolpyruvate carboxykinase* (*Pepck*), and *Thor* were
119 significantly upregulated upon PQ-feeding (Figure 1C). These findings point to an activation of *forkhead*
120 *box, sub-group O* (*foxo)*-target genes and a potentially reduced insulin signaling, despite the lack of
121 significant alterations in the expression of the Insulin-like peptides (*Ilps*) *Ilp2*, *Ilp3* and *Ilp5* (Figure 1C).

122 To test the consequences for energy mobilization and nutrient storage, we measured free glucose
123 content, as well as glycogen and triglyceride levels in whole flies after 18 hrs on control or 15mM PQ.
124 Although no changes in free glucose levels (control: 1.49±0.02µg and PQ: 1.50±0.07µg, ns p=0.954)
125 (Figure 1D) were found, we observed a clear decrease in stored glycogen (control: 1.02±0.07µg and
126 PQ: 0.33±0.08µg, ***p=0.003*) (Figure 1E) and stored triglycerides (Figure 1F) in PQ-treated flies
127 compared to control. Next, we examined histological sections of flies to define which tissues might be
128 affected. Hematoxylin and eosin (H&E) stainings showed a loss of stored lipids in the abdominal fat
129 body compared to flies kept under control conditions (Figure S1E). Fat body development, energy
130 mobilization and storage have been recently connected to the presence, cell number and subsequent
131 cross-talk of hemocytes with fat body[21], therefore we quantified GFP^+ hemocytes in *Hml/+* flies after
132 18 hrs on PQ or control food (Figure 1G-H). Our analysis did not reveal alterations in hemocyte numbers
133 and especially no oxidative stress induced loss of hemocytes (control: 243.4±24.33 hemocytes per fly
134 and PQ: 219.6±24.22 hemocytes per fly, ns *p=0.508*) (Figure 1G-H). To evaluate if hemocytes are
135 essential contributors to the stress-mediated metabolic changes and susceptibility to oxidative stress,
136 we used "hemocyte-deficient" *crq-Gal80^{ts}>reaper* (*w;tub-Gal80ts/UAS-CD8-mCherry;crq-Gal4/UAS-*
137 *reaper*) flies and tested their survival rate compared to control flies on PQ food (Figure 1I). Hemocyte-
138 deficient flies displayed a significantly higher mortality rate on 15mM PQ (43.33±6.30%) compared to
139 control flies (13.08±2.63%). Our findings show detrimental changes in energy mobilization upon

140 oxidative stress in the absence of profound over-activation of immune signaling cascades, however the
141 presence or absence of hemocytes seem to be a key determinant of the susceptibility to oxidative
142 stress in adult *Drosophila*. This strongly points to an essential role for hemocytes in controlling stress
143 response and organismal survival upon oxidative stress.

144 **Paraquat exposure generates diverse transcriptional states of adult hemocytes with specific**
145 **transcriptional state associated with oxidative stress response**

146 To gain further insights into the alterations induced in the adult fly upon oxidative stress and especially
147 to the hemocyte compartment, we decided to take advantage of unbiased single nucleus RNA-
148 sequencing (snRNA-seq). We isolated nuclei from control food and PQ-treated *Hml-DsRed.nuc* flies
149 with a modified Frankenstein protocol[22] and performed fluorescence activated nuclear sorting of
150 $DAPI^{+}Draq7^{+}$ nuclei (Figure S2A). From two independent sorts we obtained a total of 29000 nuclei
151 which were utilized for subsequent droplet-based barcoding of single nuclei, and generation of single
152 nucleus cDNA libraries. We could successfully obtain gene expression data from 11839 nuclei (Figure
153 S2B-D). Quality control analysis followed by unsupervised hierarchical clustering of all analyzed nuclei
154 using Seurat package[23] revealed 20 distinct nuclei clusters (C) with differential gene expression (Figure
155 2A). Cell identity was annotated according to the cell type-specific signatures determined by the Fly
156 Cell Atlas consortium (Figure 2A)[24]. All annotated cell types were detected in PQ-treated and control
157 flies (Figure 2B).

158 Using cell type-specific signatures, three of the clusters were annotated as hemocytes (clusters: 2, 4
159 and 11) (Figure 2A-B). Re-scaling and clustering of all 1354 identified hemocyte nuclei revealed 8
160 distinct clusters (Figure 2C). We verified hemocyte-specific signature genes across these clusters
161 including genes such as the transcription factor *Serpent* (*Srp*) and one or more of the following
162 hemocyte signature genes: *Hemolectin* (*Hml*), *croquemort* (*crq*), *Nimrod C1* (*NimC1*), *eater,* and
163 *Peroxidasin* (*Pxn*) (Figure S3A-L)[25,26]. Cluster 8 expressed various crystal cell-specific markers including
164 *lozenge* (*lz*), *pebbled* (*peb*), *prophenoloxidase 1* (*PPO1*), and *prophenoloxidase* 2 (*PPO2*), whereas all
165 other clusters seemed to be plasmatocytes (Figure S3A-L). In line with previous reports, the embryonic
166 and larval hemocyte markers *Hemese* (*He*) (data not shown) and *singed (sn)* were not expressed across
167 any of the identified clusters (Figure S3H). Interestingly, when we defined which hemocyte clusters
168 were enriched in control flies or PQ-treated flies, the two plasmatocyte clusters C1 and C7 were
169 primarily derived from control flies, whereas C2, C3, C4 and C6 are predominantly found in PQ-treated
170 flies (Figure 2D and Figure S3M). The plasmatocyte cluster C5 as well as the crystal cell cluster C8
171 presented in both conditions to similar proportions (Figure 2D and Figure S3M).

172 Next, we analyzed the TOP20 differentially expressed (DE) genes across all hemocyte clusters. We
173 found clear differences between the 7 distinct plasmatocyte clusters and the crystal cell cluster (Figure
174 2E and Table S1). The crystal cell cluster C8 showed a high expression of crystal cell specific genes
175 including *lz*, *peb*, *PPO1* and *PPO2* (Figure 2E). Plasmatocyte cluster C1, which was mostly present in
176 control conditions, had a remarkable expression of hemocyte specific marker genes such as *Hml* and
177 *Pxn,* as well as migration-associated genes including the semaphorins *Sema2a and Sema5c* (Figure 2E).
178 Yet this cluster also showed higher expression of genes contributing to metabolic regulations such as
179 the L-gulonate 3-dehydrogenase *Had2* and the gluconolactonase *regucalcin* (Figure 2E). The cluster C7
180 and C1, mostly found in control flies, substantially shared gene expression profiles. In contrast, cluster
181 C2 and C3 were nearly exclusively found in PQ-treated flies and showed expression of genes involved
182 in metabolic adaptations, with high expression of the *glucose transporter 4 enhancer factor* (*Glut4EF*)
183 or the *phosphatidate phosphatase Lipin* (*Lpin*) in C2 or the induced expression of the lipase *brummer*
184 (*bmm*), the autophagy-associated gene *Atg17* or the *lipophorin receptor LpR1*, involved in uptake of
185 neutral lipids from the hemolymph, in C3 (Figure 2E). Overall gene expression profiles in clusters C2
186 and C3 showed an induction of insulin signaling, increased autophagy and lipolysis pointing to
187 adaptation of energy mobilization in these clusters upon PQ treatment (Figure 2E). Cluster C4 was
188 characterized by a remarkable upregulation of genes involved in translation including many ribosomal
189 proteins such as *RpL8*, *RpL31* or *RpS13* (Figure 2E). Furthermore, C4 included genes associated with
190 unsaturated fatty acid metabolism such as *Desaturase 1 (Desat1)*. Similarly, cluster C5 also showed
191 induction of genes involved in fatty acid metabolism such as *ELOVL fatty acid elongase 7* (*ELOVL*)
192 (Figure 2E). Of note, we also found *Tie-like receptor tyrosine kinase* (*Tie*) specifically expressed in this
193 cluster, which is described to bind PDGF- and VEGF-related factor (Pvf) ligands and contribute to cell
194 survival and migration, as well as actin-associated binding proteins including *polychaetoid* (*pyd*) and
195 *formin 3* (*form3*). All these gene expression changes are pointing to a plasmatocyte cluster with a gene
196 expression profile associated with mobility and migration. Among all plasmatocyte clusters, we found
197 cluster C6 which presented a strong immune activation phenotype with induction of *Jak/STAT* target
198 genes including *Fasciclin 3* (*Fas3*) and *Turandot-M* (*TotM*) among its TOP20 DE genes, but also
199 activation of oxidative stress response genes such as the heat shock proteins *Hsp23*, *Hsp26* and *Hsp27*
200 or cytoskeletal genes including *myosin Myo31DF* or *spire* (*spir*) (Figure 2E).

201 Due to the partially shared expression profile of genes across hemocyte clusters, we wondered if there
202 were genes exclusively expressed in individual clusters. However, cluster C1 showed that *Sema2a*
203 seems to be exceptionally high expressed in these homeostatic plasmatocytes and genes associated
204 with metabolic regulation (e.g. *InR*, *Lpin* or *bmm*) or Jak/STAT activation (e.g. *Fas3*), as seen in PQ-
205 associated clusters, are downregulated (Figure 2F). Cluster C5 showed enrichment for genes such as
206 the transcription factor *grainy head* (*grh*) but also cytoskeletal-associated genes such as *jitterbug* (*jbug*)

207 and *form3,* suggesting a migratory potential of plasmatocytes from this cluster within their host tissues
208 (Figure 2F). Interestingly, plasmatocyte cluster C6 presented with the most profound gene expression
209 changes compared to all other clusters. Similar to our previous observations, we identified that genes
210 specifically expressed in this cluster were associated with Jak/STAT pathway activation (e.g. *Fas3*,
211 *TotM*), cytoskeletal rearrangements and migration (e.g. *Myo31DF*, *spir* or *cheerio* (*cher*)) and response
212 to oxidative stress (e.g. *Nicotinamide amidase* (*Naam*) or *Hsp23*) (Figure 2F). We also included the
213 crystal cell cluster C8 in this analysis and verified unique expression of crystal cell markers compared
214 to the seven plasmatocyte clusters (Figure 2F). Our snRNA-seq analysis revealed that adult hemocytes
215 respond differentially to oxidative stress with a specific cluster of plasmatocytes associated with
216 immune activation and stress response. Despite our findings that on systemic level we did not detect
217 a strong induction of immune activation upon oxidative stress, we now provide evidence that
218 plasmatocyte cluster C6 showed a substantial immune response towards oxidative stress.

219 **Direct response to oxidative stress *in vitro* mimics the transcriptional changes seen in cluster 6**
220 **plasmatocytes *in vivo*.**

221 Plasmatocytes responded to PQ-mediated oxidative stress in different cellular states. We defined
222 cluster C6 as a cell state which is associated with oxidative stress response and immune activation.
223 Since cluster C6 showed gene expression associated with oxidative stress and immune activation we
224 focused our further analysis on this cluster. To further substantiate our findings and address the
225 signaling pathways that could lead to diverse transcriptional states, we inferred the transcription factor
226 (TF) network based on gene expression data (Figure 3A). This analysis revealed that genes with binding
227 sites for *Xbp1* were enriched. *Xbp1* is a transcription factor associated with stress response. In addition
228 to this, the Nf-κB-related transcription factor *Relish* (*Rel*) and *kayak* (*kay*), a component of the *activator*
229 *protein-1* (*AP-1*) transcription factor complex induced by JNK signaling, were also enriched in this
230 cluster (Figure 3A). To determine if the gene expression signature of cluster C6 plasmatocytes reflects
231 a functional state of plasmatocytes directly induced by oxidative stress, we treated S2 cells, a
232 *Drosophila* plasmatocyte cell line, with different concentrations of PQ (15mM and 30mM) (Figure S4).
233 First, we performed flow cytometric analysis of ROS levels via CellROX staining after 6 and 24 hours PQ
234 treatment compared to controls (Figure S4A-B). We observed a dose-dependent increase in
235 intracellular ROS at all time points analyzed with higher ROS levels at 6 hrs (0mM: 1903±64 median
236 fluorescence intensity (MFI), 15mM: 6735±1096 MFI, and 30mM: 7435±237 MFI) compared to 24 hrs
237 (0mM: 1236±135 MFI, 15mM: 4456±228 MFI, and 30mM: 5557±303 MFI) (Figure 4C). Increase in ROS
238 and oxidative stress can lead to cellular damage such as damage in nuclear and mitochondrial DNA.

239 We next tested whether, we now aimed to test if plasmatocytes directly exposed to oxidative stress
240 might also experience these type of stress response by performing comet assays of treated and

241 untreated S2 cells. Upon PQ treatment, S2 cells showed a remarkable and dose-dependent increase in
242 DNA damage compared to untreated cells (0mM: 101.0±2.1, 5mM: 117.6±3.3, 10mM: 136.6±3.8, and
243 15mM: 147.8±5.5, data shown as olive tail moment) (Figure S4D). We were then wondering if PQ-
244 treated S2 cells would resemble cluster C6 plasmatocytes *in vivo* and performed gene expression
245 analysis of S2 cells treated with 15mM PQ after 6 and 24 hrs. Comparable to our results for cluster C6
246 *in vivo*, we found a profound induction of the Jak/STAT target genes by RTq-PCR. In S2 cells, we also
247 detected a significant increase of the Jak/STAT cytokines *upd1*, *upd2* and *upd3* (Figure S4E), which we
248 did not see before *in vivo*. Furthermore, we detected an increased expression of the JNK-target gene
249 *puckered* (*puc*), but barely any induction of metabolic genes (Figure S4E). All these results further
250 support our hypothesis that direct exposure of S2 cells with PQ *in vitro* mimics gene expression changes
251 seen in C6.

252 Because we found enrichment of genes associated with the Nf-κB-related transcription factor *Rel* in
253 cluster C6, we further verified if any other cytokines or AMPs are induced in PQ-treated S2 cells. We
254 identified a slight but significant induction of the cytokine *daw*, but no other alterations in *dpp* or the
255 AMPs *Drs*, *Dro* or *Mtk* (Figure S4F). The profound induction of Jak/STAT target genes together with the
256 activation of JNK target genes and oxidative stress induced DNA damage in S2 cells *in vitro* highly
257 support our hypothesis that cluster C6 plasmatocytes reflect a cellular state associated with the direct
258 response to oxidative stress *in vivo*. Along this line, we went back to our snRNA-seq data and
259 specifically searched for Jak/STAT target genes (*upd3*, *Socs36E*, *TotA*, *TotM* and *Fas3*) across all clusters
260 (Figure 3B). Here we identified an enriched expression of these genes in cluster C6, and a unique
261 expression of the pro-inflammatory cytokine *upd3* in cluster C6 which was not detected in any other
262 hemocyte cluster (Figure 3B). Interestingly, we also identified that *Growth arrest and DNA damage-*
263 *inducible 45* (*Gadd45*), a gene linking DNA damage signaling and stress induced JNK signaling, was
264 enriched in cluster C6 (Figure 3B). This could indicate that cluster C6 also undergoes oxidative stress
265 mediated DNA damage with subsequent JNK activation, similar to what we have seen in S2 cells *in*
266 *vitro*. Of note, the JNK target gene *puc* was found to be highly expressed across all hemocyte clusters
267 analyzed *in vivo* (Figure 3B). We looked again into the expression of metabolic genes including *Thor*
268 and *InR* as well as other cytokines such as *dpp*, *daw* or *egr* but could not detect a specific enrichment
269 in cluster C6 similar to our results from PQ-treated S2 cells *in vitro* (Figure 3B). These findings from the
270 snRNA-seq analysis *in vivo* and S2 cells *in vitro* support the hypothesis that cluster C6 plasmatocytes
271 represent a functional state of activated plasmatocytes directly responding to oxidative stress by JNK
272 signaling and Jak/STAT pathway activation. Furthermore, we found evidence that cluster C6 specifically
273 expresses the cytokine *upd3*, which could reflect an important mediator for oxidative stress response.

274

275 **Loss of canonical DNA damage signaling in adult hemocytes results in elevated *upd3* levels and a**
276 **decreased survival on oxidative stress**
277
278 We observed that hemocytes respond with a distinct gene expression pattern specific to oxidative
279 stress (Figure 1-3). Previously it has been observed that oxidative stress-induced DNA damage supports
280 immune activation in macrophages via a non-canonical DNA damage response[27]. Based on our findings,
281 we predict that also in adult hemocytes oxidative stress not only drives genome instability and
282 activates repair, but is rather essential to induce immune activation via specific gene expression
283 changes in cluster C6 plasmatocytes. To test if DNA damage signaling is involved in the response of
284 adult hemocytes to oxidative stress, we analyzed flies with a hemocyte-specific knock-down for
285 different genes of the DNA damage repair (DDR) machinery including the DNA damage sensing kinases
286 *telomere fusion* (*tefu*) and *meiotic 41* (*mei-41*) and the MRN complex protein *nbs*. Of note, by targeting
287 adult hemocytes, mostly plasmatocytes are targeted which make up 95% of all hemocytes in the adult
288 fly.
289 We generated *Hml>mei-41-IR* (*w;Hml-Gal4,UAS-2xeGFP/UAS-mei-41-IR*), *Hml>tefu-IR* (*w;Hml-*
290 *Gal4,UAS-2xeGFP/UAS-tefu-IR*), *Hml>mei41-IR;tefu-IR* (*w;Hml-Gal4,UAS-2xeGFP/UAS-mei-41-IR;UAS-*
291 *tefu-IR*) and *Hml>nbs-IR* (*w;Hml-Gal4,UAS-2xeGFP/UAS-nbs-IR*) flies (Figure S5A). First, we compared
292 their susceptibility to PQ treatment after 18 hrs and found significantly increased susceptibility to the
293 treatment across all DDR-deficient lines compared to the control genotype (*Hml/+*: 10.7±1.2%,
294 *Hml>mei-41-IR*: 40.7±4.8%, *Hml>tefu-IR*: 20.7±4.3%, *Hml>mei41-IR;tefu-IR*: 37.5±4.8% and *Hml>nbs-*
295 *IR*: 48.2±6.7%) (Figure 4A). In these flies, decreased survival after PQ did not correlate to an overall
296 reduction in lifespan on normal food and a decrease in fitness (Figure S5B).

297 Next, we inquired if DDR-deficiency in hemocytes might increase susceptibility of the fly to other
298 stresses. For this we challenged all genotypes with starvation. Importantly, we did not observe a
299 decreased survival of DDR-deficient flies on starvation compared to the control genotype, indicating
300 that the observed susceptibility to oxidative stress of flies with a DDR-deficiency in hemocytes is
301 specifically caused by oxidative stress due to PQ treatment (Figure S5C). As defects in the DDR
302 machinery in hemocytes might already affect the development during embryonic and larval stages, we
303 used a hemocyte-specific temperature-inducible knock-down of *mei-41*, *tefu* and *nbs1* which was
304 induced by a temperature shift to 29°C directly after eclosion from the pupae to induce a knockdown
305 in adult hemocytes only. We analyzed the lifespan of *Hml-Gal80^{ts}>mei-41-IR* (*w;Hml-Gal4,UAS-*
306 *2xeGFP/UAS-mei-41-IR;tub-Gal80*), *Hml-Gal80^{ts}>tefu-IR* (*w;Hml-Gal4,UAS-2xeGFP/UAS-tefu-IR;tub-*
307 *Gal80*), *Hml-Gal80^{ts}>mei-41-IR;tefu-IR* (*w;Hml-Gal4,UAS-2xeGFP/UAS-mei-41-IR;tub-Gal80/UAS-tefu-*
308 *IR*) and *Hml-Gal80^{ts}>nbs-IR* (*w;Hml-Gal4,UAS-2xeGFP/UAS-nbs-IR;tub-Gal80*) compared to control flies
309 *Hml-Gal80^{ts}/+* (*w;Hml-Gal4,UAS-2xeGFP/+;tub-Gal80*) and again found no alterations in overall

310 lifespan of all genotypes analyzed on control food except a slight decrease in lifespan of *Hml-*
311 *Gal80^{ts}>mei-41-IR;tefu-IR.* (Figure S5D). In contrast, we again found a higher susceptibility to oxidative
312 stress via PQ-feeding in the DDR-deficient lines compared to control (*Hml-Gal80^{ts}/+*: 30.3±5.2%, *Hml-*
313 *Gal80^{ts}>mei-41-IR*: 36.2±4.3%, *Hml-Gal80^{ts}>tefu-IR*: 52.4±6.9%, *Hml-Gal80^{ts}>mei-41-IR;tefu-IR*:
314 72.3±6.3% and *Hml Hml-Gal80^{ts}>nbs-IR*: 36.2±4.3%) (Figure S5E), which directly confirms our previous
315 results and conclusions (Figure 4A).

316 As we have seen before that loss of hemocytes is detrimental for the survival on oxidative stress, we
317 wanted to exclude a reduction in hemocytes in the DDR deficient fly lines as a cause of the higher
318 susceptibility to oxidative stress. We quantified GFP^{+} hemocytes in *Hml>mei-41-IR*, *Hml>tefu-IR*,
319 *Hml>mei-41-IR;tefu-IR* and *Hml>nbs-IR* flies (Figure 4B, Figure S5A). We did not find alteration in
320 hemocyte number across all fly lines on control food (with the exception of an increase in hemocytes
321 in the *Hml>tefu-IR* line), nor did we observe any effect of PQ treatment on the number of hemocytes
322 in DDR-deficient flies (Figure 4B, Figure S5A).

323 Next we analyzed if the loss of the DDR signaling machinery via knockdown of *tefu* and *mei41* results
324 in increased DNA damage in hemocytes. Comet assays of isolated hemocytes from DDR deficient flies
325 and the control genotype on PQ and control food only indicated a slight increase in DNA damage in
326 these flies, which demonstrates that the higher susceptibility of DDR deficient flies is not due to a loss
327 of hemocyte numbers or a substantial increase in DNA damage, but rather due to changes in the
328 downstream DDR-signaling events modulating immune activation of hemocytes (Figure 4C). Other
329 studies demonstrated that upon tissue damage JNK-mediated secretion of the JAK/STAT cytokines
330 upd1, upd2 and upd3 is a critical step for innate immune signaling[28,29]. Furthermore, DNA damage
331 signaling is essential to induce such an immune response and to regulate insulin signaling[30]. To
332 elucidate the implication of DDR signaling on hemocyte activation and oxidative stress resistance, we
333 measured the gene expression levels of *upd* cytokines as well as JNK and Jak/STAT targets in DDR
334 deficient flies and controls on PQ and control food. Loss of DNA damage signaling in hemocytes
335 induced a significant induction of *upd3* expression upon PQ treatment in *Hml>tefu-IR* and *Hml>mei-*
336 *41-IR;tefu-IR* flies (Figure 4D). In contrary, *upd1* and *upd2* were not significantly changed in DDR-
337 deficient flies (Figure 4D). We measured the Jak/STAT target genes *Socs36E* and *TotA* on systemic level.
338 A slight induction of *Socs36E* expression in all DDR-deficient genotypes on PQ but only *Hml>mei-41-*
339 *IR;tefu-IR* flies showed a significant induction of *Socs36e* upon PQ treatment compared to control food
340 and *Hml/+* flies on PQ (Figure 4D). *TotA* expression tended to be reduced upon PQ treatment across
341 all genotypes analyzed. However, when we checked the levels of *puc* as a *JNK signaling* target gene,
342 we found a significant induction on PQ treatment in *Hml>tefu-IR*, *Hml>mei-41-IR;tefu-IR* and *Hml>nbs-*
343 *IR* flies, which was not seen in control flies upon PQ treatment (Figure 4D). When we analyzed the gene

344 expression of genes involved in metabolism and energy mobilization, we detected a significant
345 induction and dysregulation of *Thor* and *InR* in all DDR-deficient genotypes upon PQ treatment
346 compared to control flies (Figure 4E), as well as a slight induction of *Pepck1* (Figure 4E). To exclude that
347 these changes in energy mobilization are due to altered expression of *Ilps*, we analyzed the levels of
348 *Ilp*2, *Ilp3* and *Ilp5* in all genotypes on control and PQ-food, but could not detect remarkable alterations
349 here (Figure 4E). To further exclude that the higher susceptibility of DDR-deficient flies and seen
350 alterations in stress response are due to inefficient mobilization of triglycerides, we measured stored
351 triglycerides across all genotypes and found efficient mobilization of triglyceride storage upon PQ
352 treatment in all genotypes compared to control food (Figure 4F).

353 From our results we can conclude that DDR signaling in adult hemocytes, mostly consisting of
354 plasmatocytes, essentially determines susceptibility to oxidative stress. Loss of canonical DNA damage
355 signaling in hemocytes, which normally would induce DDR or cell death, triggers enhanced non-
356 canonical DNA damage signaling such as upregulation of *JNK* signaling and elevated expression of the
357 pro-inflammatory cytokine *upd3*, as well as transcriptional alterations in energy mobilization and
358 insulin signaling. Based on our previous results on the role of hemocytes during oxidative stress, we
359 can therefore assume that this JNK activation and *upd3* induction is essentially mediated by
360 hemocytes.
361
362 **Adult hemocytes control susceptibility to oxidative stress by JNK signaling and *upd3* release**
363
364 To this point, our data suggests that oxidative stress-induced DDR in hemocytes limits immune
365 activation and stress response upon oxidative stress. In other words, enhanced DNA damage boosts
366 immune activation and therefore susceptibility to oxidative stress. As we found that increased *upd3*
367 levels correlate with a higher susceptibility to oxidative stress of flies with DDR-deficient hemocytes,
368 we aimed to test if hemocyte-derived *upd3* is a major source to regulate susceptibility to PQ-induced
369 oxidative stress. To do so, we either over-expressed *upd3* in hemocytes in *Hml>upd3* (*w;Hml-Gal4,UAS-*
370 *2xeGFP/UAS-upd3*) flies or performed a hemocyte-specific knockdown of *upd3* in *Hml>upd3-IR* (*w;Hml-*
371 *Gal4,UAS-2xeGFP/UAS-upd3-IR*) flies. Both genotypes showed a normal overall lifespan compared to
372 the *Hml/+* control (Figure S5F), but when we compared their susceptibility to PQ-induced oxidative
373 stress, *Hml>upd3* flies showed a drastically decreased survival on PQ, whereas *Hml>upd3-IR* flies did
374 not show a changed survival on PQ treatment after 18 hours (Figure 5A). We tested *upd3* expression
375 levels on a whole fly level and found a slight but not significant induction in *Hml/+* flies after PQ
376 treatment compared to control food, in line with our previous results (Figure 1B and 5B). As expected,
377 *Hml>upd3* flies showed increased levels of *upd3* in both treatment groups compared to the other
378 genotypes, but also showed a significant increase of *upd3* upon PQ compared to control food (Figure

379 5B). Surprisingly, *Hml>upd3-IR* flies still showed a slight induction of *upd3* upon PQ treatment, which
380 could potentially be derived from another cellular source after eliminating hemocyte-derived *upd3*.
381 To identify if the higher susceptibility of *Hml>upd3* flies to oxidative stress was due to reduced
382 hemocyte numbers, we quantified hemocytes across all three genotypes, but did not see any
383 significant changes of hemocyte number in both genotypes compared to *Hml/+* control flies on control
384 food and PQ (Figure 5C and Figure S5G). Only in the *Hml>upd3-IR* flies we found a reduction of
385 hemocytes between flies on control food and PQ, but without consequences for their susceptibility to
386 oxidative stress (Figure 5C and Figure S5G). Our data indicate that elevation of hemocyte-derived *upd3*
387 is sufficient to increase the mortality of adult flies on PQ-mediated oxidative stress. Yet we could not
388 exclude other cellular sources for *upd3* upon oxidative stress other than hemocytes. Therefore, we
389 wanted to probe if hemocyte-derived *upd3* is sufficient to increase the susceptibility to PQ treatment
390 in the absence of other cellular sources. We backcrossed *Hml>upd3* flies to *upd3*-deficient flies
391 (*upd3*^{null}) to generate *upd3*^{null}*;Hml>upd3* flies (*upd3*^{null}*;Hml-Gal4,UAS-2xeGFP/UAS-upd3)* and
392 compared their survival on PQ to different control genotypes (w^{1118} and *Hml/+*) and *upd3*^{null} flies (Figure
393 5D). We did not identify any differences in the susceptibility of w^{1118}, *Hml/+* and *upd3*^{null} control flies
394 to PQ treatment, however we found a significantly decreased survival in *upd3*^{null}*;Hml>upd3* flies when
395 hemocytes are overexpressing *upd3* (Figure 5D).

396 Previous studies highlighted that JNK signaling can induce *upd3* expression in hemocytes[12]. In line with
397 these reports, we found enrichment of genes with *kayak/AP-1* binding motifs in the plasmatocyte
398 subset C6 which showed further upregulation of Jak/STAT target genes and also *upd3* expression
399 (Figure 3). Therefore, we wanted to verify if *JNK* activation in hemocytes acts as a direct downstream
400 signal activated by non-canonical DNA damage signaling upon oxidative stress and subsequently
401 induces the release of the pro-inflammatory cytokine *upd3*. We either overexpressed a constitutive
402 active form of *JNKK hemipterous* (*hep*) in hemocytes using *Hml>hep[act]* (*w;Hml-Gal4,UAS-*
403 *2xeGFP/UAS-hep[act]*) flies or overexpressed a dominant-negative version of the Jun kinase *basket*
404 (*bsk*) in hemocytes using *Hml>bsk-DN* (*w;Hml-Gal4,UAS-2xeGFP/UAS-bsk-DN*). We compared their
405 survival on PQ after 18 hrs and in line with our previous results, found an increased susceptibility of
406 *Hml>hep[act*] flies to PQ treatment, but not of *Hml>bsk-DN* flies compared to the control genotype
407 (Figure 5E). We again analyzed the overall lifespan of these flies on normal food and could not find
408 differences between the genotypes (Figure S5H). Furthermore, when we analyzed *upd3* expression in
409 these flies upon PQ treatment, we found a significant induction of *upd3* expression after PQ treatment
410 in *Hml>hep[act*] compared to control food, but only a slight increase in *Hml/+* and *Hml>bsk-DN* flies
411 upon PQ feeding. These findings support a substantial role of JNK-mediated induction of *upd3* in
412 hemocytes upon oxidative stress. In summary, our data discovers a defined immune-responsive subset
413 of plasmatocytes during oxidative stress. We show that this oxidative stress-mediated immune

414 activation seems to be controlled by non-canonical DNA damage signaling resulting in *JNK* activation
415 and subsequent *upd3* expression, which can render the adult fly more susceptible to oxidative stress
416 when it is over-activated.

417

418 **Discussion**

419

420 Similar to vertebrate macrophages, oxidative stress triggers immune activation in *Drosophila*
421 hemocytes[18]. However this immune activation was not obvious on a systemic level upon PQ-mediated
422 oxidative stress. In contrast, localized oxidative stress-induced immune activation in damaged tissues
423 is an essential step of the *Drosophila* immune response to infection or injury[19,31]. However, the precise
424 contribution of *Drosophila* macrophages in this immune activation, in the organ-to-organ
425 communication during stress response and the implication in the organism's survival upon increased
426 oxidative stress remained so far ill-defined. Overall, we describe responses of adult hemocytes, namely
427 plasmatocytes, to oxidative stress with a particular subset of plasmatocytes (cluster C6) which directly
428 responds to oxidative stress by immune activation. We demonstrated that this immune activation
429 seems to be at least partially controlled by non-canonical DNA damage signaling in hemocytes. Loss of
430 *nbs*, *tefu* or *mei-41* in hemocytes renders the organism more susceptible to oxidative stress without
431 signficantly affecting oxidative stress mediated DNA damage and its repair, but with an enhanced
432 induction of JAK/STAT and JNK signaling, accompanied by changes in genes associated with energy
433 mobilization and storage. Finally, we showed that the control of hemocyte-derived *upd3* is key for the
434 survival of the organism upon oxidative stress and that induction of the *JNK/upd3* signaling axis in
435 hemocytes is sufficient to increase the susceptibility to oxidative stress. Hence, we postulate that
436 hemocyte-derived *upd3*, most likely released by the activated plasmatocyte cluster C6 during oxidative
437 stress *in vivo* and subsequently controlling energy mobilization and subsequent tissue wasting upon
438 oxidative stress.

439

440 *Drosophila* hemocytes have been described before to react to PQ-mediated or infection-mediated
441 intestinal damage via release of cytokines to promote ISC proliferation in the gut[14,17]. PQ is a widely
442 used model in *Drosophila* to induce oxidative stress via oral uptake[32]. In many reports the gut has been
443 described to be the most affected organ and ISC proliferation is an essential step to regenerate the
444 injured intestinal epithelium[33,34]. PQ treatment has been described to cause gut leakage and therefore
445 this could be a potential cause of death for the fly[14], though we did not find signs of gut leakage within
446 the 18 hours PQ treatment with a concentration of 15mM. Aside from the gut, oral PQ treatment was
447 shown to induce oxidative stress in many organs including hemocytes[35], oenocytes[36] and the brain[37],
448 indicating that the induced oxidative stress is not only localized to the gut tissue. PQ-induced oxidative

449 stress was described before to cause neurodegeneration with parkinsonism-like symptoms,
450 accompanied by strong immune activation and upregulation of *JNK* signaling in the CNS[37], an activation
451 profile similar to the identified activated plasmatocyte cluster C6 in our snRNA-seq analysis. The
452 snRNA-seq analysis further revealed distinct hemocyte clusters with seven plasmatocyte clusters and
453 one crystal cell cluster. Whereas the plasmatocyte clusters C1 and C7 seem to represent cellular states
454 found in steady state conditions only, we identified several other clusters which seemed to be exclusive
455 or at least enriched under PQ treatment. Interestingly, we only identified one cluster, C6, which
456 specifically responded to oxidative stress via immune activation and upregulation of oxidative stress
457 response genes but also *Jak/STAT* and *JNK* target genes. We postulate that these cells might be directly
458 exposed to the oxidative stress because their signature resembles the one of S2 cells directly treated
459 with PQ *in vitro*. Even though oxidative DNA damage in hemocytes was followed by immune activation
460 *in vitro* and *in vivo*, it remains to be determined if this activation is induced by cytokines derived from
461 damaged organs during oxidative stress or by the oxidative stress directly. The hypothesis that this
462 cluster is directly exposed to oxidative stress is further supported by an upregulation of genes such as
463 *Hsps* in this cluster which are known to be directly induced by oxidative stress[38]. Furthermore, we
464 found evidence that oxidative DNA damage and induced non-canonical DNA damage signaling induce
465 several of these immune activation cascades in cluster C6 plasmatocytes. This was supported by the
466 increased DNA damage in S2 cells by PQ treatment but also the enrichment of DDR-associated genes
467 such as *Gadd45* in cluster C6, which is associated with *JNK* activation and is further implicated in
468 oxidative stress induced DNA damage[37]. Constant DNA damage signaling and repair is an essential step
469 in all tissues to maintain tissue homeostasis[39].

470 In our study, we point to a potential non-canonical role of DNA damage sensing to trigger immune
471 activation and response to oxidative stress in hemocytes. We did not find indications of canonical DNA
472 damage response, such as induced apoptosis in hemocytes due to the oxidative DNA damage. Non-
473 canonical DNA damage sensing has been implicated in immune responses in vertebrates and
474 invertebrates[30,37,40,41]. It was demonstrated that vertebrate macrophages *in vitro* respond similarly to
475 immune stimuli such as infection by synergistic activation of DDR and type I interferon signaling to
476 induce downstream immune signaling cascades[27]. Here, we provide new evidence in *Drosophila* that
477 non-canonical DNA damage is used by immune cells *in vivo* to modulate and especially control their
478 immune response including pro-inflammatory cytokine release upon oxidative stress. Localized DNA
479 damage in larval epithelial cells has been shown to induce non-canonical DNA damage activity leading
480 to the secretion of *upds* and the regulation of hemocyte expansion and activation, as well as
481 subsequent hemocyte-mediated regulation of energy storage in the fat body[30]. In further support of
482 our results, one report previously demonstrated that loss of DNA damage signaling machinery induced
483 the release of *upd3* in hemocytes[14]. Most likely, the identified plasmatocyte cluster C6 is a central

484 cellular source of this signal, which needs to be further determined in future studies. Furthermore,
485 anatomical localization of this cluster and spatial distribution of the different plasmatocyte clusters
486 would be of interest. We describe a strong connection between the control of *upd3* expression by
487 hemocytes and the susceptibility of the adult fly to oxidative stress. Upon oxidative stress, we observe
488 decreased triglycerides and glycogen stores and altered gene expression such as induced expression
489 of lipolytic enzymes and other *foxo* target genes indicating energy mobilization from the adult fat body.
490 Accumulating evidence throughout our study points to an implication of hemocyte-derived *upd3* in the
491 control of energy mobilization and tissue wasting during oxidative stress. These findings are in line with
492 our previous studies where we showed that upon high fat diet hemocytes produce high levels of *upd3*
493 which induces insulin insensitivity in many tissues by activating *Jak/STAT signaling* in these organs and
494 inhibiting the insulin signaling pathway[12]. Furthermore, we and others described a central role for
495 hemocyte derived *upds* in the control of glucose metabolism in muscles during steady state and upon
496 infection[13,42]. As shown before, hemocytes produce high levels of *upd3* upon infection with
497 *Mycobacterium marinum* which also caused tissue wasting and extensive energy mobilization in a *foxo*-
498 dependent manner[11,43].

499 Our study provides further evidence that hemocytes serve as essential signaling hubs in organ-to organ
500 communication during oxidative stress, which is in line with previous immune challenge as well as
501 steady state[19,42,44]. Our findings in *Drosophila* highlight the role of macrophages for the survival on
502 oxidative stress with an urgent need for the tight control of their immune activation. We further
503 unravel the diverse responses of hemocytes towards oxidative stress which can now serve as a baseline
504 to further explore the spatiotemporal macrophage/hemocyte responses to oxidative stress. Future in
505 depth analysis of the regulation of these cellular states and their coupling to tissue repair will allow to
506 gain new insights for the treatment of diseases including cancer or neurodegenerative diseases.
507

508 **Acknowledgements and Funding**

509 The authors are very grateful to the members of the Kierdorf lab for their help and support. The
510 authors would especially like to thank M. Oberle for her exceptional help with the maintenance of the
511 Drosophila stocks and the management of the fly room. We would like to acknowledge the Lighthouse
512 Core Facility and its staff, especially J. Bodinek-Wersing and U. Jagadeshwaran, for their assistance with
513 the sorting of nuclei. The authors are especially grateful to D. Ganser and H. Fischer for the continuous
514 support throughout the study. Graphical abstract was created with BioRender.com. KK was supported
515 by project grants of the Fritz Thyssen Foundation and of the German Research Foundation (DFG). MSD
516 was supported by Wellcome Trust (207467/Z/17/Z) and Biotechnology and Biological Sciences
517 Research Council (BBSRC) (BB/W/001004/1). KK, MP, and OG were supported by the DFG through
518 project grants within SFB/TRR167 (Project ID 259373024) and by project grants within CRC1479

(Project ID 441891347). KK, MP, OG, and AC were supported by the DFG under Germany's Excellence Strategy (grant no. CIBSS—EXC-2189, Project ID 390939984). AC was further supported by the Boehringer Ingelheim Foundation (Plus3 Programme). OG was further supported by the European Research Council (ERC) through Starting Grant 337689 and Proof-of-Concept Grant 966687, and by the DFG through project grants in GRK2606 (Project ID 423813989), SFB1425 (Project ID 422681845), and SFB1160 (Project ID 256073931), as well as by the EU-H2020-MSCA-COFUND EURIdoc programme (No. 101034170). MP was further supported by the Novo Nordisk Foundation, the Ernst Jung Foundation, the DFG through project grants in SFB992 (Project ID 192904750), and SFB1160 (Project ID 256073931), a Reinhart Koselleck grant and the Gottfried Wilhelm Leibniz prize, the Ministry of Science, Research and Arts of the state of Baden-Wuerttemberg (Sonderlinie 'Neuroinflammation') and by the Alzheimer Forschung Initiative e.V. (AFI). GM was supported by a Marie Skłodowska-Curie postdoctoral fellowship.

Author Contributions

FH contributed to project planning, performed all experiments, analyzed data, edited the manuscript and prepared the figures. TM and PW performed experiments, helped with the data analysis, and edited the manuscript. CC performed the snRNA-seq experiment and bioinformatics analysis. GM performed data preprocessing and supported bioinformatics analysis. AC, MSD, KP, OG, and MP provided equipment and reagents, helped to analyze and interpret data, and edited the manuscript. KK planned and supervised the project, conceptualized the study and wrote the manuscript.

Competing Interests Statement

The authors declare no competing financial or scientific interests.

Methods Section

Drosophila melanogaster stocks:

Flies were reared on a high yeast food containing 10% brewer's yeast, 8% fructose, 2% polenta and 0.8% Agar. Propionic acid and nipagin were added to prevent bacterial or fungal growth. All crosses (except those containing the *tub-Gal80^{ts}* construct or otherwise noted) were performed at 25°C with a 12 hours dark/light cycle. The crosses with *tub-Gal80^{ts}* were performed at 18°C to ensure the inhibition of the Gal4-protein during developmental stages of the fly. The experimental male F1 flies were transferred to 29°C as soon as they hatched and were aged for six days. All transgenic lines used in this study are listed in the Table S2.

Lifespan/Survival assays:

Male flies were collected after eclosion and groups of 20 age-matched flies per genotype were housed in a food vial. The survival experiments were performed at 29°C. The vials were placed horizontal to

553 avoid that flies fall into the food and become stuck. Dead flies were counted in a daily manner. The
554 flies were transferred into a fresh food vial twice per week without CO_2 anesthesia.

555 *Paraquat treatment:*

556 Flies were maintained at 29°C for six days prior to treatment. On day six they were starved for 6 hours.
557 A filter paper soaked in 5% sucrose solution with or without 15mM Paraquat (PQ, Methyl viologen
558 hydrate, Acros Organics) was added after starvation. Flies were fed for 18 hours on the PQ containing
559 food in groups of ten. The PQ treatment was performed at 29°C in the dark[20]. To assess the survival
560 rate the dead flies per vial were counted and the percentage was calculated. The living flies were
561 further analyzed in other assays used in this study.

562 *Starvation experiments:*

563 10-20 age-matched male flies were kept in a vial containing 1% agar supplemented with 2% 1xPBS. The
564 starvation experiments were performed at 25°C. Dead flies were counted every hour. Several
565 individual experiments were performed and started on different daytimes to exclude diurnal derived
566 artifacts. The data of the individual experiments were pooled and analyzed with GraphPad Prism 9.2.0.

567 *Paraffin sections and stainings:*

568 Anaesthetized flies were washed in 75% ethanol for 5-10 seconds and transferred into 4% PFA for 30
569 minutes at room temperature. The flies were washed for 1 hour in PBS on a shaker. Subsequently the
570 flies were transferred into tissue cassettes, dehydrated and embedded in paraffin. The flies were cut
571 in 7µm thick sections de-paraffinated and stained on slides with Hematoxylin-Gill (II) for five minutes.
572 Subsequently the sections were blued in running water for ten minutes. It followed a 0.5% Eosin
573 treatment for five minutes and a final ethanol treatment with increasing concentrations until 100%.
574 The sections were transferred into Xylol and finally covered with synthetic resin and a cover slip.

575 *Semi-quantitative Real-Time PCR:*

576 Three flies were pooled and smashed in 100µl TRIzol to stabilize and isolate the RNA. Chloroform was
577 used to extract the RNA followed by an isopropanol precipitation step. The RNA was cleaned with 70%
578 ethanol and solubilized in water. A DNAse treatment was performed to digest potential genomic DNA
579 contaminations. The purified and DNAse treated RNA was written into cDNA using RevertAid Reverse
580 Transcriptase (Thermo Scientific) at 37°C for one hour. The reaction was stopped by incubating for 10
581 minutes at 70°C. The subsequent RTqPCR was done in SensiMix SYBR Green no-ROX (Meridian
582 Bioscience) and was performed on a LightCycler 480 (Roche). The qPCR cycling started with a 10-
583 minute 95°C step followed by 50 cycles with the following times and temperatures: 15s at 95°C, 15s at
584 60°C and 15s at 72°C. The gene expression levels were normalized to the value of the measured loading
585 control gene Rpl1.

586 *Confocal microscopy:*

587 The flies were anesthetized with CO2, glued on a cover slip and imaged immediately. Confocal
588 microscopy was done with a Leica SP8 microscope (Leica) and a 10x/NA0.4 Leica air objective. The
589 images were acquired in a resolution of 512x512 with a scan speed of 600 Hz. Z-Stacks with a step size
590 of 5µm and tile scans (2x2 or 2x3 images per fly) were acquired to quantify the hemocytes in whole
591 flies. The tiled images were merged with the LAS-X software (Leica) and maximum projections were

592 created using Fiji/ImageJ. The hemocytes were counted in the maximum projection images of whole
593 flies.

594 *Smurf Assay:*

595 Smurf assays were performed to check the feeding behavior as well as the gut integrity of 7 day old,
596 male flies upon PQ treatment. Brilliant Blue dye (FCF) was added into 5% sucrose solution in a
597 concentration of 1% (w/v). PQ was added in concentrations of 2mM, 15mM and 30mM. Control food
598 was 5% sucrose and 1% Brilliant Blue without PQ. The flies were fed with blue food according the PQ-
599 treatment protocol, as described above. Flies were analyzed after 18h of feeding on brilliant-blue food.
600 Three kinds of flies were distinguished. Flies that did not eat at all were excluded. Flies with a blue gut
601 or crop were classified as "non-smurf". Flies which turned completely blue or showed distribution of
602 blue dye outside the gut were classified as "smurf".

603 *Thin Layer Chromatography (TLC):*

604 Each sample in the TLC analysis contains 10 flies of the respective genotype. The flies were starved for
605 one hour before they were anesthetized with CO2 and transferred into 100µl chloroform:methanol
606 (3:1) on ice. The flies were centrifuged for 5 minutes at 15,000g at 4°C and subsequently homogenized
607 with a pestle. The sample was centrifuged again with the same settings. Lard was dissolved in
608 chloroform:methanol (3:1) and served as triglyceride control (standard 1). Standard 1 was used to
609 produce a standard curve with decreasing triglyceride concentrations. The samples and the standard
610 curve were loaded on a glass silica gel plate (Millipore). The mobile phase in the TLC chamber was
611 made with hexane:diethylether (4:1). The plate was placed in the chamber until the solvent front
612 reached the upper end of the plate. The plate was taken out, air dried and stained with ceric
613 ammonium heptamolybdate (CAM). Subsequently the plate was incubated at 80°C for 2 hours to
614 visualize the stained triglyceride bands. Images were taken with a gel documentation system (gelONE).
615 Triglyceride density was measured and the concentrations were calculated according the pre-
616 determined concentrations of the standard curve. Image analysis and calculations were done using
617 ImageJ.

618 *Glucose Assay:*

619 Seven day old male flies were used for the analysis. They were treated for 18h with PQ or sucrose
620 respectively. Subsequently the flies were starved for one hour to bring all flies into the same metabolic
621 state. Three flies were pooled as one sample and manually homogenized in 75µl TE + 0.1% Triton X-
622 100 (Sigma Aldrich). The samples were incubated for 20min at 75°C to inactivate any intrinsic
623 enzymatic activity. 5µl of the samples were loaded into a flat-bottom 96-well plate. Each sample was
624 measured four times to measure glucose, trehalose, glycogen and the fly background respectively. The
625 fly background was determined by diluting the fly sample with water. Glucose reagent (Sentinel
626 Diagnostics) was added to the fly sample to measure the glucose levels. Trehalase (Sigma Aldrich) or
627 amyloglucosidase (Sigma Aldrich) was added to the glucose reagent to measure trehalose or glycogen
628 respectively. Plates were incubated for 24h at 37°C before the colorimetric measurement was
629 performed at a wavelength of 492nm on a Tecan® Spark plate reader. The concentrations were
630 calculated according to standards loaded on the same plate.

631 *Nuclei FACS sorting:*

632 100 male *Hml-dsRed.nuc* flies per sample were homogenized in 500µl ice-cold EZ nuclei lysis buffer
633 (Sigma). Another 500µl EZ lysis buffer was added and the nuclei were incubated for five minutes on
634 ice. Following a pre-filtration step with a 70µm cell strainer (Miltenyi filters) the nuclei were
635 centrifuged at 500g for six minutes at 4°C. The pellet was resuspended and incubated in 1ml of EZ lysis
636 buffer for five minutes on ice following a second centrifugation step with previous used settings. After
637 discarding the supernatant, 500µl of nuclei wash and resuspension buffer (1x PBS; 1% BSA; 0.2U/µl
638 RNase inhibitor, NEB) was added without resuspending the pellet and incubated for 5 minutes on ice.
639 Subsequently the pellet was resuspended with additional 500µl nuclei wash and resuspension buffer.
640 The nuclei were centrifuged using previous settings and subsequently washed with 1ml of nuclei wash
641 and resuspension buffer. After centrifugation the pellet was resuspended and incubated for 15
642 minutes with nuclei staining solution containing DAPI (1:1000) and DRAQ7 (1:100). The nuclei were
643 washed once with 1ml nuclei wash and resuspension buffer. After centrifugation the pellet was
644 dissolved in 200µl wash and resuspension buffer, filtered through a 40µm filter and sorted on a BD
645 FACS ARIAIII. A duplet exclusion was performed by gating on singlets in FSC-A vs. FSC-W plot.
646 Subsequently DRAQ7+DAPI+ events were sorted into nuclei wash and resuspension buffer.

647 *Single nucleus library preparation and sequencing:*

648 For single nucleus library preparation, nuclei were loaded onto a Chromium Single Cell 3' G Chip (10X
649 Genomics) to generate single-nucleus gel beads in emulsion (GEM) according to the manufacturer's
650 instructions without modifications using Chromium Next GEM Single Cell 3' Reagents Kit v3.1 (10X
651 Genomics). In order to multiplex the samples for sequencing, Single Index Kit T Set A (10x Genomics)
652 was used for library preparation according to the manufacturer's instructions. The cDNA content and
653 size of post-sample index PCR samples was analyzed using a 2100 BioAnalyzer (Agilent). Library
654 quantification was done using NEB Next® Library Quant Kit for Illumina® (New England Biolabs)
655 following manufacturer's instructions. Sequencing libraries were loaded on an Illumina Nextseq 550
656 flow cell, with sequencing settings according to the recommendations of 10× Genomics. Sample de-
657 multiplexing was done using built-in BCL2FASTQ. Cell Ranger v6 software was implemented for gene
658 alignment to the fly genome. The *Drosophila melanogaster* genome assembly and annotation file were
659 downloaded from Ensembl (Release 104). The annotation files were filtered as suggested by 10x
660 Genomics, to keep only the categories of interest (i.e. protein coding genes, long intergenic noncoding
661 RNAs, antisense, pseudogenes). Cell Ranger v6 with the "include-intron" parameter was used for the
662 generation of the count data.

663 *snRNA-seq data analysis*

664 Downstream analysis implemented the SoupX v1 and Seurat v4 R-based packages. The matrix for each
665 sample was loaded using the SoupX package[45] and ambient RNA contamination was calculated using
666 the default setting. The corrected matrix together with metadata on treatment were used to create an
667 object in Seurat v4[23]. Doublet detection was done using the DoubletFinder package v2[46]. After doublet
668 exclusion, a combined object was created from the list by using the "merge" function. Nuclei with <
669 5% of mitochondrial contamination and between 400 and 1,700 genes expressed were retained for
670 further analysis. The filtered raw count matrix was log-normalized within each nucleus. The top 3,000
671 variable genes were calculated by Seurat using the variance stabilizing transformation selection
672 method and data were scaled. The variable genes were used to perform principal component analysis
673 (PCA) and the top 20 principal components were used for the unsupervised clustering. Seurat applies
674 a graph-based clustering approach: the "FindNeighbors" function uses the number of principal

675 components (dims = 20) to construct the k-nearest neighbors graph based on the Euclidean distance
676 in PCA space, and the "FindClusters" function applies the Louvain algorithm to iteratively group nuclei
677 (resolution = 1). We then used the PCA embedding to generate an UMAP for cluster visualization. For
678 each cluster, differentially expressed genes (DEGs) were calculated using the "FindMarkers" and
679 "FindAllMarkers" function with default parameters with adjusted $P < 0.05$ using Bonferroni correction.
680 The DEGs were used to assign cell type identity to clusters based on known cell lineage markers
681 described in previously published study[25]. To understand the impact of Paraquat treatment on each
682 cluster, "FindMarkers" function was used to compare "control" vs "Paraquat" treated cells per cluster.
683 Based on the DEGs obtained from this analysis, volcano plots were created using the EnhancedVolcano
684 package v1[47]. UMAP visualizations, Feature plots and dot plots for snRNA-seq data were generated
685 using in-built plotting functionality of Seurat.

686 *Subclustering of hemocytes and further analysis:*

687 Based on the cell identity and known hemocyte marker genes from a previous study[25], sub-clusterings
688 were performed using the same unsupervised algorithm and downstream analysis. After removing
689 non-hemocyte clusters, final sub-clustering was done with a modification that "FindNeighbors"
690 function was run with dims = 10 and "FindClusters" function was run with resolution 0.8. Based on the
691 DEGs found by the "FindAllMarkers" function (parameters: only.pos = T, test.use= "MAST") a heat map
692 was plotted for TOP 20 DE genes per clusters.

693 *Regulation network analysis of hemocyte clusters:*

694 In order to determine the transcription factor activity, regulon analysis was performed using the R
695 package SCENIC (v1.3.1)[48]. To remove noise, genes with low expression levels or low positive rates
696 were filtered using the "geneFiltering" function with default settings to obtain a filtered matrix which
697 was used to build co-expression network using the "runCorrelation" and "runGENIE3" functions. Gene
698 regulatory networks (GRNs) were built and scored using the default parameters. Potential regulons
699 based on DNA-motif analysis were selected by using RcisTarget and active gene networks were
700 identified by AUCell. Regulon activity for each cell was calculated as the average normalized expression
701 of putative target genes. Regulon activity matrix was exported which was used to create a new 'AUC'
702 assay using "CreateAssayObject" function of Seurat. "DoHeatmap" function from Seurat was used to
703 plot scaled TF activity in individual hemocytes.

704 *S2 Cell Culture, CellROX staining and flow cytometry:*

705 Drosophila S2 cells (Invitrogen™) were cultured in Schneider's Drosophila medium (Gibco™) at 26°C
706 and atmospheric oxygen and carbon dioxide conditions. The medium contained 10% FCS and 1%
707 penicillin/streptomycin. PQ was added into the medium in concentrations of 15mM or 30mM to
708 investigate the influence on the production of reactive oxygen species (ROS). Control cells remained
709 untreated. To visualize ROS and oxidative stress, the cells were stained with CellROX™ Deep Red
710 Reagent (Invitrogen) for 30 minutes directly in the medium in a concentration of 1:500 at 26°C. The
711 cells were washed twice with 1xPBS containing 2mM EDTA. In order to stain dead cells DAPI was added
712 to the samples in a concentration of 1:1000. Samples were acquired using a BD LSRFortessa™ (BD
713 Biosciences) and analyzed with FlowJo analysis software.

714 *COMET assays:*

715 Comet assays were performed to analyze the amount of DNA damage in S2 cells treated with PQ. S2
716 cells were treated with 15mM or 30mM PQ for 24h. The cells were brought into a concentration of
717 $1.8x10^5$ cells/ml. Low melting agarose (LMA) was boiled at 90°C and subsequently cooled down to 37°C.
718 The cells were diluted in low melting agarose (LMA) at a ratio of 1:10 (cells:LMA) and transferred onto
719 a CometSlide™ (Trevigen). To ensure proper attachment of the LMA, the slides were cooled for 30
720 minutes at 4°C. The lysis was performed for one hour at 4°C. Therefore the slides were submerged in
721 CometAssay® Lysis Solution (Trevigen). Subsequently the cells were submerged in alkaline unwinding
722 solution (200mM NaOH, 1mM EDTA, pH 13) for 1h at 4°C. The electrophoresis was performed under
723 alkaline conditions (pH13) for 30 minutes with a current of 20V (1V/cm). The slides were neutralized
724 with ddH_2O, dehydrated with 37% ethanol and dried properly at 37°C before they were stained with
725 SYBR™Gold (Invitrogen) for 30 minutes. Comets were imaged with an Olympus BX61 fluorescence
726 microscope. Comet data was analyzed via TriTrek CometScore 2.0.0.38 software.

727 *Statistical analysis and data handling:*

728 Statistical significance of real-time qPCR, Paraquat survival, hemocyte quantification, TLC, Glucose
729 assay, CellROX and comet assay data was calculated with an unpaired t-test or one-way ANOVA as
730 indicated in the figure legends. Lifespan/survival assays were analyzed using Log-Rank and Wilcoxon
731 test. Significance digits indicate the following significance levels: *$p<0.05$, **$p<0.01$, ***$p<0.001$,
732 ****$p<0.0001$. Significance tests were performed using GraphPad Prism 9 software. Data handling of
733 snRNAseq data is described above.

734 **Data availability**

735

736 snRNA-seq data will be publicly available as of the date of publication. Microscopy, flow cytometry and
737 survival data reported in this paper will be shared by the lead contact upon request. Any additional
738 information required to reanalyze the data reported in this paper is available from the lead contact
739 upon request.

740

741 **References**

742 1. Pham-Huy, L.A., He, H., and Pham-Huy, C. (2008). Free Radicals, Antioxidants in Disease and
743 Health. Int J Biomed Sci *4*, 89–96.

744 2. Sinenko, S.A., Shim, J., and Banerjee, U. (2011). Oxidative stress in the haematopoietic niche
745 regulates the cellular immune response in Drosophila. EMBO Rep *13*, 83–89.
746 10.1038/embor.2011.223.

747 3. Herb, M., and Schramm, M. (2021). Functions of ROS in Macrophages and Antimicrobial
748 Immunity. Antioxidants (Basel) *10*, 313. 10.3390/antiox10020313.

749 4. Nathan, C., and Cunningham-Bussel, A. (2013). Beyond oxidative stress: an immunologist's guide
750 to reactive oxygen species. Nat Rev Immunol *13*, 349–361. 10.1038/nri3423.

751 5. Finkel, T., and Holbrook, N.J. (2000). Oxidants, oxidative stress and the biology of ageing. Nature
752 *408*, 239–247. 10.1038/35041687.

753 6. Moghadam, Z.M., Henneke, P., and Kolter, J. (2021). From Flies to Men: ROS and the NADPH
754 Oxidase in Phagocytes. Frontiers in Cell and Developmental Biology *9*, 618.
755 10.3389/fcell.2021.628991.

756 7. Meister, M., and Lagueux, M. (2003). Drosophila blood cells. Cell Microbiol *5*, 573–580.
757 10.1046/j.1462-5822.2003.00302.x.

758 8. Banerjee, U., Girard, J.R., Goins, L.M., and Spratford, C.M. (2019). Drosophila as a Genetic Model
759 for Hematopoiesis. Genetics *211*, 367–417. 10.1534/genetics.118.300223.

760 9. Gold, K.S., and Brückner, K. (2014). Drosophila as a model for the two myeloid blood cell systems
761 in vertebrates. Exp. Hematol. *42*, 717–727. 10.1016/j.exphem.2014.06.002.

762 10. Holz, A., Bossinger, B., Strasser, T., Janning, W., and Klapper, R. (2003). The two origins of
763 hemocytes in Drosophila. Development *130*, 4955–4962. 10.1242/dev.00702.

764 11. Péan, C.B., Schiebler, M., Tan, S.W.S., Sharrock, J.A., Kierdorf, K., Brown, K.P., Maserumule, M.C.,
765 Menezes, S., Pilátová, M., Bronda, K., et al. (2017). Regulation of phagocyte triglyceride by a
766 STAT-ATG2 pathway controls mycobacterial infection. Nat Commun *8*, 14642.
767 10.1038/ncomms14642.

768 12. Woodcock, K.J., Kierdorf, K., Pouchelon, C.A., Vivancos, V., Dionne, M.S., and Geissmann, F.
769 (2015). Macrophage-derived upd3 cytokine causes impaired glucose homeostasis and reduced
770 lifespan in Drosophila fed a lipid-rich diet. Immunity *42*, 133–144.
771 10.1016/j.immuni.2014.12.023.

772 13. Kierdorf, K., Hersperger, F., Sharrock, J., Vincent, C.M., Ustaoglu, P., Dou, J., Gyoergy, A., Groß,
773 O., Siekhaus, D.E., and Dionne, M.S. (2020). Muscle function and homeostasis require cytokine
774 inhibition of AKT activity in Drosophila. Elife *9*. 10.7554/eLife.51595.

775 14. Ayyaz, A., Li, H., and Jasper, H. (2015). Haemocytes control stem cell activity in the Drosophila
776 intestine. Nat. Cell Biol. *17*, 736–748. 10.1038/ncb3174.

777 15. Myers, A.L., Harris, C.M., Choe, K.-M., and Brennan, C.A. (2018). Inflammatory production of
778 reactive oxygen species by Drosophila hemocytes activates cellular immune defenses.
779 Biochemical and Biophysical Research Communications *505*, 726–732.
780 10.1016/j.bbrc.2018.09.126.

781 16. Fogarty, C.E., Diwanji, N., Lindblad, J.L., Tare, M., Amcheslavsky, A., Makhijani, K., Brückner, K.,
782 Fan, Y., and Bergmann, A. (2016). Extracellular Reactive Oxygen Species Drive Apoptosis-Induced
783 Proliferation via Drosophila Macrophages. Current Biology *26*, 575–584.
784 10.1016/j.cub.2015.12.064.

785 17. Chakrabarti, S., Dudzic, J.P., Li, X., Collas, E.J., Boquete, J.-P., and Lemaitre, B. (2016). Remote
786 Control of Intestinal Stem Cell Activity by Haemocytes in Drosophila. PLoS Genet *12*, e1006089.
787 10.1371/journal.pgen.1006089.

788 18. Chakrabarti, S., and Visweswariah, S.S. (2020). Intramacrophage ROS Primes the Innate Immune
789 System via JAK/STAT and Toll Activation. Cell Reports *33*, 108368. 10.1016/j.celrep.2020.108368.

790 19. Wu, S.-C., Liao, C.-W., Pan, R.-L., and Juang, J.-L. (2012). Infection-Induced Intestinal Oxidative
791 Stress Triggers Organ-to-Organ Immunological Communication in Drosophila. Cell Host &
792 Microbe *11*, 410–417. 10.1016/j.chom.2012.03.004.

793 20. Wang, M.C., Bohmann, D., and Jasper, H. (2003). JNK Signaling Confers Tolerance to Oxidative
794 Stress and Extends Lifespan in Drosophila. Developmental Cell *5*, 811–816. 10.1016/S1534-
795 5807(03)00323-X.

796 21. Cox, N., Crozet, L., Holtman, I.R., Loyher, P.-L., Lazarov, T., White, J.B., Mass, E., Stanley, E.R.,
797 Elemento, O., Glass, C.K., et al. (2021). Diet-regulated production of PDGFcc by macrophages
798 controls energy storage. Science *373*. 10.1126/science.abe9383.

799 22. Martelotto, L. (2020). 'Frankenstein' protocol for nuclei isolation from fresh and frozen tissue for
800 snRNAseq. 10.17504/PROTOCOLS.IO.3FKGJKW.

801 23. Hao, Y., Hao, S., Andersen-Nissen, E., Mauck, W.M., Zheng, S., Butler, A., Lee, M.J., Wilk, A.J.,
802 Darby, C., Zager, M., et al. (2021). Integrated analysis of multimodal single-cell data. Cell *184*,
803 3573-3587.e29. 10.1016/j.cell.2021.04.048.

804 24. Li, H., Janssens, J., De Waegeneer, M., Kolluru, S.S., Davie, K., Gardeux, V., Saelens, W., David,
805 F.P.A., Brbić, M., Spanier, K., et al. (2022). Fly Cell Atlas: A single-nucleus transcriptomic atlas of
806 the adult fruit fly. Science *375*, eabk2432. 10.1126/science.abk2432.

807 25. Cattenoz, P.B., Sakr, R., Pavlidaki, A., Delaporte, C., Riba, A., Molina, N., Hariharan, N.,
808 Mukherjee, T., and Giangrande, A. (2020). Temporal specificity and heterogeneity of Drosophila
809 immune cells. EMBO J *39*, e104486. 10.15252/embj.2020104486.

810 26. Tattikota, S.G., Cho, B., Liu, Y., Hu, Y., Barrera, V., Steinbaugh, M.J., Yoon, S.-H., Comjean, A., Li,
811 F., Dervis, F., et al. (2020). A single-cell survey of Drosophila blood. eLife *9*, e54818.
812 10.7554/eLife.54818.

813 27. Morales, A.J., Carrero, J.A., Hung, P.J., Tubbs, A.T., Andrews, J.M., Edelson, B.T., Calderon, B.,
814 Innes, C.L., Paules, R.S., Payton, J.E., et al. (2017). A type I IFN-dependent DNA damage response
815 regulates the genetic program and inflammasome activation in macrophages. eLife *6*, e24655.
816 10.7554/eLife.24655.

817 28. Jiang, H., Patel, P.H., Kohlmaier, A., Grenley, M.O., McEwen, D.G., and Edgar, B.A. (2009).
818 Cytokine/Jak/Stat Signaling Mediates Regeneration and Homeostasis in the Drosophila Midgut.
819 Cell *137*, 1343–1355. 10.1016/j.cell.2009.05.014.

820 29. Pastor-Pareja, J.C., Wu, M., and Xu, T. (2008). An innate immune response of blood cells to
821 tumors and tissue damage in Drosophila. Dis Model Mech *1*, 144–154; discussion 153.
822 10.1242/dmm.000950.

823 30. Karpac, J., Younger, A., and Jasper, H. (2011). Dynamic coordination of innate immune signaling
824 and Insulin signaling regulates systemic responses to localized DNA damage. Dev Cell *20*, 841–
825 854. 10.1016/j.devcel.2011.05.011.

826 31. Louradour, I., Sharma, A., Morin-Poulard, I., Letourneau, M., Vincent, A., Crozatier, M., and
827 Vanzo, N. (2017). Reactive oxygen species-dependent Toll/NF-κB activation in the Drosophila
828 hematopoietic niche confers resistance to wasp parasitism. eLife *6*, e25496.
829 10.7554/eLife.25496.

830 32. Paraquat administration in Drosophila for use in metabolic studies of oxidative stress (2011).
831 Analytical Biochemistry *419*, 345–347. 10.1016/j.ab.2011.08.023.

832 33. Jiang, H., Grenley, M.O., Bravo, M.-J., Blumhagen, R.Z., and Edgar, B.A. (2011). EGFR/Ras/MAPK
833 signaling mediates adult midgut epithelial homeostasis and regeneration in Drosophila. Cell Stem
834 Cell *8*, 84–95. 10.1016/j.stem.2010.11.026.

835 34. Patel, P.H., Pénalva, C., Kardorff, M., Roca, M., Pavlović, B., Thiel, A., Teleman, A.A., and Edgar,
836 B.A. (2019). Damage sensing by a Nox-Ask1-MKK3-p38 signaling pathway mediates regeneration
837 in the adult Drosophila midgut. Nat Commun *10*, 4365. 10.1038/s41467-019-12336-w.

838 35. Azad, P., Ryu, J., and Haddad, G.G. (2011). Distinct role of Hsp70 in Drosophila hemocytes during
839 severe hypoxia. Free Radic Biol Med *51*, 530–538. 10.1016/j.freeradbiomed.2011.05.005.

840 36. Huang, K., Chen, W., Zhu, F., Li, P.W.-L., Kapahi, P., and Bai, H. (2019). RiboTag translatomic
841 profiling of Drosophila oenocytes under aging and induced oxidative stress. BMC Genomics *20*,
842 50. 10.1186/s12864-018-5404-4.

843 37. Maitra, U., Scaglione, M.N., Chtarbanova, S., and O'Donnell, J.M. (2019). Innate immune
844 responses to paraquat exposure in a Drosophila model of Parkinson's disease. Sci Rep *9*, 12714.
845 10.1038/s41598-019-48977-6.

846 38. Donovan, M.R., and Marr, M.T. (2016). dFOXO Activates Large and Small Heat Shock Protein
847 Genes in Response to Oxidative Stress to Maintain Proteostasis in Drosophila*. Journal of
848 Biological Chemistry *291*, 19042–19050. 10.1074/jbc.M116.723049.

849 39. Khan, C., Muliyil, S., and Rao, B.J. (2019). Genome Damage Sensing Leads to Tissue Homeostasis
850 in Drosophila. Int Rev Cell Mol Biol *345*, 173–224. 10.1016/bs.ircmb.2018.12.001.

851 40. Dunphy, G., Flannery, S.M., Almine, J.F., Connolly, D.J., Paulus, C., Jønsson, K.L., Jakobsen, M.R.,
852 Nevels, M.M., Bowie, A.G., and Unterholzner, L. (2018). Non-canonical Activation of the DNA
853 Sensing Adaptor STING by ATM and IFI16 Mediates NF-κB Signaling after Nuclear DNA Damage.
854 Mol Cell *71*, 745-760.e5. 10.1016/j.molcel.2018.07.034.

855 41. Bednarski, J.J., and Sleckman, B.P. (2019). At the intersection of DNA damage and immune
856 responses. Nat Rev Immunol *19*, 231–242. 10.1038/s41577-019-0135-6.

857 42. Yang, H., Kronhamn, J., Ekström, J., Korkut, G.G., and Hultmark, D. (2015). JAK/STAT signaling in
858 Drosophila muscles controls the cellular immune response against parasitoid infection. EMBO
859 Rep *16*, 1664–1672. 10.15252/embr.201540277.

860 43. Dionne, M.S., Pham, L.N., Shirasu-Hiza, M., and Schneider, D.S. (2006). Akt and FOXO
861 dysregulation contribute to infection-induced wasting in Drosophila. Curr Biol *16*, 1977–1985.
862 10.1016/j.cub.2006.08.052.

863 44. Yang, H., and Hultmark, D. (2016). Tissue communication in a systemic immune response of
864 Drosophila. Fly (Austin) *10*, 115–122. 10.1080/19336934.2016.1182269.

865 45. Young, M.D., and Behjati, S. (2020). SoupX removes ambient RNA contamination from droplet-
866 based single-cell RNA sequencing data. Gigascience *9*, giaa151. 10.1093/gigascience/giaa151.

867 46. McGinnis, C.S., Murrow, L.M., and Gartner, Z.J. (2019). DoubletFinder: Doublet Detection in
868 Single-Cell RNA Sequencing Data Using Artificial Nearest Neighbors. Cell Syst *8*, 329-337.e4.
869 10.1016/j.cels.2019.03.003.

870 47. Blighe, K. (2021). EnhancedVolcano: publication-ready volcano plots with enhanced colouring
871 and labeling.

872 48. Aibar, S., González-Blas, C.B., Moerman, T., Huynh-Thu, V.A., Imrichova, H., Hulselmans, G.,
873 Rambow, F., Marine, J.-C., Geurts, P., Aerts, J., et al. (2017). SCENIC: single-cell regulatory
874 network inference and clustering. Nat Methods *14*, 1083–1086. 10.1038/nmeth.4463.

875 **Figure Legends**

876

877 **Figure 1. Loss of hemocytes increases the susceptibility of adult Drosophila to oxidative stress by**
878 **Paraquat feeding.** (A) Survival of *Hml/+* flies with control food (n=20) and 15mM Paraquat (n=28) at
879 29°C. Five independent experiments were performed. Student's unpaired t-test: ****p<0.0001, each
880 data point represents a sample with 10 flies. (B-C) RTqPCR of whole flies were performed to investigate
881 gene-expressions of the JAK-STAT-signaling pathway (B) and insulin-signaling pathway (C). All
882 transcript levels were normalized to the expression of the loading control *Rpl1* and are shown in
883 arbitrary units [au]. Each data point (n=5) represents a sample of three whole flies. Student's unpaired
884 t-tests were performed for each transcript to compare the gene-expression between control and
885 treated flies: **p<0.01; ***p<0.001; ****p<0.0001. (D) Glucose and (E) glycogen levels of whole flies
886 were measured in control and PQ-treated flies. Each dot (n=3) represents a sample containing three
887 flies. Student's unpaired t-test: **p<0.01. (F) Triglyceride (TG) amounts were determined via thin-layer
888 chromatography. Student's unpaired t-test: **p<0.01. (G) Representative images of 7 day old
889 *HmlΔ4>eGFP* flies treated with 5% sucrose solution and 15mM PQ respectively. Scale bars = 500µm.
890 (H) Hemocyte quantification of 7 day old *HmlΔ4>eGFP* flies treated with control food (5% sucrose
891 solution) (n=5) or 15mM Paraquat (n=5). Each data point represents one fly. Statistical significance was
892 tested using student's unpaired t-test: p=0.508. (I) Survival of *crq-Gal80^{ts}/+* control flies (n=13) and
893 hemocyte depleted *crq-Gal80^{ts}>reaper* flies (n=7) on control food (n=20) and 15mM Paraquat (n=28)
894 at 29°C. Student's unpaired t-test: ****p<0.0001, each data point represents a sample with 10 flies.

895 **Figure 2. Unbiased single nuclei transcriptomic profiling identified diverse transcriptomic states of**
896 **hemocytes associated with oxidative stress response.** (A) Uniform Manifold Approximation and
897 Projection (UMAP) visualization of single nucleus states from flies exposed to 15mM PQ containing or
898 control food. Dashed lines indicate the broad cell types. Male accessory gland main cells (MAG),
899 Malpighian tubule principal cells (MTC), male germline cells (MGC), outer photoreceptor cells (PRC),
900 tracheolar cells (TC), epithelial cells (EC). Colors indicate distinct clusters. n=11839 nuclei are shown.
901 (B) UMAP visualization of nuclei from **A** colored by treatment. Nuclei from control group are labeled
902 in red and nuclei from PQ group are labeled in blue. Dashed lines indicate the broad cell type as **A**. (C)
903 UMAP visualization of hemocytes from **A** after sub-setting and re-clustering. Colors and dashed lines
904 indicate distinct clusters. n=1354 nuclei are shown. (D) UMAP visualization of hemocytes clusters
905 colored by treatment. Nuclei from control group are labeled in red and nuclei from PQ group are
906 labeled in blue. Dashed lines indicate distinct clusters. n=1354 nuclei are shown. (E) Heat map of 20
907 genes enriched in each hemocytes cluster. Gene names are indicated on the left. Colors in the heat
908 map correspond to normalized scaled expression. (F) Volcano plots comparing pseudo bulk gene
909 expression of individual hemocytes cluster vs all remaining hemocytes. The $-\log_{10}$-transformed
910 adjusted P value (P adjusted, y-axis) is plotted against the $\log_2$-transformed fold change (FC) in
911 expression between the indicated cluster vs remaining hemocytes (x-axis). Genes under $\log_2$ FC and –
912 Log_{10} P value cut off are shown in grey (NS). Genes above $\log_2$ FC but under P value cut off in green,
913 Genes under $\log_2$ FC and above $-\text{Log}_{10}$ P value cut off are shown in blue and genes above $\log_2$ FC and –
914 Log_{10} P value cut off are shown in red.

915 **Figure 3: A specific cluster of plasmatocytes responds to oxidative stress with immune activation by**
916 **Jak/STAT, DDR and JNK signaling.** (A) Key transcription factors (TFs) regulating hemocytes states. Heat
917 map of scaled TF activity at a single cell level in hemocytes states from **Figure 2C**. Colors in the heat
918 map correspond to scaled expression. Numbers on top indicate the cluster identity. Labels on the left
919 and right indicate the TFs. (B) Feature plots showing scaled expression of selected genes associated

920 with JAK/STAT signaling (*upd3*, *Socs36E*, *TotA*, *TotM*, *Fas3*), JNK and DNA damage signaling (*puc*,
921 *Gadd45*), insulin signaling (*Thor*, *InR*), TGFβ signaling (*dpp*, *daw*) and TNF signaling (*egr*).

922 **Figure 4**: **Loss of non-canonical DNA damage signaling activity in hemocytes leads to an increase in**
923 **systemic *upd3* levels and a higher susceptibility to oxidative stress**. (A) Survival of *Hml/+* (n= 28),
924 *Hml>mei41-IR (n*= 23); *Hml>tefu-IR (n*= 24); *Hml>mei41-IR,tefu-IR (n*= 16) and *Hml>nbs-IR* (n= 22) flies
925 on control food and PQ. Each data point represents a sample of 10 flies. Mean ± SEM is shown. Three
926 independent experiments were performed. One-way ANOVA: ****p<0.001*; *****p<0.0001*. (B)
927 Hemocyte quantification of *Hml/+* control flies and DDR-knockdowns on control food (C) and 15mM
928 Paraquat (P). Each data point represents one fly (n=5 for all groups). Mean ± SEM is shown. One way
929 ANOVA: *Hml/+* (C) vs *Hml>tefu-IR* (C), ***p=0.0052*; *Hml>tefu-IR* (C) vs *Hml>tefu-IR* (P), **p=0.03* (C)
930 Comet assay of isolated hemocytes from *Hml/+* (C: n=73; P: n=129), *Hml>mei41-IR* (C: n=119; P: n=132)
931 and *Hml>tefu-IR* (C: n=175; P: n=125) - flies on control food and PQ. Olive tail moment of comet assays
932 of sorted hemocyte nuclei is shown. One-way ANOVA: *p<0.05; ***p<0.001; ****p<0.0001. (D) Gene
933 expression analysis for *Jak/STAT* target genes via RT-qPCR in *Hml/+* control flies and DDR-knockdowns
934 on control food (C) and 15mM Paraquat (P). All transcript levels were normalized to the expression of
935 the loading control *Rpl1* and are shown in arbitrary units [au]. Each data point (n=5) represents a
936 sample of three individual flies. Mean ± SEM is shown. Two-way ANOVA: **p<0.05*; ***p<0.01*; ***
937 *p<0.001*; *****p<0.0001*. (E) Gene expression analysis for insulin signaling target genes and *Ilps* via RT-
938 qPCR in *Hml/+* control flies and DDR-knockdowns on control food (C) and 15mM Paraquat (P). All
939 transcript levels were normalized to the expression of the loading control *Rpl1* and are shown in
940 arbitrary units [au]. Each data point (n=5) represents a sample of three individual flies. Mean ± SEM is
941 shown. Two-way ANOVA: **p<0.05*; ***p<0.01*; *** *p<0.001*; *****p<0.0001*. (F) Triglyceride (TG) levels
942 of *Hml/+*, *Hml>mei41-IR*, *Hml>tefu-IR, Hml>mei41-IR,tefu-IR* and *Hml>nbs-IR* flies on control food and
943 PQ determined via thin-layer chromatography (TLC). One representative TLC is shown (left panel).
944 Quantification thereof is shown on the right. Each data point (n=4 per group) represents a sample of
945 ten individual flies. Mean ± SEM is shown. n.d. = not detectable. One-way ANOVA was performed for
946 both groups (15mM PQ and control) separately: **p=0.0106*.

947 **Figure 5: Hemocyte-derived *upd3* controls susceptibility to oxidative stress in adult *Drosophila***. (A)
948 Survival of *Hml/+* (n=28), *Hml>upd3-IR* (n=27) and *Hml>upd3* (n=26) flies on 15mM PQ food. Each data
949 point represents a sample of 10-15 flies. Mean ± SEM is shown. Three independent experiments were
950 performed. One-way ANOVA: *****p<0.0001*. (B) Gene expression analysis for *upd3* via RT-qPCR in
951 *Hml/+, Hml>upd3-IR* and *Hml>upd3* flies on control food (-) and 15mM Paraquat (+). Each data point
952 (n=5-6) represents a sample of three individual flies. Mean ± SEM is shown. Two-way ANOVA:
953 *****p<0.0001*. (C) Hemocyte quantifications in *Hml/+, Hml>upd3-IR* and *Hml>upd3* flies on control
954 food and 15mM PQ food. Each data point represents one fly (n= 5-6). Mean ± SEM is shown. One-way
955 ANOVA: **p<0.01. (D) Survival of w^{1118} (n=17), *Hml/+* (n=16), $upd3^{null}$ (n=11) *and* $upd3^{null}$*;Hml>upd3*
956 flies (n=16) on 15mM PQ food at 29°C. Each data point represents a sample with 10-15 flies. Mean ±
957 SEM is shown. One-way ANOVA: *****p<0.0001*. (E) Survival of *Hml/+* (n=78), *Hml>hep[act]* (n=38) and
958 *Hml>bsk-DN* (n=80) flies on 15mM PQ food. Each data point represents a sample with 10 flies. Mean ±
959 SEM is shown. One-way ANOVA: ***p<0.01*; *****p<0.0001*. (F) Gene expression analysis for *upd3* via
960 RT-qPCR of *Hml/+*, *Hml>hep[act]* and *Hml>bsk-DN* flies on control food (-) and 15mM Paraquat (+).
961 Each data point (n=5-6) represents a sample of three individual flies. Mean ± SEM is shown. Two-way
962 ANOVA: **p<0.05.*

963

964 **Supplementary Figure Legends**
965
966 **Figure S1: Paraquat-induced oxidative stress does not cause gut leakage, but detrimental changes in**
967 **triglyceride storage in the fat body.** (A) Survival of *Hml/+* flies treated with control food (n=8), 2mM
968 PQ (n=8), 15mM PQ (n=9) and 30mM PQ (n=8). Each data point represents a sample of 10 flies. Mean
969 ± SEM is shown. One-way ANOVA: ***p<0.01*; ****p<0.0001*. (B) Smurf assay to test the gut integrity
970 of 7 day old *Hml/+* flies treated with 2mM PQ (n=79), 15mM PQ (n=90), 30mM PQ (n=80) and controls
971 (n=80). Data was pooled from two independent experiments. (C) Gene expression analysis for *AMP*
972 genes via RT-qPCR in whole flies on control food (C) and 15mM Paraquat (P). All transcript levels were
973 normalized to the expression of the loading control *Rpl1* and are shown in arbitrary units [au]. Each
974 data point (n=5) represents a sample of three individual flies. Mean ± SEM is shown. (D) Gene
975 expression analysis for *dpp*, *daw* and *eiger* via RT-qPCR in whole flies on control food (C) and 15mM
976 Paraquat (P). All transcript levels were normalized to the expression of the loading control *Rpl1* and
977 are shown in arbitrary units [au]. Each data point (n=5) represents a sample of three individual flies.
978 Mean ± SEM is shown. (E) Representative light microscopic images of HE stained control flies (left
979 panels) and flies treated with 15mM PQ (right panels). Inserts indicate location of higher magnification
980 images below. Scale bar (overview) = 500 µm, scale bar (inserts) = 100 µm.

981 **Figure S2: Gating strategy for the FACS isolation of nuclei from control and PQ-treated flies.** (A) Flow
982 cytometric sorting strategy of nuclei used for the snRNA-seq. Doublet exclusion was performed via
983 gating on DRAQ7 single positive nuclei. $DRAQ7^{+}DAPI^{+}$ double positive events were considered to be
984 nuclei and were sorted for the snRNA-seq. (B) Violin plot indicating number of genes identified in
985 analyzed nuclei of the sorted samples. Color code is indicated in legend. (C) Violin plot indicating RNA
986 counts of the analyzed nuclei of each sorted sample. Color code is indicated in legend. (D) Violin plot
987 indicating percentage of mitochondrial genes detected in the nuclei of each sorted samples. Color code
988 is indicated in legend.

989 **Figure S3: Specific signature genes identify plasmatocyte and crystal cell clusters within the eight**
990 **identified hemocyte clusters.** (A) Dot plot of hemocyte signature gene-expression according to
991 Cattenoz et al[25]. Color code is indicated in legend. (B)-(L) Feature plots for expression levels of
992 respective hemocyte signature genes across all hemocyte clusters. Color-code, indicating the
993 expression levels of the respective genes, is shown on the right side of each graph. Gene names are
994 indicated above plots shown. (M) Bar plot representing distribution of nuclei derived from flies under
995 control condition (red) and flies treated with 15mM PQ (turquoise) across all eight identified hemocyte
996 clusters. Each cluster is shown as one bar. Total number of hemocytes in the respective cluster is
997 indicated below.

998 **Figure S4: PQ treatment of S2 cells *in vitro* induces reactive oxygen species, immune activation and**
999 **DNA damage.** (A) Gating strategy of flow cytometric analysis of control or PQ-treated S2-cells stained
1000 for reactive oxygen species (ROS) with CellROX. Control cells, 15mM PQ treated and 30mM PQ treated
1001 cells are shown in the first, second and third row respectively. After doublet exclusion, dead cells were
1002 excluded via DAPI staining. The amount of ROS was determined in the last gate were the CellROX
1003 staining is shown. (B) Representative FACS histograms of cells treated with PQ and analyzed via CellROX
1004 staining. Gates indicate the cut-off for determining $CellROX^{+}$ cells. (C) Mean fluorescence intensity
1005 (MFI) of FACS analyzed, $CellROX^{+}$ cells. Data were generated from three independent experiments
1006 (n=3). One-way ANOVA: **p<0.05; **p<0.01; ***p<0.001; ****p<0.0001*. (D) Comet assay of S2 cells
1007 treated without PQ (n=351), 5mM PQ (n=208), 10mM PQ (n=129) and 15mM PQ (n=71). Assay was

1008 performed in two independent experiments. Data of one representative assay are shown as violin plots
1009 with median (red), second and third quartile. One-way ANOVA: ****p<0.001; ****p>0.0001*. (E-F) Gene
1010 expression analysis of genes associated with JAK-STAT signaling, JNK signaling, insulin signaling is
1011 shown in (E) and TGFβ signaling and AMPs is shown in (F). S2-cells treated with 15mM PQ for six or 24
1012 hours. Controls were untreated. Each dot represents a sample containing RNA of 50.000 cells. One-
1013 way ANOVA: **p<0.05; **p<0.01; ***p<0.001; ****p<0.0001*.

1014 **Figure S5: Loss of DNA damage, upd3 or JNK signaling in hemocytes alters susceptibility to oxidative**
1015 **stress but not overall lifespan.** (A) Representative images of *Hml/+* flies and DDR-Knockdown flies on
1016 control food (left panels) and treated with 15mM PQ (right panels). Five individual flies per group were
1017 analyzed. (B) Lifespan analysis of *Hml/+* (n=251), *Hml>mei-41-IR* (n=231), *Hml>tefu-IR* (n=219),
1018 *Hml>mei-41-IR;tefu-IR* (n=144) and *Hml>nbs-IR* flies (n=299). *Hml/+* vs. *Hml>mei-41-IR*: Log-rank test
1019 *****p<0.0001*, X^2=172.2; Wilcoxon test *****p<0.0001*, X^2=155.9. *Hml/+* vs. *Hml>tefu-IR*: Log-rank test
1020 *****p<0.0001*, X^2=56.09; Wilcoxon test *****p<0.0001*, X^2=50.95. *Hml/+* vs. *Hml>mei-41-IR;tefu-IR*:
1021 Log-rank test ns, X^2=3.1; Wilcoxon test ****p=0.0005*, X^2=12.11. *Hml/+* vs *Hml>nbs-IR*: Log-rank test
1022 *****p<0.0001*, X^2=60.90; Wilcoxon test *****p<0.0001*, X^2=50.21. Data was obtained from three
1023 independent experiments. (C) Starvation survival of *Hml/+* (n=607), *Hml>mei-41-IR* (n=421), *Hml>tefu-*
1024 *IR* (n=480), *Hml>mei-41-IR;tefu-IR* (n=266) and *Hml>nbs-IR* (n=341) flies. *Hml/+* vs. *Hml>mei-41-IR*: Log-
1025 rank test ***p=0.0052*, X^2=7.81; Wilcoxon test ns, X^2=0.02. *Hml/+* vs. *Hml>tefu-IR*: Log-rank test ns,
1026 X^2=0.03; Wilcoxon test **p=0.0153*, X^2=5.88. *Hml/+* vs. *Hml>mei-41-IR;tefu-IR*: Log-rank test ns, X^2=0.21;
1027 Wilcoxon test **p=0.019*, X^2=5.51. *Hml/+* vs *Hml>nbs-IR*: Log-rank test ****p=0.0003*, X^2=13.30; Wilcoxon
1028 test ns, X^2=1.24. Data was obtained from two independent experiments. (D) Lifespan analysis of *Hml-*
1029 *Gal80^{ts}/+* (n=127), *Hml-Gal80^{ts}>mei-41-IR* (n=140), *Hml-Gal80^{ts}>tefu-IR* (n=164), *Hml-Gal80^{ts}>mei-41-*
1030 *IR;tefu-IR* (n=101) and *Hml-Gal80^{ts}>nbs-IR* flies (n=157). *Hml-Gal80^{ts}/+* vs. *Hml-Gal80^{ts}>mei-41-IR*: Log-
1031 rank test *****p<0.0001*, chi^2=21.80; Wilcoxon test *****p<0.0001*, X^2=18.48. *Hml-Gal80^{ts}/+* vs. *Hml-*
1032 *Gal80^{ts}>tefu-IR*: Log-rank test ****p=0.0003*, X^2=13.20; Wilcoxon test **p=0.033*, X^2=4.56. *Hml-Gal80^{ts}/+*
1033 vs. *Hml-Gal80^{ts}>mei-41-IR;tefu-IR*: Log-rank test **p=0.0429*, X^2=4.10; Wilcoxon test ****p=0.0001*,
1034 X^2=14.95. *Hml-Gal80^{ts}/+* vs *Hml-Gal80^{ts}>nbs-IR*: Log-rank test ***p=0.0047*, X^2=7.99; Wilcoxon test ns,
1035 X^2=1.68. Data was obtained from five independent experiments. (E) Survival of *Hml-Gal80^{ts}/+* (n=23),
1036 *Hml-Gal80^{ts}>mei-41-IR* (n=28), *Hml-Gal80^{ts}>tefu-IR* (n=18), *Hml-Gal80^{ts}>mei-41-IR;tefu-IR* (n=13) and
1037 *Hml-Gal80^{ts}>nbs-IR* flies (n=31) on PQ food. Each dot represents a sample with ten flies. Mean ± SEM
1038 is shown. One-way ANOVA **p<0.05*; *****p<0.0001*. Data was obtained from five independent
1039 experiments. (F) Lifespan analysis of *Hml/+ (n=266), Hml>upd3-IR (n=269),* and *Hml>upd3* flies (n=193).
1040 *Hml/+* vs. *Hml>upd3-IR*: Log-rank test *****p<0.0001*, X^2=96.03; Wilcoxon test *****p<0.0001*, X^2=81.16.
1041 *Hml/+* vs. *Hml>upd3*: Log-rank test *****p<0.0001*, X^2=15.33; Wilcoxon test **p=0.0124*, X^2=6.26. Results
1042 are shown from two independent experiments. (G) Representative images of *Hml/+, Hml>upd3-IR* and
1043 *Hml>upd3* flies on control food (left panels) and treated with 15mM PQ (right panels). Six individual
1044 flies per group were analyzed. (H) Lifespan analysis of *Hml/+* (n=281), *Hml>hep[act]* (n=117), and
1045 *Hml>bsk-DN* (n=273) flies. *Hml/+* vs. *Hml>hep[act]*; Log-rank test: n.s.; p=0.69, X^2=0.16; Wilcoxon test:
1046 n.s. p=0.18, X^2=1.77. *Hml/+* vs. *Hml>bsk-DN*: Log-rank test: *****p<0.0001*, X^2=25.31; Wilcoxon test:
1047 *****p<0.0001*, X^2=23.61. Data was obtained from two independent experiments.

1048 **Table S1: Differentially expressed genes in hemocyte clusters C1-C8.**

1049 **Table S2: Transgenic *Drosophila* lines and primers used in the study.**

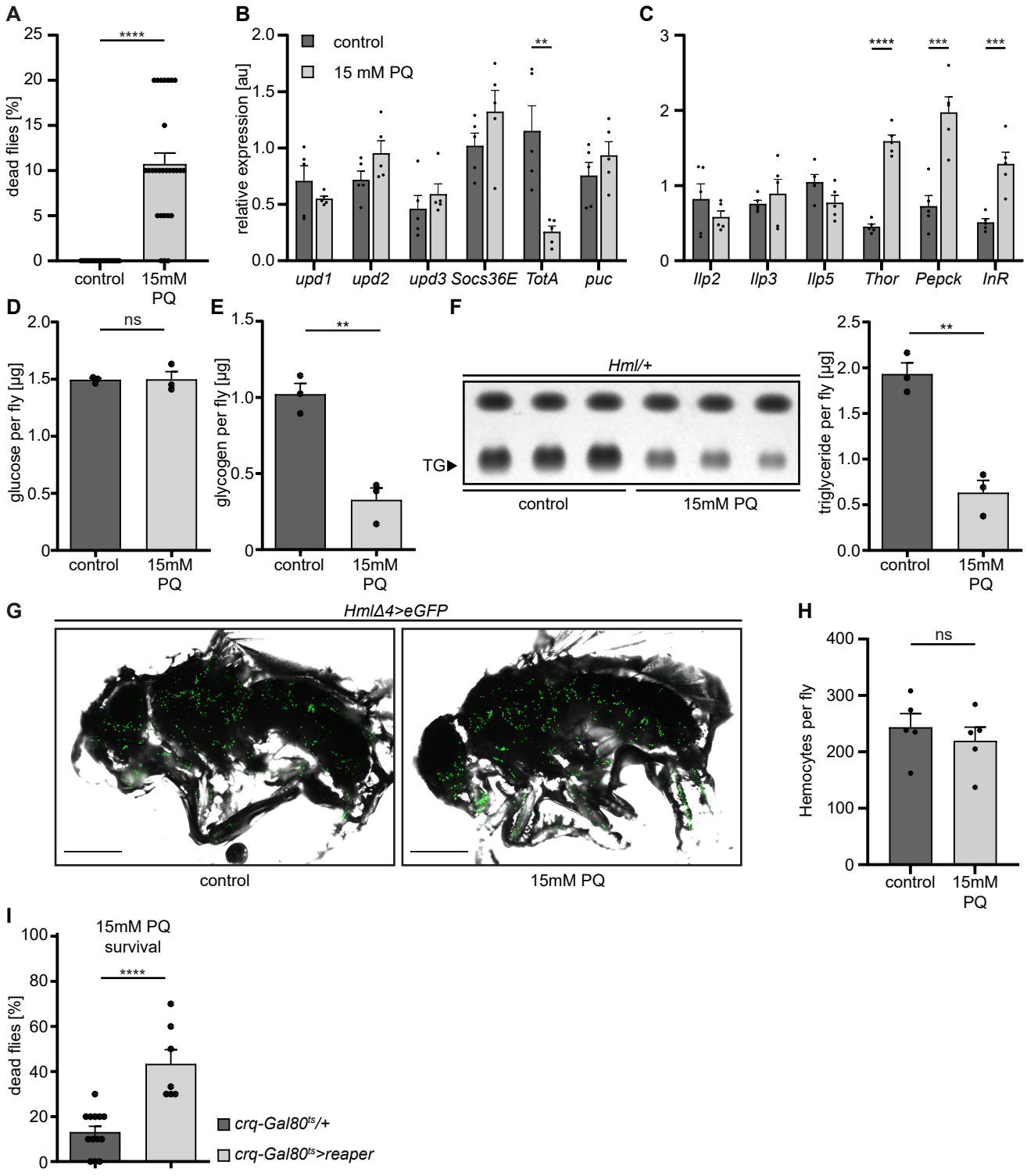
A
dead flies [%]
****
control
15mM PQ
B
relative expression [au]
control
15 mM PQ
**
upd1
upd2
upd3
Socs36E
TotA
puc
C
****
***
***
Ilp2
Ilp3
Ilp5
Thor
Pepck
InR
D
glucose per fly [µg]
ns
control
15mM PQ
E
glycogen per fly [µg]
**
control
15mM PQ
F
Hml/+
TG
control
15mM PQ
triglyceride per fly [µg]
**
control
15mM PQ
G
HmlΔ4>eGFP
control
15mM PQ
H
Hemocytes per fly
ns
control
15mM PQ
I
15mM PQ survival
dead flies [%]
****
crq-Gal80ts/+
crq-Gal80ts>reaper

Figure 1

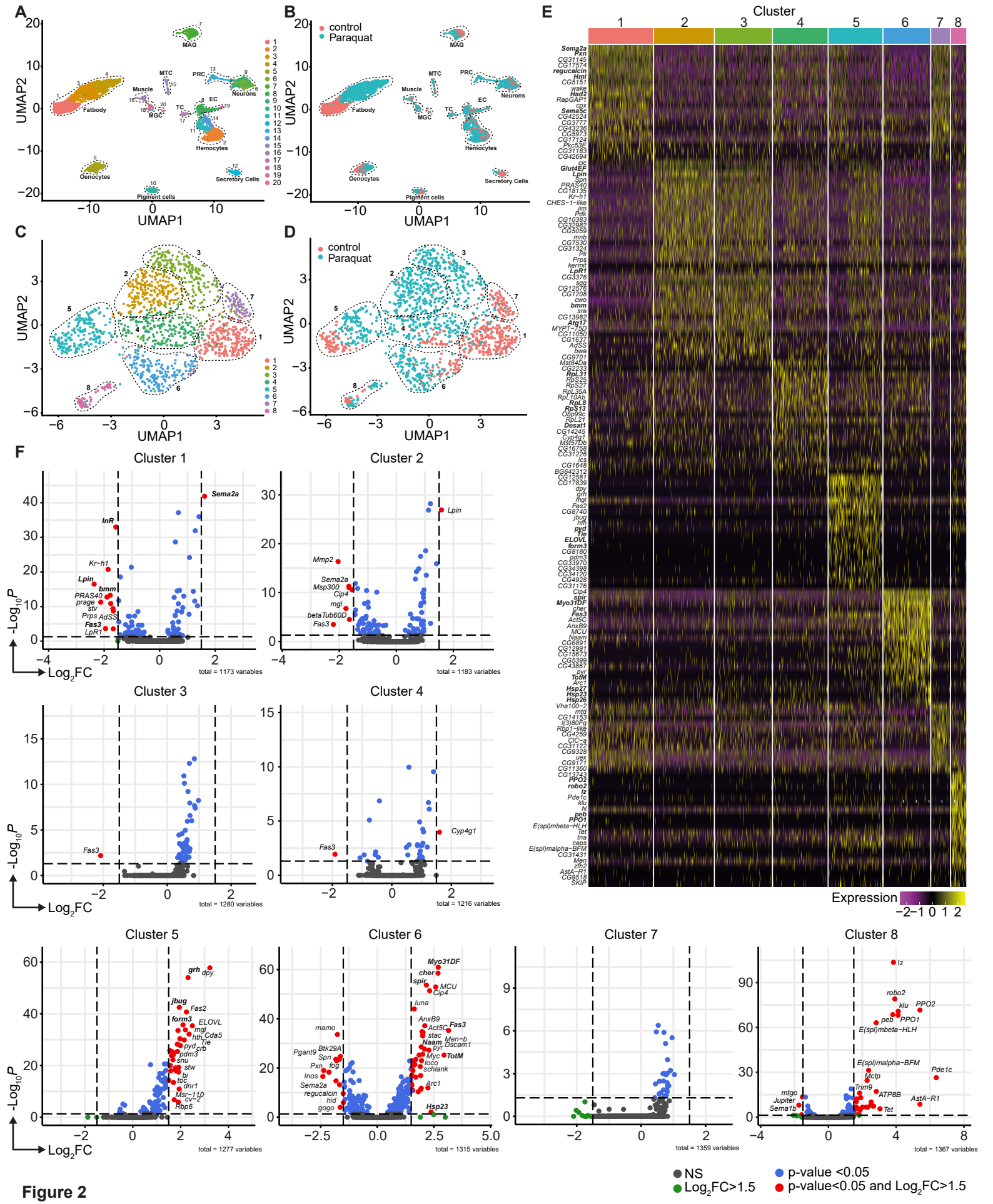
A
B
C
D
E
F
UMAP1
UMAP2
control
Paraquat
MAG
Muscle
MTC
PRC
Neurons
Fatbody
MGC
TC
EC
Hemocytes
Oenocytes
Secretory Cells
Pigment cells
Cluster
Expression
Cluster 1
Cluster 2
Cluster 3
Cluster 4
Cluster 5
Cluster 6
Cluster 7
Cluster 8
-Log10P
Log2FC
total = 1173 variables
total = 1183 variables
total = 1280 variables
total = 1216 variables
total = 1277 variables
total = 1315 variables
total = 1359 variables
total = 1367 variables
NS
Log2FC>1.5
p-value <0.05
p-value<0.05 and Log2FC>1.5

Figure 2

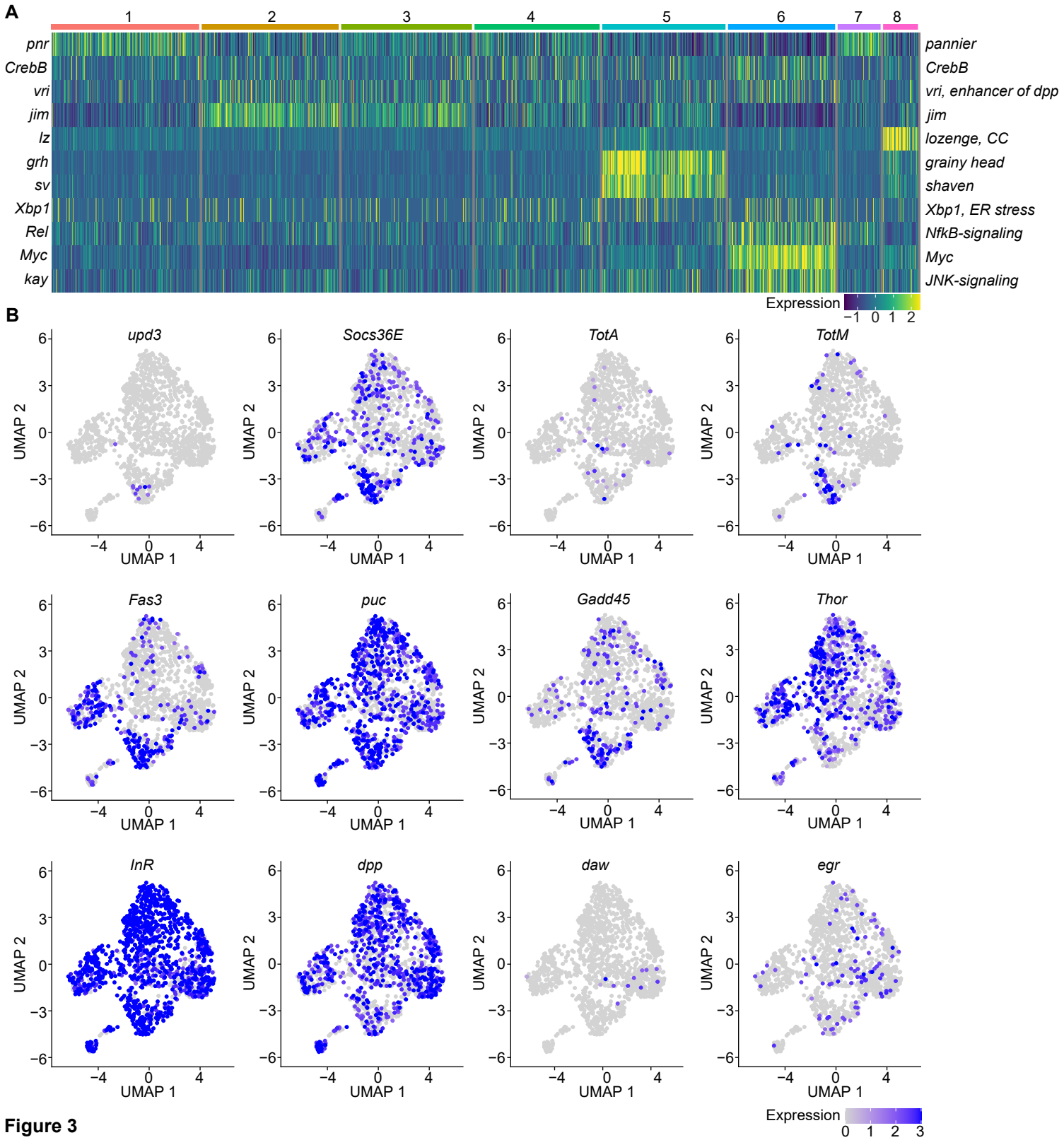
A
1
2
3
4
5
6
7
8
pnr
CrebB
vri
jim
lz
grh
sv
Xbp1
Rel
Myc
kay
pannier
CrebB
vri, enhancer of dpp
jim
lozenge, CC
grainy head
shaven
Xbp1, ER stress
NfkB-signaling
Myc
JNK-signaling
Expression
−1 0 1 2
B
upd3
Socs36E
TotA
TotM
Fas3
puc
Gadd45
Thor
InR
dpp
daw
egr
UMAP 1
UMAP 2
Expression
0 1 2 3

Figure 3

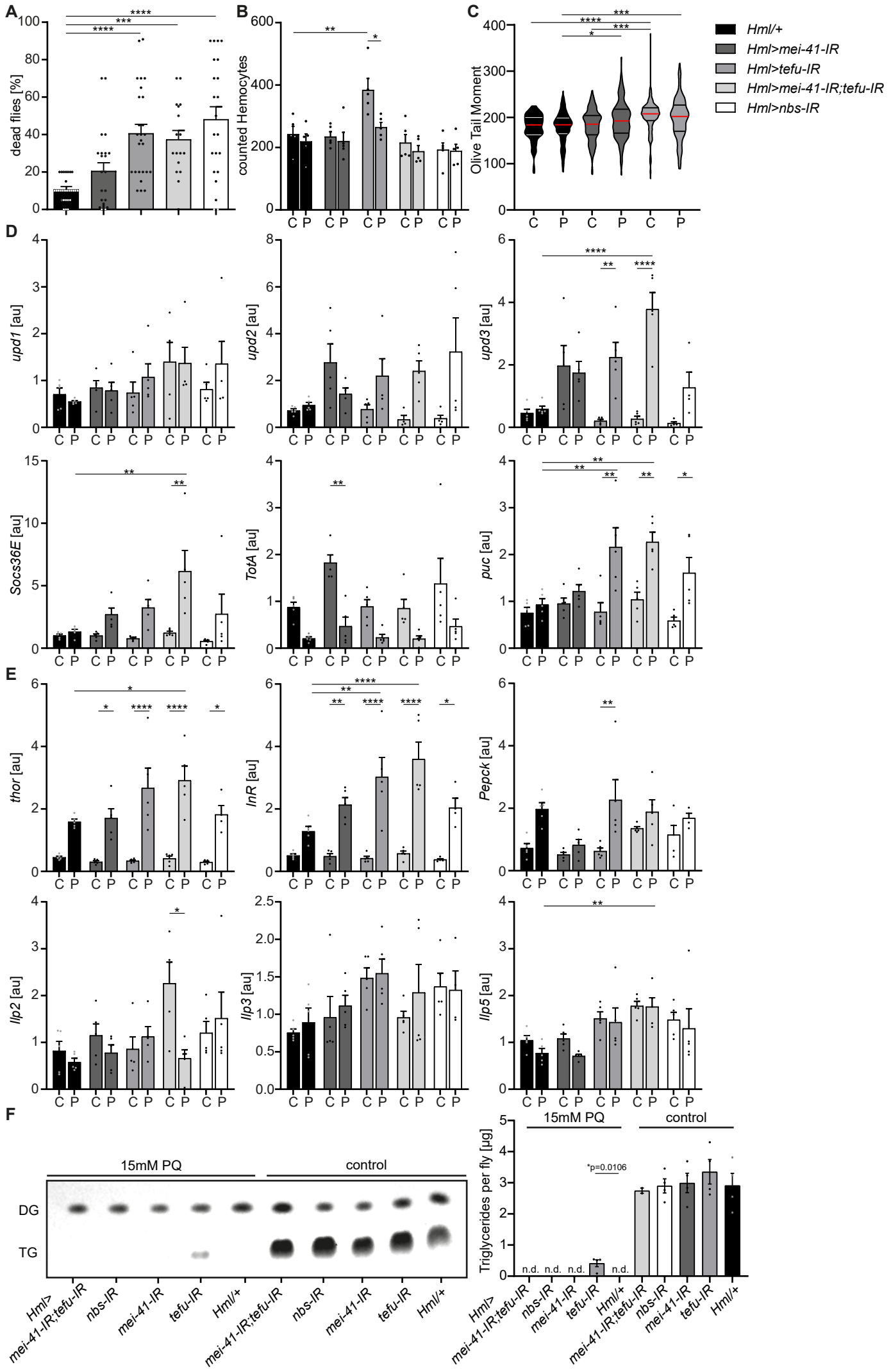
A
dead flies [%]
B
counted Hemocytes
C
Olive Tail Moment
Hml/+
Hml>mei-41-IR
Hml>tefu-IR
Hml>mei-41-IR;tefu-IR
Hml>nbs-IR
D
upd1 [au]
upd2 [au]
upd3 [au]
Socs36E [au]
TotA [au]
puc [au]
E
thor [au]
InR [au]
Pepck [au]
Ilp2 [au]
Ilp3 [au]
Ilp5 [au]
F
15mM PQ
control
DG
TG
Triglycerides per fly [µg]
*p=0.0106
n.d.
Hml>mei-41-IR;tefu-IR
nbs-IR
mei-41-IR
tefu-IR
Hml/+

Figure 4

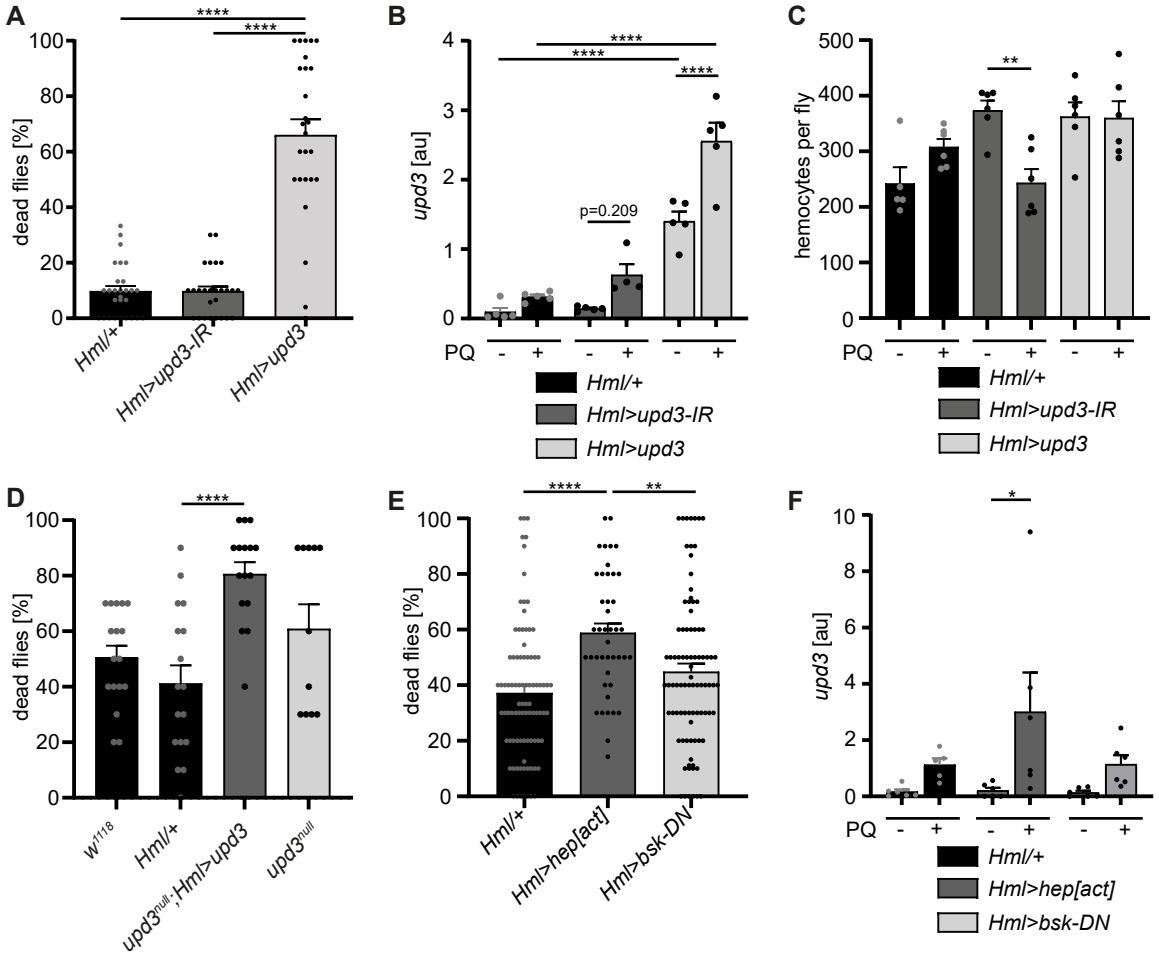
A
dead flies [%]
Hml/+
Hml>upd3-IR
Hml>upd3
B
upd3 [au]
p=0.209
PQ
Hml/+
Hml>upd3-IR
Hml>upd3
C
hemocytes per fly
PQ
Hml/+
Hml>upd3-IR
Hml>upd3
D
dead flies [%]
w1118
Hml/+
upd3null;Hml>upd3
upd3null
E
dead flies [%]
Hml/+
Hml>hep[act]
Hml>bsk-DN
F
upd3 [au]
PQ
Hml/+
Hml>hep[act]
Hml>bsk-DN

Figure 5

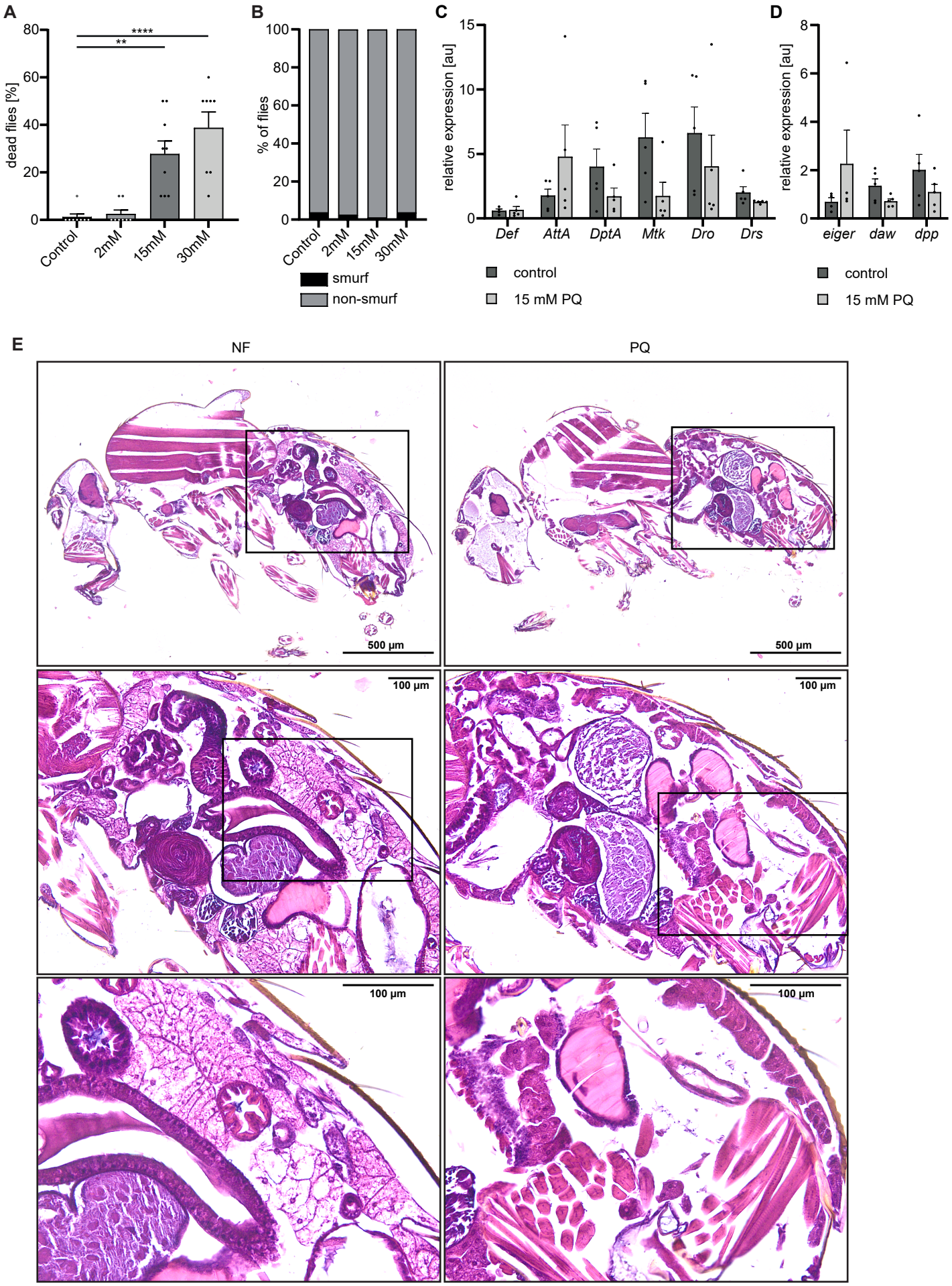
A
dead flies [%]
80
60
40
20
0
****
**
Control
2mM
15mM
30mM
B
% of flies
100
80
60
40
20
0
Control
2mM
15mM
30mM
smurf
non-smurf
C
relative expression [au]
15
10
5
0
Def
AttA
DptA
Mtk
Dro
Drs
control
15 mM PQ
D
relative expression [au]
8
6
4
2
0
eiger
daw
dpp
control
15 mM PQ
E
NF
PQ
500 µm
500 µm
100 µm
100 µm
100 µm
100 µm

Figure S1

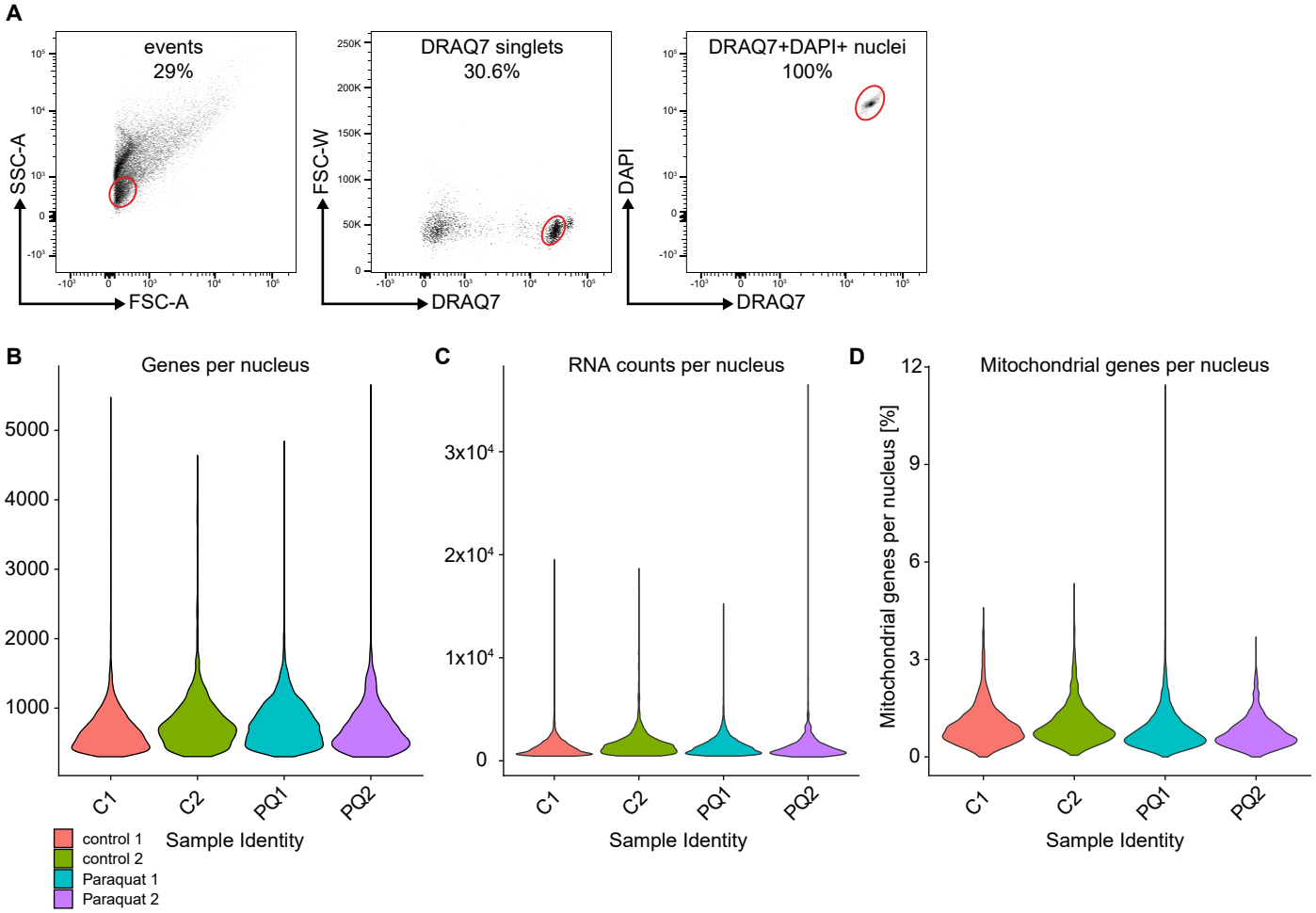
A
events
29%
SSC-A
FSC-A
DRAQ7 singlets
30.6%
FSC-W
DRAQ7
DRAQ7+DAPI+ nuclei
100%
DAPI
DRAQ7
B
Genes per nucleus
C
RNA counts per nucleus
D
Mitochondrial genes per nucleus
Mitochondrial genes per nucleus [%]
C1
C2
PQ1
PQ2
Sample Identity
control 1
control 2
Paraquat 1
Paraquat 2

Figure S2

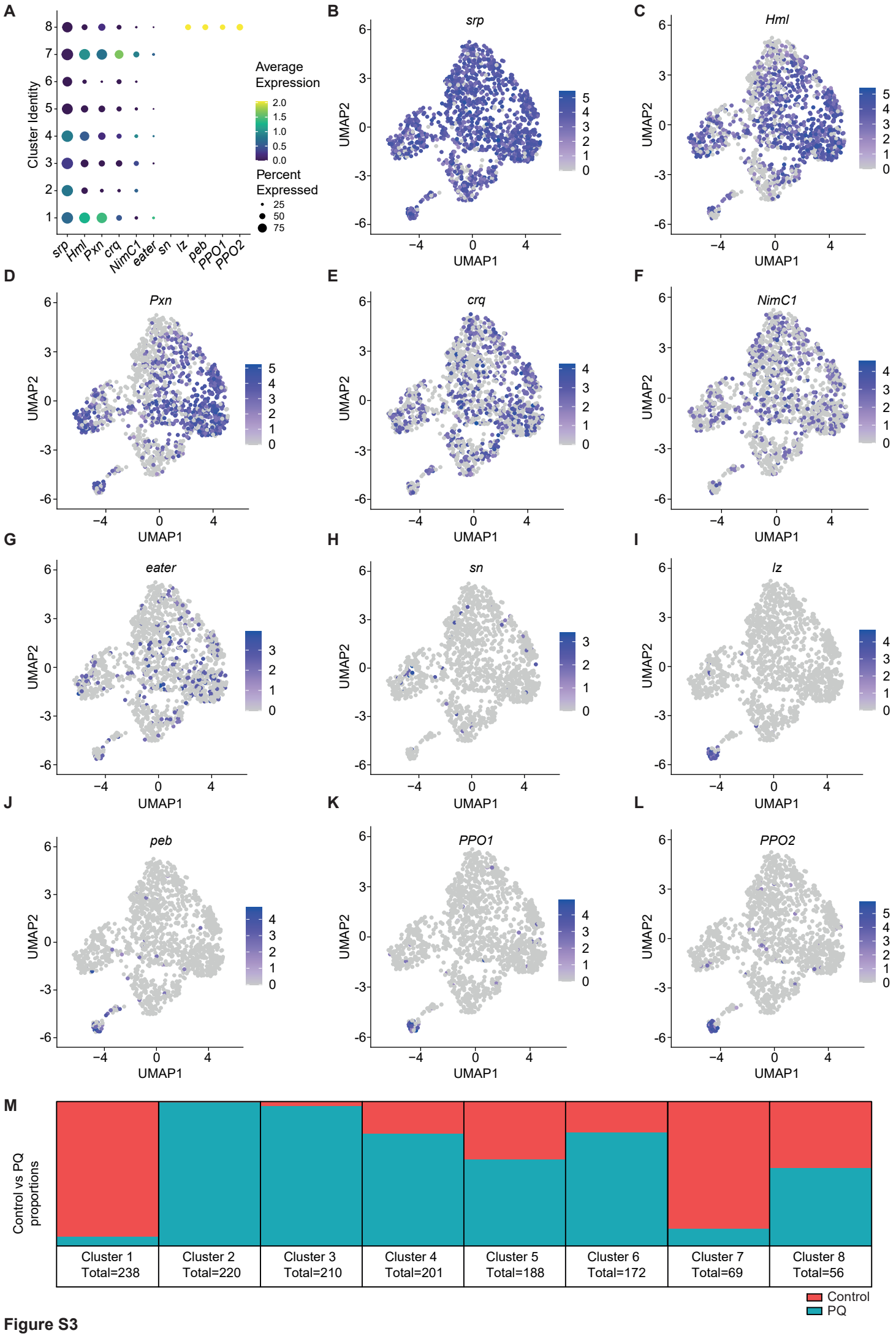
A
Cluster Identity
Average Expression
Percent Expressed
srp
Hml
Pxn
crq
NimC1
eater
sn
lz
peb
PPO1
PPO2
B
srp
C
Hml
D
Pxn
E
crq
F
NimC1
G
eater
H
sn
I
lz
J
peb
K
PPO1
L
PPO2
UMAP1
UMAP2
M
Control vs PQ proportions
Cluster 1 Total=238
Cluster 2 Total=220
Cluster 3 Total=210
Cluster 4 Total=201
Cluster 5 Total=188
Cluster 6 Total=172
Cluster 7 Total=69
Cluster 8 Total=56
Control
PQ

Figure S3

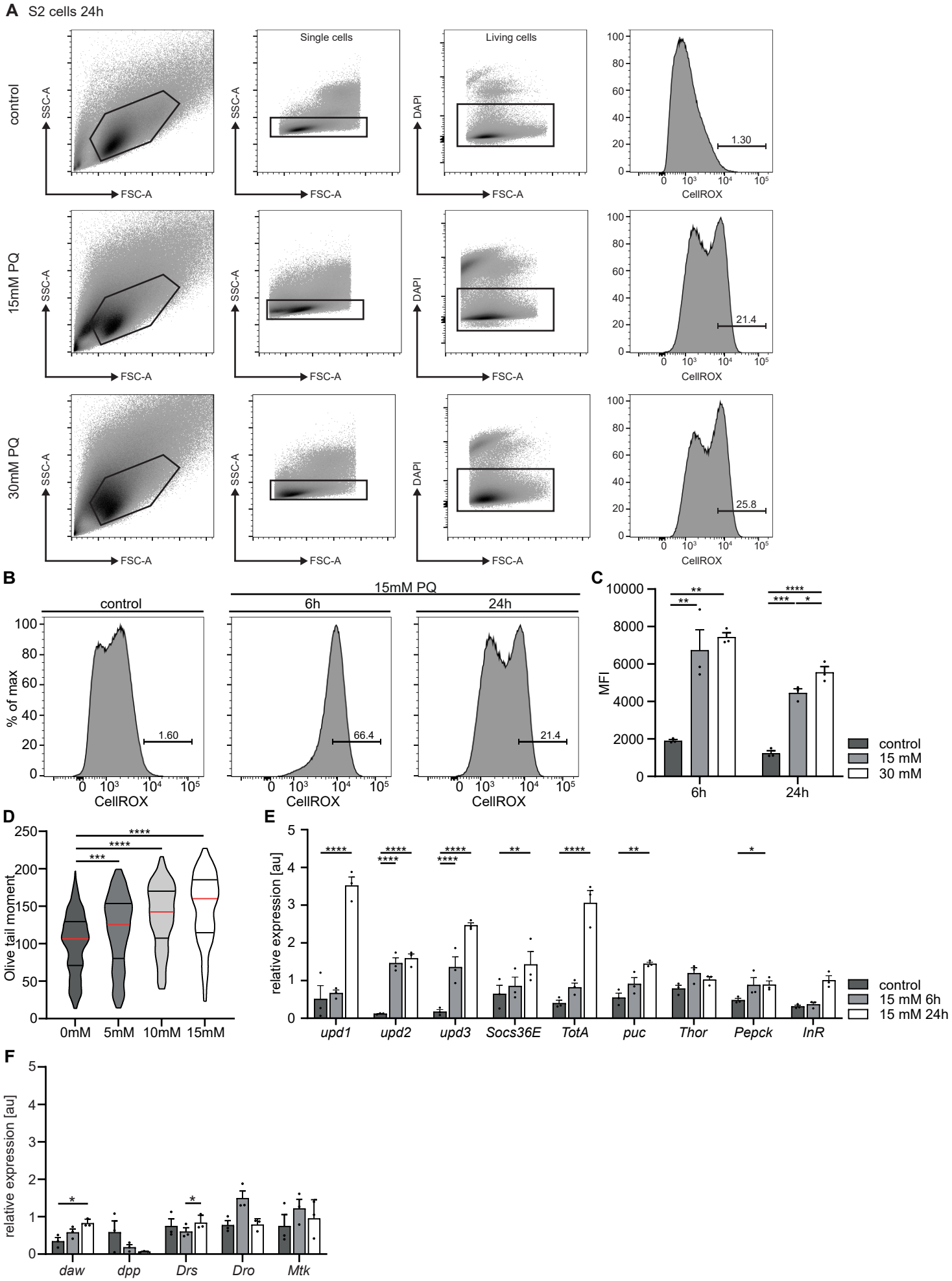
A
S2 cells 24h
control
15mM PQ
30mM PQ
SSC-A
FSC-A
Single cells
Living cells
DAPI
CellROX
1.30
21.4
25.8
B
control
15mM PQ
6h
24h
% of max
1.60
66.4
21.4
C
MFI
control
15 mM
30 mM
6h
24h
D
Olive tail moment
0mM
5mM
10mM
15mM
E
relative expression [au]
control
15 mM 6h
15 mM 24h
upd1
upd2
upd3
Socs36E
TotA
puc
Thor
Pepck
InR
F
relative expression [au]
daw
dpp
Drs
Dro
Mtk

Figure S4

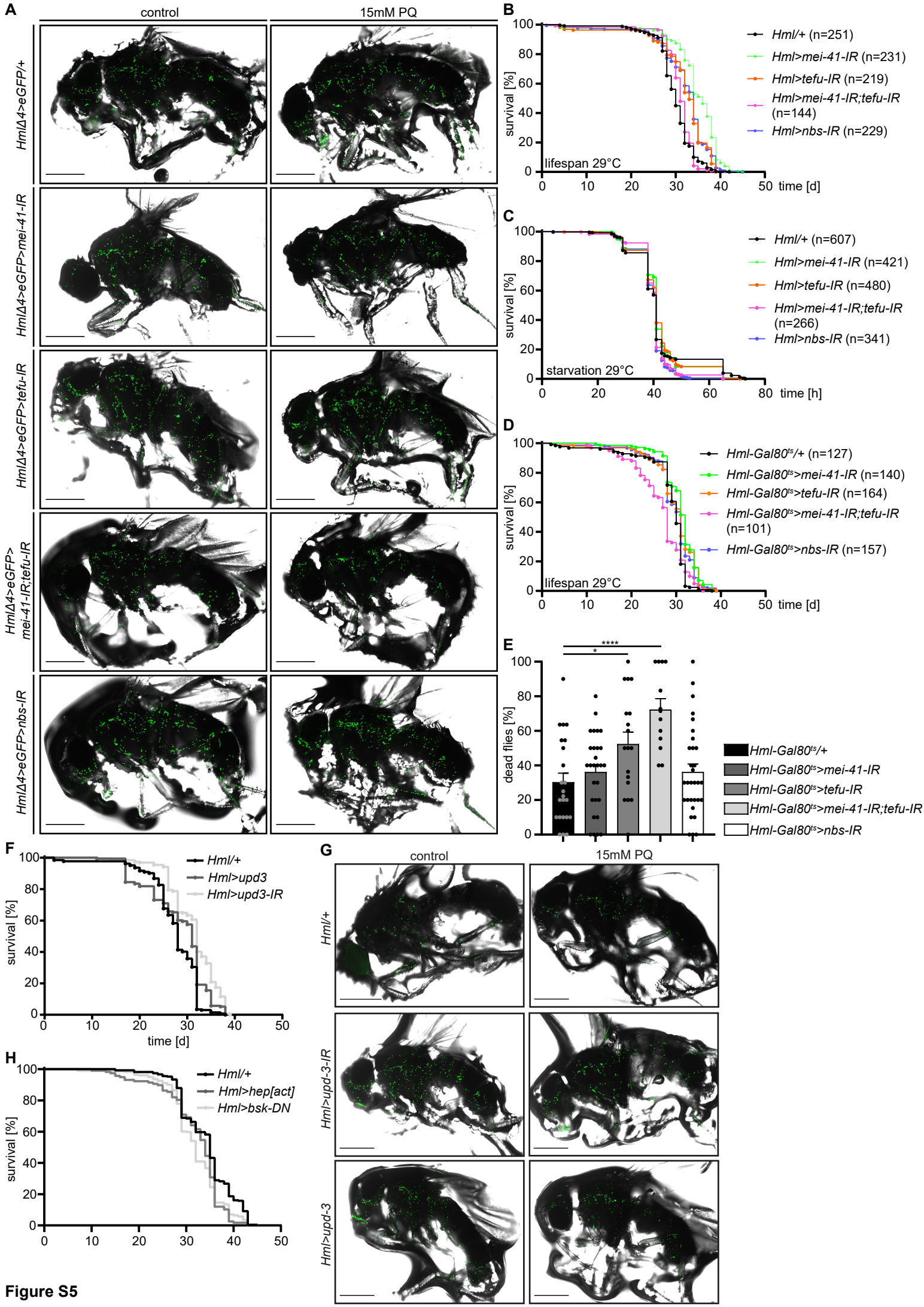
A
control
15mM PQ
HmlΔ4>eGFP/+
HmlΔ4>eGFP>mei-41-IR
HmlΔ4>eGFP>tefu-IR
HmlΔ4>eGFP>mei-41-IR;tefu-IR
HmlΔ4>eGFP>nbs-IR
B
survival [%]
lifespan 29°C
time [d]
Hml/+ (n=251)
Hml>mei-41-IR (n=231)
Hml>tefu-IR (n=219)
Hml>mei-41-IR;tefu-IR (n=144)
Hml>nbs-IR (n=229)
C
survival [%]
starvation 29°C
time [h]
Hml/+ (n=607)
Hml>mei-41-IR (n=421)
Hml>tefu-IR (n=480)
Hml>mei-41-IR;tefu-IR (n=266)
Hml>nbs-IR (n=341)
D
survival [%]
lifespan 29°C
time [d]
Hml-Gal80ts/+ (n=127)
Hml-Gal80ts>mei-41-IR (n=140)
Hml-Gal80ts>tefu-IR (n=164)
Hml-Gal80ts>mei-41-IR;tefu-IR (n=101)
Hml-Gal80ts>nbs-IR (n=157)
E
dead flies [%]
****
*
Hml-Gal80ts/+
Hml-Gal80ts>mei-41-IR
Hml-Gal80ts>tefu-IR
Hml-Gal80ts>mei-41-IR;tefu-IR
Hml-Gal80ts>nbs-IR
F
survival [%]
time [d]
Hml/+
Hml>upd3
Hml>upd3-IR
G
control
15mM PQ
Hml/+
Hml>upd-3-IR
Hml>upd-3
H
survival [%]
Hml/+
Hml>hep[act]
Hml>bsk-DN

Figure S5

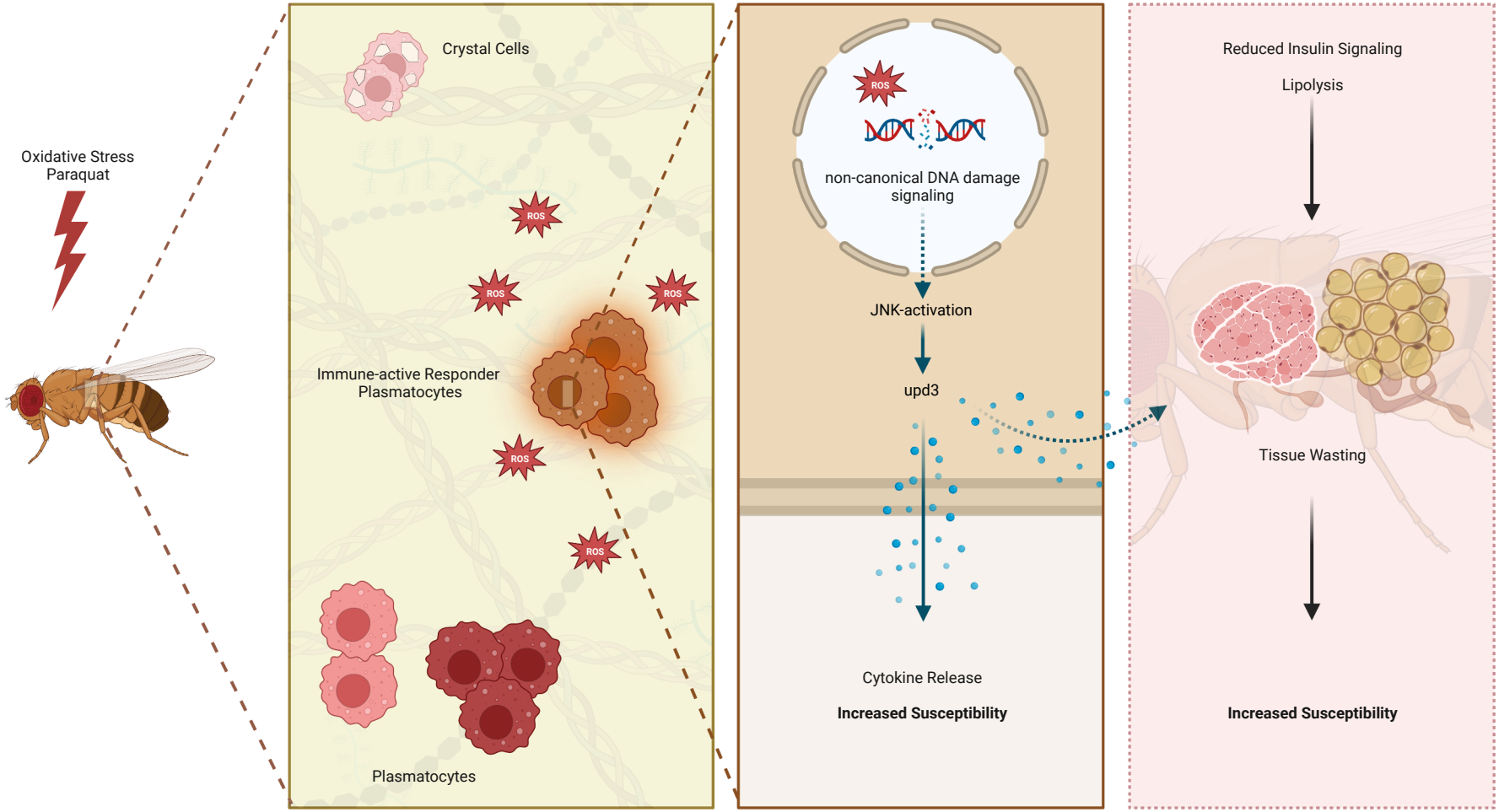
Oxidative Stress
Paraquat
Crystal Cells
ROS
ROS
ROS
ROS
ROS
Immune-active Responder
Plasmatocytes
Plasmatocytes
ROS
non-canonical DNA damage
signaling
JNK-activation
upd3
Cytokine Release
Increased Susceptibility
Reduced Insulin Signaling
Lipolysis
Tissue Wasting
Increased Susceptibility

Gene name	p-value	Average Log2 Fold Change	pct.1	pct.2	adjusted p-value	ter Ider
Sema2a	1.72E-44	1.6162889276056	0.807	0.371	2.06E-40	1
Pxn	7.35E-41	1.41812388559959	0.861	0.475	8.77E-37	1
CG5953	1.68E-39	-2.67460628121596	0.126	0.567	2.00E-35	1
CG31145	1.12E-37	1.12782433966876	0.929	0.706	1.34E-33	1
InR	1.28E-37	-1.57869976883602	0.655	0.895	1.52E-33	1
CG17574	1.03E-36	1.24918727582247	0.857	0.578	1.23E-32	1
regucalcin	4.30E-33	1.27904682829312	0.819	0.425	5.12E-29	1
Ten-m	2.97E-31	0.673576667842315	1	0.995	3.55E-27	1
Hml	3.24E-28	1.07332943120508	0.891	0.6	3.87E-24	1
Kr-h1	5.16E-27	-1.85748232917306	0.168	0.547	6.16E-23	1
Lpin	9.76E-27	-2.35909191337391	0.055	0.363	1.16E-22	1
CG10383	2.93E-26	-2.1714142846315	0.067	0.393	3.50E-22	1
pum	3.83E-26	0.565683740182448	1	0.993	4.57E-22	1
CG5151	4.40E-24	0.909497502163978	0.924	0.769	5.25E-20	1
cv-c	2.38E-23	-1.02161516685926	0.824	0.942	2.83E-19	1
cwo	7.93E-23	-1.41352854268449	0.345	0.688	9.47E-19	1
wake	3.34E-21	1.26219505400736	0.609	0.396	3.99E-17	1
bmm	1.72E-20	-1.78085022951387	0.109	0.414	2.05E-16	1
stv	5.54E-20	-2.12213745323016	0.034	0.282	6.60E-16	1
Had2	7.11E-20	1.20912954095074	0.534	0.28	8.48E-16	1
PRAS40	9.16E-20	-1.89630346158984	0.105	0.402	1.09E-15	1
CG46385	9.82E-20	-1.27716569989531	0.55	0.791	1.17E-15	1
AdSS	2.15E-19	-1.68347697076142	0.013	0.227	2.56E-15	1
Ppn	6.90E-18	0.634534332066303	1	0.958	8.23E-14	1
CG31324	7.52E-18	-1.86668574690431	0.126	0.402	8.97E-14	1
prage	1.06E-17	-1.7614500508477	0.076	0.337	1.27E-13	1
RapGAP1	1.14E-17	0.867906201854038	0.866	0.673	1.36E-13	1
mamo	1.51E-17	0.710986211589814	0.95	0.828	1.80E-13	1
Pdk	1.78E-17	-1.47359080963743	0.189	0.479	2.12E-13	1
cpx	2.63E-17	1.3623783240176	0.382	0.183	3.13E-13	1
psq	3.13E-16	0.672179838899004	0.916	0.799	3.73E-12	1
CG18135	1.27E-15	-1.67122855998694	0.16	0.388	1.52E-11	1
pan	1.79E-15	0.833970229628373	0.84	0.712	2.14E-11	1
Prps	3.81E-15	-1.66969042516105	0.16	0.392	4.54E-11	1
uex	1.03E-14	0.793185206779205	0.693	0.524	1.23E-10	1
CG32982	2.82E-14	-1.63902398259109	0.231	0.48	3.37E-10	1
Prosap	5.43E-14	0.522203366409648	0.975	0.94	6.48E-10	1
mtd	7.81E-14	0.628844989319082	0.895	0.73	9.31E-10	1
sgg	8.95E-14	-0.783173366563123	0.647	0.844	1.07E-09	1
Sema5c	1.34E-13	1.05855006119846	0.66	0.48	1.60E-09	1
CG42524	1.60E-13	0.918363789912115	0.529	0.331	1.91E-09	1
h	1.79E-12	-1.12890169350037	0.176	0.425	2.13E-08	1
aay	3.17E-12	-1.22856960361341	0.017	0.17	3.78E-08	1
cact	5.87E-12	-1.00974512443576	0.227	0.465	7.00E-08	1
CG3777	2.00E-11	1.08685920707846	0.366	0.195	2.39E-07	1
hdc	2.07E-11	0.554701003283501	0.945	0.856	2.46E-07	1
Syp	2.17E-11	0.561237457815474	0.933	0.833	2.59E-07	1
puc	2.42E-11	-1.08151243010921	0.353	0.591	2.89E-07	1
mbc	3.96E-11	0.824278803439878	0.567	0.464	4.73E-07	1
Xrp1	4.17E-11	-0.899936680519057	0.525	0.747	4.97E-07	1
GstD1	6.85E-11	-1.46778443765202	0.113	0.316	8.17E-07	1
LpR1	2.90E-10	-1.67255391987075	0.05	0.196	3.46E-06	1
CG31637	3.71E-10	0.742259847605879	0.588	0.473	4.43E-06	1
MtnA	3.74E-10	-0.996960575060986	0.13	0.329	4.46E-06	1
Thor	4.05E-10	-1.11070878838343	0.223	0.44	4.84E-06	1
CG3961	7.23E-10	0.826903706064792	0.521	0.342	8.63E-06	1
CG43236	7.76E-10	1.24631405471821	0.256	0.113	9.26E-06	1
GlcAT-P	1.74E-09	0.679829365423647	0.672	0.502	2.07E-05	1
CG5973	2.00E-09	0.88857173863944	0.399	0.225	2.39E-05	1

CG41378	2.44E-09	0.589301057255471	0.681	0.591	2.91E-05	1
CG9171	3.44E-09	0.780961631706464	0.454	0.334	4.10E-05	1
CG1208	4.23E-09	-0.957227641172127	0.092	0.268	5.05E-05	1
CG18067	4.79E-09	-1.09200724019655	0.08	0.143	5.72E-05	1
CG9328	5.04E-09	0.709281110277145	0.571	0.461	6.02E-05	1
Fas3	6.68E-09	-1.95084157860347	0.084	0.25	7.97E-05	1
Pgant9	1.00E-08	0.471976960778431	0.832	0.678	0.0001192872674	1
CG17124	1.18E-08	0.836099956143777	0.529	0.406	0.0001403088514	1
Btk29A	1.38E-08	0.498342115510994	0.895	0.748	0.0001650178191	1
l(1)G0196	1.71E-08	0.667277641680846	0.534	0.377	0.0002035352832	1
Glut4EF	1.90E-08	-0.762351700584293	0.815	0.909	0.0002263830098	1
Pkc53E	1.97E-08	1.01542295397375	0.185	0.092	0.0002349523186	1
CG17839	1.99E-08	-1.75071198562369	0.021	0.139	0.0002376518743	1
pnr	2.15E-08	0.599439270211903	0.639	0.536	0.0002558924772	1
Mob2	2.40E-08	-0.640082251405746	0.744	0.86	0.0002860050165	1
app	3.51E-08	0.68648866871702	0.454	0.375	0.0004186461574	1
CG7530	3.53E-08	-1.20392773499384	0.042	0.176	0.000420906438	1
CG11089	3.78E-08	-0.781307579960688	0.021	0.134	0.0004505298267	1
mnb	3.84E-08	-0.853724446464037	0.231	0.429	0.0004576146008	1
kuz	4.59E-08	0.487305344345348	0.891	0.806	0.0005479753289	1
shep	4.62E-08	0.298010781569423	1	0.983	0.0005516911908	1
sra	5.19E-08	-0.866504549208023	0.092	0.245	0.0006194198595	1
GEFmeso	5.57E-08	-0.77528594666364	0.269	0.471	0.0006641153134	1
Fer1HCH	5.98E-08	-0.854784429231019	0.374	0.574	0.0007133554414	1
CG3376	6.54E-08	-0.826736322745281	0.29	0.487	0.0007806630444	1
CG11050	6.93E-08	-1.03466909268403	0.017	0.123	0.0008266022201	1
flw	7.20E-08	0.699439025698075	0.429	0.342	0.0008586965528	1
Fer2LCH	7.71E-08	-0.846246192920253	0.399	0.593	0.0009200951794	1
Atg8a	7.90E-08	-0.890773238039883	0.197	0.387	0.0009429852175	1
RpLP2	8.03E-08	-0.914837371368728	0.101	0.223	0.000958245699	1
MESR3	8.05E-08	0.476518466147037	0.777	0.737	0.0009599613228	1
CG1943	8.25E-08	-0.89107268761854	0.08	0.228	0.0009841059195	1
MFS17	9.22E-08	0.5075814500755	0.739	0.676	0.0010997311335	1
kay	1.13E-07	-0.878906221519471	0.252	0.449	0.0013536604973	1
Galphao	1.16E-07	0.705821802694266	0.378	0.289	0.0013800459548	1
jim	1.23E-07	-0.758217961491641	0.29	0.49	0.0014731075302	1
CenG1A	1.36E-07	-0.886976326588646	0.059	0.189	0.0016206334068	1
nkd	1.55E-07	-1.13184051364839	0.071	0.22	0.0018448773239	1
Gadd45	1.60E-07	-1.23122821108162	0.038	0.167	0.0019057734757	1
ham	1.60E-07	0.776409621653134	0.349	0.249	0.0019090341541	1
CG31183	1.72E-07	0.911780341748128	0.197	0.116	0.0020511758122	1
DIP-lambda	1.79E-07	0.635778759623991	0.609	0.481	0.0021354995767	1
Rala	1.85E-07	0.488000922359868	0.538	0.495	0.0022025343261	1
rl	1.92E-07	0.297637562467301	0.987	0.962	0.0022862467339	1
CG45050	2.14E-07	-0.507568053467238	0.601	0.777	0.0025531962561	1
cnc	2.41E-07	-0.555608400181908	0.546	0.724	0.0028748986268	1
ena	2.66E-07	0.618931723957947	0.689	0.562	0.003177817324	1
CG42694	3.12E-07	0.869007202597888	0.172	0.086	0.0037222474249	1
Pect	3.14E-07	-0.579660852394219	0.155	0.307	0.0037509397615	1
Nrg	3.39E-07	-1.41785238300148	0.042	0.163	0.0040495504716	1
DIP-alpha	3.98E-07	-0.346847706927715	0.479	0.667	0.0047506508805	1
RpL19	4.50E-07	-1.0050479210697	0.168	0.324	0.0053724101269	1
fax	5.59E-07	-0.702951603870904	0.466	0.646	0.0066640922243	1
anne	5.73E-07	0.449471080325161	0.294	0.269	0.0068384972439	1
Dbp80	5.88E-07	0.486783544825669	0.752	0.676	0.0070159424913	1
cv-2	6.37E-07	-1.1675648172023	0.013	0.101	0.0076013815535	1
oys	6.66E-07	-0.715235001283986	0.147	0.298	0.0079442614984	1
ush	6.70E-07	0.491086221355686	0.811	0.704	0.0079867474648	1
Atg18b	6.90E-07	-0.808639549487901	0.126	0.277	0.0082315557717	1
CG3168	7.09E-07	-1.16081411057093	0.025	0.126	0.0084616542786	1

SCaMC	7.70E-07	-0.964803852969327	0.147	0.315	0.0091879744672	1
CG33144	8.07E-07	0.626423054989156	0.521	0.404	0.0096230270426	1
unc-13	8.23E-07	0.504624297794107	0.664	0.566	0.0098153757634	1
unk	8.34E-07	-0.850913581121446	0.097	0.244	0.0099449356685	1
caps	8.90E-07	-1.27628185867807	0.021	0.121	0.0106223344233	1
ref(2)P	8.98E-07	-0.691841259610093	0.063	0.19	0.0107094094945	1
spri	9.11E-07	0.413174863145775	0.798	0.745	0.0108644513389	1
Col4a1	9.39E-07	0.347456471036864	0.975	0.914	0.011204823691	1
lbk	9.61E-07	-0.66898761046754	0.45	0.611	0.0114620343279	1
CG13868	9.69E-07	-0.800653207137174	0.244	0.431	0.0115612216315	1
RpS9	1.03E-06	-0.777165015480121	0.13	0.272	0.0123223720699	1
Tgi	1.10E-06	0.700543226084842	0.298	0.205	0.0131223248221	1
Atg1	1.21E-06	-0.821693401454341	0.16	0.321	0.0144800775601	1
Fim	1.22E-06	-0.687396611960331	0.223	0.398	0.0144970747972	1
apolpp	1.23E-06	0.616339242102445	0.487	0.323	0.0147099741076	1
Gel	1.25E-06	0.577170649446541	0.353	0.286	0.0148551303544	1
Cals	1.46E-06	0.450055656061303	0.252	0.248	0.0173716656995	1
raskol	1.72E-06	0.557872487311775	0.248	0.214	0.0205192029799	1
CG15784	1.74E-06	-0.874017661182743	0.025	0.116	0.0207170936386	1
NimC4	1.86E-06	-1.23285349214299	0.017	0.11	0.0221781717796	1
Gyf	1.93E-06	0.436956094792022	0.336	0.319	0.0229834154549	1
DOR	1.97E-06	0.682730029576101	0.357	0.282	0.0235462956914	1
AnxB9	2.08E-06	-0.86925550072843	0.189	0.354	0.0248469271135	1
NaCP60E	2.12E-06	0.709163779147426	0.319	0.226	0.0253255879948	1
ckn	2.27E-06	0.647770714633008	0.286	0.218	0.0271084416435	1
Hex-A	2.45E-06	-0.744773545889198	0.155	0.314	0.0292173304358	1
Pde9	2.45E-06	0.592106944441244	0.681	0.576	0.0292591450487	1
Lmpt	2.47E-06	-1.14665742238657	0.029	0.134	0.0295060331424	1
CG14207	2.48E-06	-0.762754583101828	0.017	0.105	0.0295790473666	1
Hsc70Cb	2.64E-06	-0.439465747494038	0.139	0.266	0.031441860985	1
dl	2.85E-06	-1.10191444839634	0.038	0.15	0.0340444808043	1
CG33298	3.01E-06	0.544607820502207	0.5	0.413	0.035909077181	1
CG18628	3.46E-06	-0.670396252537318	0.029	0.13	0.0412265399215	1
RhoGAP15B	3.50E-06	-0.705549564268354	0.105	0.234	0.0417682814539	1
shot	3.60E-06	0.344190828372803	0.912	0.893	0.0429487156919	1
Ubi-p63E	3.68E-06	-0.945505349517211	0.265	0.439	0.0438398236124	1
Mct1	3.78E-06	-0.318052359710765	0.092	0.181	0.0450511946113	1
Pcyt1	3.97E-06	-0.618343558098732	0.046	0.144	0.0473767316392	1
step	3.97E-06	-0.299349649800543	0.298	0.449	0.0473965504767	1
cic	3.33E-32	1.19541168195356	0.991	0.949	3.98E-28	2
Glut4EF.1	2.39E-31	1.12721129448769	0.968	0.878	2.85E-27	2
Lpin.1	3.52E-29	1.58315817044524	0.605	0.253	4.20E-25	2
Spn.1	5.61E-24	1.02886009630333	0.855	0.637	6.69E-20	2
Mmp2.1	1.63E-22	-2.04204533407427	0.168	0.517	1.94E-18	2
Mob2.1	6.65E-21	0.849549961080278	0.936	0.821	7.93E-17	2
sgg.1	5.73E-20	0.784872050008015	0.95	0.782	6.84E-16	2
PRAS40.1	6.18E-20	1.41120326595323	0.577	0.307	7.37E-16	2
CG18135.1	6.50E-19	1.28283186774196	0.541	0.311	7.75E-15	2
InR.1	4.29E-18	0.706142605520689	0.973	0.83	5.12E-14	2
Kr-h1.1	1.64E-17	1.0526172627847	0.7	0.439	1.96E-13	2
Pvr	9.81E-17	0.667890403245941	0.968	0.86	1.17E-12	2
Crtc.1	1.22E-16	0.928646068162169	0.7	0.5	1.45E-12	2
RhoGAP71E	2.33E-16	-1.43544309961527	0.309	0.601	2.78E-12	2
Cip4	3.71E-16	-1.54971488700007	0.286	0.58	4.42E-12	2
Sema2a.1	3.81E-16	-1.65984354425531	0.209	0.493	4.54E-12	2
Msp300	4.28E-16	-1.6642604378789	0.355	0.613	5.11E-12	2
CHES-1-like.1	5.81E-16	0.947789176012077	0.491	0.351	6.93E-12	2
jim.1	3.19E-15	0.947161862808102	0.641	0.42	3.81E-11	2
Pdk.1	1.07E-14	0.968747964075999	0.627	0.39	1.27E-10	2
CG12163	1.39E-14	0.834244537295691	0.691	0.537	1.65E-10	2

luna	1.43E-14	-1.04232564512513	0.65	0.835	1.70E-10	2
Pxn.1	2.15E-14	-1.35680989449939	0.309	0.587	2.56E-10	2
CG5953.1	3.20E-14	0.875665367552621	0.705	0.449	3.82E-10	2
CG10383.1	3.84E-14	1.06755201854884	0.545	0.295	4.59E-10	2
CG32982.1	7.96E-14	1.17456063663202	0.614	0.402	9.50E-10	2
cwo.1	1.38E-13	0.871098428939009	0.759	0.603	1.64E-09	2
regucalcin.1	2.64E-13	-0.991607533679677	0.259	0.539	3.15E-09	2
CG5059.1	3.21E-13	0.951045835900925	0.518	0.315	3.83E-09	2
egh.1	5.87E-13	-1.11513053688925	0.195	0.465	7.01E-09	2
mnb.1	9.41E-13	0.950868218349842	0.582	0.358	1.12E-08	2
CG7530.1	9.77E-13	1.24389124768074	0.273	0.129	1.16E-08	2
Dyrk2	1.01E-12	0.853053473445721	0.714	0.535	1.20E-08	2
CG31324.1	1.26E-12	1.04728328164989	0.545	0.317	1.50E-08	2
Pli.1	1.63E-12	0.967006483452418	0.591	0.377	1.94E-08	2
hdc.1	2.04E-12	-0.684330599383186	0.75	0.895	2.44E-08	2
Pax	3.87E-12	-1.44562111964136	0.064	0.261	4.62E-08	2
CG13868.1	4.42E-12	0.920318408574457	0.555	0.368	5.27E-08	2
alphaTub84B	5.44E-12	-1.1886492004544	0.073	0.269	6.49E-08	2
spir	5.92E-12	-1.42650737584219	0.255	0.493	7.06E-08	2
CG10543	7.12E-12	0.678590209091547	0.809	0.722	8.50E-08	2
mgl	7.49E-12	-1.76541559996217	0.123	0.355	8.93E-08	2
CG17574.1	1.54E-11	-0.981551244196897	0.427	0.665	1.84E-07	2
gish	2.02E-11	-0.980362013105583	0.277	0.542	2.41E-07	2
Rtnl1	4.17E-11	-1.32707942986465	0.009	0.142	4.98E-07	2
RanBPM.1	4.42E-11	0.910915814933915	0.414	0.262	5.27E-07	2
flw.1	5.70E-11	-1.05941674741121	0.164	0.394	6.80E-07	2
Moe	5.97E-11	-0.780539783643164	0.264	0.511	7.12E-07	2
zip	6.38E-11	-1.07556340897062	0.123	0.338	7.61E-07	2
Prps.1	9.54E-11	0.959630745905299	0.459	0.33	1.14E-06	2
aqz	1.49E-10	0.494790937258879	0.964	0.885	1.78E-06	2
Act42A.1	2.01E-10	-1.27551684128559	0.036	0.199	2.40E-06	2
NimB4	2.83E-10	0.674907069920365	0.477	0.378	3.38E-06	2
CG3376.1	3.50E-10	0.864209488463082	0.605	0.423	4.18E-06	2
sr	4.38E-10	0.721354529893485	0.668	0.51	5.22E-06	2
CG32486	4.38E-10	0.634747292474779	0.632	0.523	5.23E-06	2
Atg1.1	5.04E-10	0.881977993627787	0.391	0.274	6.02E-06	2
Fas3.1	6.29E-10	-2.20776027118582	0.082	0.247	7.51E-06	2
betaTub60D	7.38E-10	-1.64440847219498	0.095	0.285	8.80E-06	2
CG43867	1.31E-09	-1.45046487725163	0.036	0.189	1.56E-05	2
uex.1	1.44E-09	-0.613377371428332	0.355	0.592	1.71E-05	2
bmm.1	2.00E-09	0.890654957476672	0.527	0.329	2.38E-05	2
MYPT-75D	2.81E-09	0.79569912620648	0.705	0.509	3.35E-05	2
AdSS.1	3.33E-09	0.944885039893061	0.309	0.167	3.97E-05	2
Thor.1	3.93E-09	0.885166445563009	0.545	0.374	4.68E-05	2
CG46385.1	4.45E-09	0.618168058523458	0.85	0.73	5.31E-05	2
CrebA.1	4.56E-09	-1.25194175486553	0.095	0.288	5.45E-05	2
drpr	5.92E-09	0.571670515955866	0.855	0.733	7.06E-05	2
l(3)L1231	6.01E-09	0.49919896664013	0.773	0.719	7.17E-05	2
lbk.1	7.27E-09	0.621526784486822	0.673	0.566	8.67E-05	2
CG5888.1	1.05E-08	-0.832188794458463	0.164	0.355	0.0001247100174	2
Atg17.1	1.08E-08	0.744417727042563	0.455	0.315	0.0001293242728	2
CG42524.1	1.10E-08	-0.800872528130593	0.195	0.399	0.0001309477845	2
chic	1.24E-08	-0.656245667159821	0.205	0.399	0.0001479907508	2
kermit	1.54E-08	0.96548080714328	0.136	0.051	0.0001839946231	2
app.1	1.70E-08	-0.861512227317622	0.214	0.422	0.0002024502334	2
CG5973.1	1.82E-08	-1.19047473183274	0.105	0.284	0.0002172632261	2
sra.1	1.87E-08	0.881504914886091	0.345	0.194	0.0002234223209	2
CG32767	2.07E-08	0.659562052264535	0.714	0.598	0.0002471850368	2
B4	2.21E-08	-1.16031768700246	0.023	0.151	0.0002635498778	2
fs(1)h.1	2.22E-08	0.501816734502216	0.709	0.677	0.0002643449454	2

LpR1.1	2.84E-08	1.19990133337143	0.291	0.148	0.0003382891428	2
Smr	2.86E-08	0.478389654168635	0.886	0.851	0.0003414890402	2
scb	2.99E-08	-1.11904068052272	0.036	0.171	0.0003571605052	2
Cam	3.21E-08	-0.965880044453312	0.345	0.542	0.0003825427851	2
foxo	3.29E-08	0.602016224720276	0.659	0.531	0.000392318678	2
pigs.1	3.42E-08	-0.729468200242131	0.391	0.62	0.0004078230554	2
CG4250.1	4.19E-08	-0.917121772619201	0.191	0.385	0.0004999273267	2
LanA.1	5.38E-08	-0.927599870487512	0.077	0.229	0.0006422806663	2
Had2.1	6.29E-08	-1.0002872853694	0.164	0.355	0.0007505387299	2
CG4404.1	6.31E-08	0.900651281177832	0.264	0.147	0.000752970037	2
Mkp3	6.55E-08	-1.15735381651856	0.15	0.347	0.0007810880881	2
CG8679	9.27E-08	0.848005899252338	0.127	0.058	0.0011054095865	2
CG9005	9.39E-08	0.730316459973993	0.482	0.366	0.0011195555836	2
CG43236.1	1.02E-07	-1.22634590298012	0.032	0.158	0.0012205681593	2
px	1.17E-07	0.469620741623282	0.805	0.77	0.0013955682118	2
crq	1.22E-07	-0.384619420870882	0.282	0.465	0.001451022152	2
Sap47	1.64E-07	0.6651615404365	0.495	0.408	0.0019543406032	2
Naam	1.80E-07	-1.35169595421129	0.114	0.278	0.0021510827333	2
bbc	1.94E-07	-0.882725592866563	0.095	0.25	0.0023197101389	2
Blimp-1	1.98E-07	0.517219208748204	0.614	0.553	0.0023624640631	2
Atg18b.1	2.03E-07	0.70809520954086	0.35	0.232	0.0024214176824	2
CG9003	2.43E-07	0.689013159215575	0.455	0.306	0.0029031258161	2
Frl	2.65E-07	-0.910499008156447	0.236	0.426	0.0031653083577	2
norpA	2.92E-07	-0.664092053526328	0.282	0.478	0.0034889322981	2
CG6191	2.96E-07	0.829465829646994	0.182	0.105	0.0035251250917	2
zfh1	3.07E-07	0.43192433274305	0.973	0.901	0.003657789726	2
Gapvd1	3.14E-07	0.77456655045068	0.155	0.079	0.0037492631228	2
firl.1	3.31E-07	-1.25016564022784	0.032	0.152	0.0039431561506	2
EDTP	3.43E-07	0.853396843837101	0.314	0.187	0.0040869305675	2
kst	3.99E-07	-0.789578024564893	0.082	0.216	0.0047573231353	2
PDZ-GEF	4.02E-07	0.620671775255476	0.336	0.257	0.0047912966989	2
CG9674.1	4.13E-07	0.592728164231881	0.459	0.286	0.0049242204882	2
klar.1	4.36E-07	-0.637603212393463	0.405	0.61	0.0052062131118	2
CG1208.1	4.61E-07	0.940504074341949	0.364	0.213	0.0054980847809	2
CG42674	4.87E-07	-1.11975083963627	0.027	0.138	0.0058097273242	2
sick	5.29E-07	-1.10874063741184	0.018	0.12	0.0063124265669	2
apolpp.1	5.65E-07	-0.484966789351918	0.214	0.378	0.0067364518964	2
Sema2b.1	5.95E-07	0.701128333840265	0.323	0.26	0.0071023909702	2
dikar	6.05E-07	0.521892858499395	0.436	0.382	0.0072215174958	2
CG32264.1	6.08E-07	-0.747078267325779	0.286	0.476	0.0072485563173	2
wake.1	6.16E-07	-0.981227405482643	0.273	0.464	0.0073512136279	2
CG3328	6.20E-07	0.514715221769952	0.595	0.534	0.0073982103138	2
hfp	6.54E-07	0.632404434845659	0.318	0.24	0.0078047611841	2
sno	7.38E-07	0.718987770502164	0.209	0.142	0.0088016169177	2
Hml.1	7.41E-07	-0.890346183795403	0.532	0.674	0.0088448580523	2
shep.1	7.50E-07	-0.368158084917997	0.973	0.989	0.0089464704031	2
CG12065	8.60E-07	0.48926749804893	0.668	0.593	0.0102583490433	2
CG42668	9.33E-07	-0.8849367709824	0.1	0.252	0.0111332538965	2
SCaMC.1	9.45E-07	0.626013497382698	0.323	0.279	0.0112695761843	2
CG12576.1	9.61E-07	0.753726058791556	0.373	0.254	0.0114582417781	2
cora.1	9.63E-07	-0.611849603610952	0.323	0.517	0.0114835313021	2
Tlk.1	9.97E-07	0.422565927339984	0.686	0.679	0.0118901864165	2
eEF2.1	1.17E-06	0.269476637928111	0.268	0.323	0.0139890084013	2
unk.1	1.22E-06	0.821838940621414	0.323	0.198	0.0145429599808	2
mbc.1	1.31E-06	-0.602637841078507	0.323	0.512	0.0156243611504	2
Cyp4ac3	1.33E-06	0.840257999284449	0.132	0.058	0.0159025923617	2
CG6891	1.42E-06	-1.14844764825421	0.009	0.101	0.0169462687609	2
CG18171	1.59E-06	0.581074290374027	0.364	0.3	0.0189333451202	2
AdipoR	1.60E-06	0.567926158355136	0.182	0.163	0.019076946305	2
CG3777.1	1.65E-06	-1.00692406543775	0.095	0.25	0.0196490849722	2

ATP8A	1.81E-06	-1.04249562880634	0.059	0.186	0.0215972184798	2
cdi	1.89E-06	-0.798662699249844	0.159	0.327	0.0224938357141	2
CG6357	1.93E-06	-0.627334010467367	0.027	0.116	0.0230538865779	2
bves	1.96E-06	-0.783450624635608	0.114	0.257	0.023362860474	2
Ziz.1	2.04E-06	0.761145297965434	0.441	0.313	0.024368734496	2
RhoGAP93B	2.27E-06	-0.531962321187022	0.055	0.148	0.0271190493159	2
mtgo	2.50E-06	0.313741275203546	0.982	0.96	0.0298301051757	2
Socs16D	2.60E-06	0.674151710806568	0.164	0.12	0.0310267286548	2
bwa.1	2.63E-06	0.76708554948304	0.25	0.14	0.0313409377672	2
rudhira	2.68E-06	0.534243210113484	0.664	0.556	0.0319140138117	2
Ran	2.79E-06	-0.530657885828707	0.027	0.107	0.0332476502147	2
tai	3.01E-06	0.424228940053434	0.877	0.809	0.0359101742163	2
Pdcd4.1	3.06E-06	0.623098869165216	0.168	0.13	0.0364708681396	2
Syp.1	3.10E-06	-0.455943655547646	0.75	0.87	0.0369837365466	2
pan.1	3.12E-06	-0.468904520929707	0.591	0.762	0.0372056461885	2
l(3)80Fg.1	3.13E-06	-0.733575388281955	0.477	0.635	0.0373874540942	2
Usp15-31	4.03E-06	-0.945177399349594	0.045	0.158	0.0480454013456	2
Kr-h1.2	2.16E-18	0.849086392291416	0.762	0.43	2.57E-14	3
CG10383.2	9.80E-17	0.696271900127146	0.586	0.29	1.17E-12	3
InR.2	1.53E-16	0.522828663316981	0.981	0.83	1.82E-12	3
CG3376.2	2.31E-16	0.813070251115809	0.714	0.405	2.75E-12	3
Pvr.1	1.83E-15	0.53802432953129	0.99	0.857	2.18E-11	3
sgg.2	3.00E-15	0.694113895516637	0.929	0.788	3.58E-11	3
CG12576.2	7.33E-15	0.687553815789311	0.49	0.234	8.75E-11	3
CG32982.2	8.72E-15	1.04962281726703	0.662	0.395	1.04E-10	3
CG1208.2	1.60E-14	0.754602376706507	0.448	0.199	1.91E-10	3
Lpin.2	1.70E-14	0.707664256638977	0.543	0.267	2.03E-10	3
cwo.2	1.92E-14	0.650525095816118	0.852	0.588	2.29E-10	3
bmm.2	2.65E-13	0.977922987003129	0.59	0.319	3.17E-09	3
sra.2	2.95E-13	0.855297818172686	0.414	0.183	3.52E-09	3
PDZ-GEF.1	4.99E-13	0.537590570955192	0.457	0.236	5.95E-09	3
CG13982	7.34E-13	1.01822440967123	0.371	0.137	8.76E-09	3
Atg17.2	8.70E-13	0.767421715351092	0.562	0.296	1.04E-08	3
Ser	4.70E-12	0.5078077752485	0.571	0.326	5.60E-08	3
uex.2	4.81E-12	-0.514067780633636	0.576	0.549	5.74E-08	3
Pdk.2	5.79E-12	0.712998979833129	0.648	0.388	6.90E-08	3
CG5953.2	6.08E-12	0.309978404864284	0.695	0.453	7.26E-08	3
NimB4.1	6.65E-12	0.392947481077724	0.586	0.36	7.93E-08	3
MYPT-75D.1	6.93E-12	0.878228608070454	0.743	0.503	8.27E-08	3
CG32486.1	7.44E-12	0.448066824007923	0.752	0.502	8.88E-08	3
C1GalTA.2	3.93E-11	0.436919414415815	0.433	0.244	4.69E-07	3
CG1943.2	4.48E-11	0.383535886547904	0.352	0.175	5.34E-07	3
lbk.2	5.68E-11	0.629899469437275	0.776	0.548	6.77E-07	3
Hsc70-4.1	8.07E-11	-0.575325679415239	0.314	0.289	9.62E-07	3
Pkn.1	8.95E-11	0.422685533002747	0.729	0.488	1.07E-06	3
Myc.1	1.13E-10	-0.878014980252786	0.462	0.467	1.35E-06	3
Spn.2	1.58E-10	0.462651190649179	0.867	0.637	1.89E-06	3
flfl.2	1.68E-10	0.399352113170937	0.314	0.159	2.00E-06	3
CG12054	1.78E-10	0.289973211454242	0.41	0.237	2.12E-06	3
mam	2.16E-10	0.345877289015632	0.571	0.364	2.57E-06	3
hep	2.20E-10	0.260588721827463	0.424	0.263	2.62E-06	3
Fer2LCH.1	3.64E-10	0.522366238916377	0.752	0.524	4.34E-06	3
cv-c.2	3.69E-10	0.366434481482135	0.99	0.909	4.40E-06	3
CG12065.1	4.23E-10	0.383441963048982	0.8	0.569	5.05E-06	3
cpo.1	5.18E-10	-0.370192429015233	0.776	0.688	6.18E-06	3
CG46385.2	5.31E-10	0.526170347930775	0.9	0.722	6.33E-06	3
CG12163.1	5.36E-10	0.448970023724559	0.757	0.526	6.39E-06	3
pcs.2	5.51E-10	0.272977131105791	0.324	0.181	6.57E-06	3
sbr.1	5.94E-10	0.258938557552162	0.405	0.25	7.09E-06	3
Pdp1.1	7.99E-10	-0.543294912740076	0.595	0.6	9.53E-06	3

PRAS40.2	8.54E-10	0.412201035736534	0.529	0.318	1.02E-05	3
Crtc.2	8.65E-10	0.530938171588458	0.729	0.497	1.03E-05	3
Atg18b.2	9.25E-10	0.6222932972772	0.424	0.219	1.10E-05	3
Karl	1.38E-09	0.458184354282332	0.929	0.761	1.65E-05	3
CG5059.2	1.70E-09	0.370315415360736	0.519	0.316	2.03E-05	3
Mbs	2.22E-09	0.508289410347841	0.576	0.35	2.65E-05	3
Msp300.1	2.30E-09	-0.898480609839093	0.5	0.584	2.75E-05	3
CG12012.2	2.32E-09	0.392779927230301	0.319	0.166	2.76E-05	3
RpS26	2.54E-09	-0.398812928534632	0.295	0.241	3.03E-05	3
CG6966	2.56E-09	0.333949808330341	0.424	0.264	3.06E-05	3
hid.1	2.97E-09	0.488209504711279	0.557	0.338	3.54E-05	3
CG4404.2	3.00E-09	0.516892476346466	0.29	0.143	3.58E-05	3
REPTOR.2	3.01E-09	0.431159125398005	0.786	0.562	3.59E-05	3
kay.1	4.09E-09	-0.260598608058797	0.495	0.4	4.87E-05	3
Mob2.2	4.20E-09	0.565266403025322	0.938	0.821	5.00E-05	3
CG11050.1	4.39E-09	0.680356183908367	0.229	0.081	5.24E-05	3
Sema2b.2	4.68E-09	0.627136010716301	0.443	0.239	5.59E-05	3
Eip74EF.2	4.70E-09	0.460158259573872	0.762	0.55	5.60E-05	3
Yeti	6.92E-09	-0.330125724090943	0.362	0.328	8.25E-05	3
Exn.1	7.51E-09	0.540975005527516	0.495	0.282	8.96E-05	3
Trpm.1	8.01E-09	0.293946504299909	0.619	0.426	9.56E-05	3
Glut4EF.2	8.16E-09	0.38422557478599	0.976	0.877	9.74E-05	3
CG17574.2	8.34E-09	-0.572717797838628	0.595	0.633	9.95E-05	3
CG32091.1	9.38E-09	0.458497470469013	0.833	0.64	0.0001119451324	3
Socs36E.1	1.02E-08	-0.801027323306203	0.243	0.24	0.0001215241989	3
CG31324.2	1.17E-08	0.646469083815031	0.543	0.32	0.0001397308338	3
cpx.2	1.20E-08	-1.06609529217803	0.171	0.226	0.0001428886025	3
Tis11.1	1.20E-08	0.311591789666597	0.938	0.78	0.0001431780378	3
SCaMC.2	1.30E-08	0.368790725168412	0.438	0.258	0.0001548489269	3
Sik3	1.67E-08	0.376075207720654	0.381	0.225	0.0001987182623	3
Sox14	1.76E-08	0.478436311128424	0.281	0.142	0.0002100187538	3
sqd.1	1.82E-08	-0.33875278166946	0.638	0.57	0.0002176161316	3
ced-6.1	1.84E-08	0.373435495807289	0.652	0.448	0.0002198523049	3
Khc-73.1	1.96E-08	0.342135380234682	0.452	0.283	0.0002336171674	3
Cip4.1	2.08E-08	-0.739019569644458	0.529	0.533	0.0002484229711	3
CG31689.1	2.21E-08	0.512482986036712	0.629	0.413	0.0002639860894	3
Naprt.2	2.21E-08	0.334169019294527	0.29	0.165	0.000264065254	3
gogo.1	2.26E-08	0.623079095346855	0.348	0.178	0.0002701680169	3
g.2	2.47E-08	0.480548386013048	0.314	0.158	0.0002950868223	3
Jupiter	2.73E-08	0.284955352094502	0.962	0.819	0.0003258858971	3
RpL28.1	2.76E-08	-0.484008635781098	0.371	0.328	0.0003296901308	3
Cyp6v1	2.76E-08	0.302721798703909	0.233	0.127	0.0003297381576	3
CG5151.2	2.83E-08	-0.519198062392515	0.81	0.794	0.0003380961571	3
Fas3.2	2.98E-08	-2.08423873323704	0.095	0.244	0.0003550787487	3
RpL27A.1	3.11E-08	-0.936221332547622	0.319	0.389	0.0003707514009	3
Plp.1	3.18E-08	-0.271812220377899	0.252	0.209	0.0003788215939	3
RpL10Ab.1	3.93E-08	-0.530402756488546	0.281	0.256	0.0004686723609	3
14-3-3zeta	4.03E-08	-0.353735238514262	0.39	0.362	0.0004804483084	3
RpS17.1	4.05E-08	-0.566154031742435	0.243	0.213	0.0004827073597	3
Dscam1.1	4.89E-08	-0.395695649811587	0.29	0.253	0.0005835100557	3
mnb.2	5.68E-08	0.622393756179635	0.581	0.36	0.0006773179386	3
Sap-r.1	5.73E-08	0.460008990155399	0.614	0.403	0.0006836004789	3
drpr.1	5.73E-08	0.389938649906924	0.886	0.729	0.0006840183032	3
pigs.2	6.21E-08	-0.269236985846659	0.652	0.57	0.0007412480262	3
Prps.2	6.66E-08	0.387119495207165	0.514	0.321	0.0007945008441	3
Mondo.1	7.30E-08	0.250336446814534	0.305	0.183	0.0008702342357	3
scrib	7.61E-08	-0.705655211568932	0.257	0.319	0.0009074996368	3
Fer1HCH.1	8.47E-08	0.293939080916089	0.705	0.509	0.0010104534855	3
alc.1	8.70E-08	0.349162525789013	0.414	0.256	0.0010372851868	3
CG1637	8.90E-08	0.665309870256895	0.31	0.146	0.0010617099769	3

rhea.1	8.99E-08	-0.283865877224216	0.424	0.36	0.0010718324418	3
AdSS.2	9.10E-08	0.710755943252319	0.333	0.164	0.0010857200246	3
CycG.1	9.66E-08	0.376727738386363	0.886	0.72	0.0011527913938	3
Svil.1	9.91E-08	-0.578130857424555	0.424	0.432	0.0011824791164	3
step.1	1.01E-07	0.434981171956066	0.595	0.392	0.0012019623599	3
cno.2	1.05E-07	0.569723463877752	0.524	0.318	0.0012568437945	3
GstD1.1	1.13E-07	-0.678042301621328	0.305	0.276	0.0013426060425	3
bip2	1.14E-07	0.41450956210642	0.59	0.398	0.0013628129654	3
RpS7.1	1.21E-07	-0.824659573032428	0.252	0.308	0.0014418273314	3
RpL31	1.24E-07	-0.659107482172964	0.233	0.258	0.0014737213326	3
Rab7.2	1.24E-07	0.393586754064347	0.238	0.116	0.0014775374165	3
sta	1.33E-07	-0.590671465740614	0.267	0.277	0.0015898437711	3
spin.1	1.36E-07	0.267709939339253	0.557	0.38	0.0016272720175	3
RpS25	1.42E-07	-0.527509481559156	0.248	0.233	0.0016880106565	3
mt:CoI.1	1.42E-07	-0.740829073451362	0.171	0.202	0.0016988561446	3
scyl	1.52E-07	0.257798356479547	0.676	0.485	0.0018088653105	3
bwa.2	1.56E-07	0.69512900797887	0.286	0.134	0.0018586927866	3
Pxn.2	1.58E-07	-0.669537258304447	0.514	0.548	0.0018886163763	3
RpL32.1	1.60E-07	-0.851860973425808	0.233	0.291	0.0019067764293	3
bin3	1.61E-07	0.272371084313564	0.3	0.178	0.0019195955219	3
Mapmodulin.2	1.74E-07	0.286289595239454	0.286	0.164	0.0020707321309	3
vir-1.2	1.90E-07	-0.805144701589895	0.324	0.302	0.0022627799209	3
Su(z)2	1.97E-07	0.498668076380089	0.143	0.054	0.0023531089434	3
CG30046	2.00E-07	0.361917917856802	0.281	0.161	0.0023833862942	3
CG13907	2.01E-07	0.298592822637415	0.314	0.195	0.0024011743145	3
fax.1	2.02E-07	0.337173289590805	0.776	0.585	0.0024059514477	3
jim.2	2.13E-07	0.54228903310569	0.633	0.423	0.0025392322781	3
RhoGAP71E.1	2.15E-07	-0.447852934556401	0.557	0.554	0.0025706317926	3
CG42542	2.38E-07	0.478636599801107	0.429	0.249	0.0028450535246	3
ABCD	2.56E-07	0.326501450413701	0.357	0.215	0.0030534693076	3
CG2233	2.59E-07	-0.962829874020814	0.014	0.117	0.0030876297252	3
Arc1.1	2.95E-07	-1.15832771323043	0.129	0.105	0.0035136855845	3
RhoGAP15B.1	3.11E-07	0.412188794903409	0.338	0.189	0.0037057827618	3
unk.2	3.21E-07	0.351699301912965	0.333	0.198	0.0038265729013	3
CDase	3.29E-07	0.435904002467194	0.119	0.041	0.003921575169	3
Paip2.2	3.37E-07	0.572028661417677	0.386	0.213	0.0040246082144	3
RpL24	3.52E-07	-0.781852243536358	0.205	0.284	0.0042039813924	3
mgl.1	3.77E-07	-1.33800885922457	0.219	0.335	0.0045009382488	3
RpS18.1	3.99E-07	-0.339401166326109	0.367	0.306	0.0047629639362	3
l(3)L1231.1	4.48E-07	0.329946636979948	0.867	0.702	0.0053443740247	3
RpL23	4.50E-07	-0.561894308299002	0.324	0.332	0.005368457617	3
CG18135.2	4.64E-07	0.617394661193937	0.514	0.318	0.0055339359816	3
RpS9.1	4.67E-07	-0.353985176265118	0.29	0.239	0.0055650699525	3
RpS28b.1	4.70E-07	-0.446749363516989	0.229	0.224	0.0056057982855	3
RpS8.1	5.01E-07	-0.405661030803671	0.376	0.321	0.0059808346066	3
CG42524.2	5.02E-07	-0.475024691134287	0.343	0.37	0.0059843710565	3
CG30089.2	5.24E-07	0.261249322738689	0.538	0.378	0.0062482482018	3
SREBP.2	5.93E-07	0.307792326681031	0.281	0.162	0.0070692174326	3
Drat.2	5.94E-07	0.31062657592985	0.305	0.175	0.0070800321465	3
Dmtn	6.31E-07	0.327814009715068	0.476	0.307	0.0075328502768	3
Mur2B	6.39E-07	0.256812392964107	0.643	0.461	0.0076188835376	3
RpL23A	6.90E-07	-0.485206056940219	0.19	0.172	0.008233482379	3
CHES-1-like.2	7.96E-07	0.304930363857806	0.505	0.35	0.0094924215257	3
CG15309	8.33E-07	0.316732491364971	0.21	0.112	0.0099426614076	3
CG34331	8.34E-07	0.272484698543709	0.214	0.115	0.0099512388176	3
lap.1	9.65E-07	0.291217241649805	0.571	0.406	0.0115143742148	3
Act5C.2	1.05E-06	-0.718492462585442	0.319	0.373	0.0125372713084	3
Haspin.1	1.08E-06	-0.263881477708771	0.252	0.227	0.0128973166231	3
wake.2	1.16E-06	-0.717902303664886	0.395	0.44	0.0138234089329	3
CG17754.1	1.22E-06	0.352825258196109	0.252	0.147	0.01454090019	3

Idh.1	1.32E-06	0.47071493844447	0.257	0.127	0.0157702373821	3
MCPH1.1	1.44E-06	0.299773997393448	0.248	0.139	0.0171540032584	3
CG1578.1	1.50E-06	0.303397702844113	0.395	0.25	0.0179091675479	3
Vha100-2.2	1.63E-06	-0.290233274570722	0.243	0.221	0.0194731974896	3
CG4080	1.73E-06	0.453273173341873	0.643	0.455	0.0206855729776	3
spg.2	1.78E-06	0.27932920473449	0.224	0.127	0.0212368083416	3
slpr.1	1.79E-06	0.482027791170556	0.229	0.114	0.0213913066739	3
CG4911	1.81E-06	0.308791238940375	0.238	0.133	0.0215517240641	3
Hipk	1.97E-06	0.341370287086756	0.714	0.526	0.0235150416282	3
Btk29A.2	2.01E-06	0.308511029581569	0.89	0.752	0.0239259589941	3
CG5080.2	2.17E-06	0.529087035480707	0.676	0.492	0.025842776748	3
Drak.2	2.20E-06	-0.481048868160896	0.495	0.51	0.0262691320042	3
galla-1.1	2.28E-06	0.319554020568064	0.2	0.101	0.0271926682298	3
hzg.1	2.38E-06	-0.369598537275305	0.176	0.168	0.0283579715486	3
Ald1.1	2.55E-06	-0.509622021165498	0.352	0.333	0.0304233635789	3
Gdh.1	2.62E-06	0.448072267857711	0.176	0.069	0.0312160608755	3
Vha100-1	2.63E-06	0.253451676775692	0.2	0.111	0.0313612297596	3
RpL34b	2.76E-06	-0.57725843181108	0.21	0.219	0.0328891679406	3
px.1	2.89E-06	0.250845609889354	0.9	0.753	0.034481170945	3
nmo	2.89E-06	-0.269589399241302	0.305	0.256	0.0345304024922	3
CG10082.1	3.14E-06	0.375694724495009	0.41	0.254	0.0375032770788	3
spir.1	3.16E-06	-0.411063912667716	0.495	0.447	0.0376663975412	3
cdi.1	3.24E-06	-0.506935838745604	0.3	0.3	0.0386916178478	3
CG9701.2	3.39E-06	0.770959129656833	0.2	0.083	0.0404647993976	3
sm	3.46E-06	-0.335147193269629	0.276	0.236	0.0412242080082	3
Drs	3.86E-06	-1.05291109019903	0.095	0.12	0.046011558018	3
CG2201	3.96E-06	-0.454333141174861	0.124	0.133	0.0472267430268	3
COX6B	3.99E-06	-0.36554939886172	0.129	0.117	0.0475824351414	3
Dyrk2.1	4.05E-06	0.451670796271031	0.719	0.536	0.0483210629738	3
sky.1	4.10E-06	0.276816346360274	0.786	0.62	0.0488678612909	3
flw.2	4.15E-06	-0.697295119808303	0.319	0.364	0.0495102534689	3
eEF1alpha1.2	4.87E-15	0.936512974405452	0.582	0.512	5.81E-11	4
Mst84Da.2	2.47E-14	1.40178832329455	0.328	0.132	2.95E-10	4
CG2233.1	1.04E-13	1.70921282310769	0.269	0.072	1.24E-09	4
Ppn.1	1.75E-13	0.573812859313076	1	0.96	2.09E-09	4
RpL31.1	7.31E-13	1.02602864494543	0.353	0.237	8.72E-09	4
RpS25.1	8.20E-12	1.23038825332276	0.398	0.207	9.78E-08	4
RpS27.2	8.96E-12	1.04673095157903	0.433	0.291	1.07E-07	4
Inos	2.30E-11	0.934065383544328	0.647	0.496	2.74E-07	4
RpL35A.2	3.19E-11	1.06509709814655	0.348	0.197	3.80E-07	4
RpL10Ab.2	3.99E-11	1.04183140861749	0.398	0.236	4.76E-07	4
RpL8.1	1.17E-10	1.0022098768417	0.388	0.25	1.40E-06	4
RpS13	2.40E-10	1.00355774172317	0.343	0.223	2.86E-06	4
Eip93F	2.60E-10	-0.418309412214887	0.985	0.994	3.10E-06	4
Obp99c.1	5.75E-10	1.19125783576766	0.219	0.101	6.86E-06	4
eEF2.3	1.36E-09	0.86496703020927	0.438	0.293	1.62E-05	4
RpL21.3	1.76E-09	0.980992584980417	0.373	0.258	2.10E-05	4
InR.3	1.90E-09	-0.753364690938545	0.786	0.865	2.26E-05	4
cathD	1.93E-09	0.94248068035287	0.284	0.206	2.30E-05	4
RpL28.2	2.10E-09	0.848639585298234	0.393	0.325	2.51E-05	4
lilli	4.84E-09	-0.401832750203563	0.522	0.745	5.77E-05	4
CG42788.1	5.48E-09	0.560930526408355	0.249	0.273	6.53E-05	4
RpL36.1	8.43E-09	0.833488732415874	0.338	0.27	0.0001005049702	4
RpL27A.2	9.82E-09	0.951674393531336	0.488	0.359	0.0001171976524	4
Desat1	1.10E-08	1.25922089966806	0.299	0.123	0.0001310042436	4
CG14245.2	1.28E-08	1.48861045886729	0.184	0.122	0.0001531400763	4
Cyp4g1	1.54E-08	1.6019592741483	0.388	0.216	0.0001838880091	4
mt:CoI.2	1.98E-08	0.895754009549248	0.269	0.185	0.0002359639526	4
RpL7.1	2.21E-08	0.787699614082168	0.284	0.237	0.0002637711947	4
RpL14.1	3.07E-08	0.950569661812994	0.393	0.293	0.0003657621768	4

RpL26.1	3.63E-08	0.825926687183751	0.358	0.258	0.0004324959924	4
RpL11.1	3.82E-08	0.915399562271482	0.284	0.181	0.0004554489176	4
RpS18.2	3.85E-08	0.835421002656854	0.418	0.298	0.0004590924476	4
RpLP2.1	4.09E-08	0.933668704778794	0.299	0.185	0.0004873714561	4
RpS17.2	4.53E-08	0.956449930690613	0.274	0.208	0.0005403780805	4
RpS4.1	4.57E-08	0.930326547651795	0.299	0.194	0.0005446540289	4
RpL32.2	5.43E-08	0.800309994515723	0.353	0.27	0.0006482585785	4
RpS28b.2	5.75E-08	0.789266049796187	0.294	0.213	0.0006858379777	4
RpS9.2	6.47E-08	0.866319936579521	0.353	0.229	0.0007717550211	4
Mst57Db.1	6.94E-08	0.975357685007016	0.239	0.132	0.0008273844736	4
RpL37A.2	7.45E-08	0.905939482988465	0.264	0.183	0.0008887458359	4
CG7766.1	1.00E-07	0.461148893953984	0.159	0.151	0.0011929832451	4
CG16758.2	1.37E-07	0.965261139420053	0.224	0.083	0.0016327588955	4
CG3662	1.43E-07	0.469142020835293	0.348	0.342	0.0017095520177	4
RpL15.2	1.48E-07	0.782977793221353	0.383	0.301	0.0017641374001	4
CG3124	1.59E-07	0.900602917115372	0.134	0.041	0.0018910633316	4
RpL35.2	1.66E-07	0.885003987811209	0.303	0.207	0.0019859994015	4
awd.1	1.80E-07	0.749329366441465	0.154	0.11	0.0021484763553	4
CG31226	1.89E-07	1.0360316318312	0.154	0.07	0.0022500251929	4
CG46059	2.00E-07	0.924620677194567	0.129	0.058	0.0023814788958	4
lcs.1	2.00E-07	1.10696260766346	0.299	0.179	0.0023896805679	4
RpL27.2	2.08E-07	0.822916658281648	0.323	0.255	0.002476929629	4
hppy.1	2.32E-07	-0.440018169501951	0.418	0.612	0.0027715626103	4
RpS10b.1	2.64E-07	0.926697540535153	0.358	0.225	0.0031531232743	4
RpS29.1	2.79E-07	0.957249279952114	0.303	0.187	0.0033335550456	4
Got2.1	2.89E-07	0.854938545094138	0.149	0.081	0.0034506100868	4
CG1648.2	3.17E-07	1.33185631644574	0.144	0.131	0.0037844584854	4
Fas3.3	3.23E-07	-1.91053722997782	0.09	0.243	0.0038575051936	4
CG6503.1	3.76E-07	0.603863347571765	0.129	0.03	0.0044809976208	4
NimB2	4.77E-07	0.583198470892037	0.274	0.236	0.0056851982599	4
RpL41	4.88E-07	0.862004488945127	0.428	0.266	0.0058158039883	4
RpS21.2	4.91E-07	0.955580163037721	0.373	0.229	0.0058558672993	4
CG42674.2	5.44E-07	-1.26018001888435	0.025	0.137	0.0064934879881	4
RpLP1.2	6.10E-07	0.957366301745282	0.338	0.221	0.0072741148874	4
CG5080.3	7.81E-07	0.64708037773412	0.567	0.512	0.0093125110188	4
GEFmeso.2	8.33E-07	-0.728258227337812	0.279	0.463	0.0099400895899	4
RpL13	9.82E-07	0.734919036458735	0.313	0.24	0.0117105504636	4
SPARC.1	1.18E-06	0.539156076959753	0.612	0.504	0.014040481405	4
RpL39	1.33E-06	0.905872765503611	0.299	0.21	0.0158160142638	4
lectin-24Db.2	1.34E-06	0.590311077077747	0.154	0.13	0.0160222604234	4
RpS2	1.39E-06	0.785997249939405	0.294	0.179	0.0165553115987	4
spir.2	1.44E-06	-0.927837056568672	0.289	0.483	0.0172045819257	4
RpS30.2	1.45E-06	0.856448823048755	0.333	0.218	0.0172542704014	4
hid.2	1.80E-06	-0.816190021028425	0.219	0.398	0.0214215289675	4
RpS3.1	1.80E-06	0.805111843744539	0.264	0.176	0.0214739394391	4
ocn	1.81E-06	0.958231088555501	0.129	0.059	0.0216298143537	4
ATPsynD	1.88E-06	0.745081337576209	0.129	0.069	0.0223913075574	4
BG642312	2.08E-06	1.00667528995515	0.139	0.061	0.0248015088112	4
bun.2	2.21E-06	-0.543297858608794	0.741	0.856	0.0264117493109	4
Mob2.3	2.33E-06	-0.56132333335042	0.736	0.857	0.0277377655985	4
Fim.1	2.34E-06	-0.785863753753718	0.219	0.393	0.0278658755866	4
prage.3	2.44E-06	-1.06953997362873	0.149	0.316	0.0291408158703	4
ACC.1	2.45E-06	0.906031095266012	0.189	0.128	0.0292752276677	4
RpL3.2	2.60E-06	0.72043225732193	0.328	0.25	0.0309685624609	4
msi.1	2.80E-06	-0.455198301508616	0.786	0.866	0.0334549378003	4
eEF1beta	2.99E-06	0.781371077295109	0.189	0.115	0.0356383556195	4
Hml.3	3.02E-06	0.49004949729222	0.776	0.629	0.0360826224148	4
MtnA.2	3.15E-06	0.802305348256153	0.388	0.278	0.0375415473756	4
Ance-5.1	3.23E-06	0.678788230226699	0.204	0.142	0.038561643987	4
Diap1	3.57E-06	-0.673537839246777	0.308	0.491	0.0425425598263	4

RpL7A	3.64E-06	0.619031392969284	0.323	0.261	0.043446558823	4
Abl	3.76E-06	-0.642103574193539	0.542	0.718	0.0448824420554	4
CG12581	4.11E-64	2.82073566819943	0.449	0.018	4.90E-60	5
CG17839.4	2.68E-58	3.19678083316368	0.52	0.05	3.20E-54	5
dpy	2.73E-38	3.22234795432207	0.313	0.015	3.25E-34	5
grh	9.70E-38	2.31071028239617	0.313	0.018	1.16E-33	5
mgl.3	2.11E-37	2.20247650886107	0.667	0.258	2.51E-33	5
Fas2	4.54E-30	2.24365654798538	0.308	0.031	5.41E-26	5
CG8740.2	9.09E-30	1.98749658913401	0.348	0.045	1.08E-25	5
jbug	2.32E-28	1.94439806490792	0.212	0.006	2.77E-24	5
hth.1	4.79E-27	2.35617531642719	0.323	0.051	5.72E-23	5
pyd.3	8.07E-26	2.15195615123538	0.333	0.059	9.62E-22	5
Tie	3.04E-25	1.97086686390188	0.217	0.018	3.62E-21	5
ELOVL	6.37E-25	2.49057173809767	0.202	0.009	7.60E-21	5
CG11073	8.20E-25	1.62162396221701	0.187	0.008	9.78E-21	5
Cda5	1.23E-24	1.88911439980088	0.207	0.012	1.47E-20	5
form3	1.80E-24	2.10059258851659	0.212	0.011	2.15E-20	5
ed.3	7.62E-24	1.70717090481219	0.505	0.166	9.09E-20	5
CG8180	1.56E-23	1.95936684071358	0.192	0.007	1.86E-19	5
siz.2	7.35E-23	1.6145715724054	0.424	0.112	8.76E-19	5
Dys.4	1.11E-22	1.68648376984811	0.439	0.124	1.32E-18	5
Fas3.4	1.40E-21	0.740040421736059	0.51	0.172	1.67E-17	5
crb	1.92E-21	1.8612541026741	0.247	0.029	2.30E-17	5
pdm3	7.41E-21	1.9893085475526	0.172	0.009	8.84E-17	5
vvl	5.18E-20	1.6488445273231	0.227	0.027	6.18E-16	5
CG33970	7.52E-20	2.47638364006136	0.177	0.009	8.97E-16	5
CG30460	8.12E-20	1.79893620154641	0.232	0.031	9.69E-16	5
CG6040	2.38E-19	1.63768078666897	0.227	0.027	2.84E-15	5
snu	6.47E-19	1.56896348929837	0.202	0.027	7.71E-15	5
CG6959	9.00E-19	1.4640148539517	0.237	0.036	1.07E-14	5
Nost	9.12E-19	1.681069501888	0.258	0.039	1.09E-14	5
CG34398	1.38E-18	2.00995807423664	0.187	0.015	1.65E-14	5
ASPP	1.71E-18	1.55009034812052	0.187	0.015	2.04E-14	5
CG34120	1.73E-18	2.11789091546304	0.177	0.015	2.06E-14	5
CG33110	1.84E-18	1.82893213718574	0.167	0.009	2.19E-14	5
RhoGEF64C	1.01E-17	1.86715077044877	0.146	0.006	1.20E-13	5
stw	1.39E-17	1.67894677716945	0.197	0.022	1.66E-13	5
CG32521.1	2.48E-17	1.66952939618763	0.308	0.075	2.95E-13	5
Lmpt.3	4.80E-17	1.78451867233145	0.323	0.081	5.73E-13	5
CG12814	1.72E-16	1.52891565534872	0.187	0.018	2.05E-12	5
sick.2	2.07E-16	1.77174169570269	0.298	0.07	2.47E-12	5
Hpd	2.19E-16	1.91712496610647	0.172	0.019	2.62E-12	5
CG9628	2.82E-16	1.31158121504037	0.192	0.026	3.36E-12	5
bru2	2.84E-16	1.58655364951058	0.237	0.045	3.38E-12	5
Wdr62.1	5.03E-16	1.05557899070494	0.631	0.414	6.00E-12	5
CG4928	6.79E-16	1.9502324555258	0.222	0.06	8.10E-12	5
nahoda	8.30E-16	1.32407828962826	0.131	0.007	9.90E-12	5
CG32694	1.38E-15	1.66292824532561	0.141	0.013	1.64E-11	5
CG3655	1.54E-15	1.5264063626582	0.187	0.022	1.83E-11	5
ovo	2.11E-15	1.42745667265416	0.131	0.007	2.51E-11	5
CG41520.1	2.31E-15	1.60384376653916	0.424	0.175	2.75E-11	5
sv	1.13E-14	1.82047943010866	0.116	0.006	1.34E-10	5
toc.4	1.72E-14	1.50651753746865	0.268	0.069	2.05E-10	5
rdgA.1	2.10E-14	1.2632522646121	0.359	0.119	2.51E-10	5
CG32137	2.59E-14	1.3400543319881	0.177	0.021	3.09E-10	5
CG43759	4.04E-14	1.49044387881662	0.146	0.015	4.81E-10	5
sprt	4.20E-14	1.38049650307373	0.146	0.013	5.01E-10	5
Best2	4.97E-14	1.13091497059409	0.157	0.017	5.92E-10	5
Msr-110	5.15E-14	1.9421799805343	0.227	0.061	6.15E-10	5
bi	7.70E-14	1.91041749806079	0.106	0.004	9.19E-10	5

Ets98B	7.97E-14	1.2618869936624	0.162	0.019	9.51E-10	5
dnr1	1.01E-13	1.7032370656918	0.182	0.033	1.20E-09	5
CG2841	1.14E-13	1.51223662813052	0.141	0.013	1.36E-09	5
Kank	1.24E-13	1.38086229442623	0.167	0.025	1.48E-09	5
sdt	1.86E-13	1.3487670185576	0.242	0.052	2.22E-09	5
CG31176	4.56E-13	1.98079071726863	0.121	0.009	5.44E-09	5
Gs2.1	6.60E-13	1.36957612865016	0.348	0.124	7.88E-09	5
Ptp10D	2.14E-12	1.36668166083459	0.232	0.055	2.55E-08	5
CG14830	2.32E-12	1.09474833398214	0.101	0.006	2.77E-08	5
pio	2.70E-12	1.18730742732376	0.116	0.009	3.22E-08	5
bowl	2.87E-12	1.08745390986779	0.121	0.009	3.42E-08	5
Sp1	4.05E-12	1.24641551397887	0.106	0.007	4.84E-08	5
CG17834	4.64E-12	1.55379997105354	0.141	0.02	5.54E-08	5
Amph	1.60E-11	1.3699469373971	0.232	0.057	1.90E-07	5
CG6398	1.79E-11	1.15822038833728	0.126	0.014	2.14E-07	5
CG3168.1	2.05E-11	1.32410909072678	0.253	0.084	2.44E-07	5
osp	2.73E-11	1.25999074713829	0.212	0.052	3.25E-07	5
CG6409.1	5.27E-11	1.28922596837188	0.192	0.077	6.29E-07	5
caps.3	6.65E-11	1.12616355405047	0.263	0.076	7.93E-07	5
CG32264.3	1.14E-10	0.854978197923121	0.652	0.411	1.36E-06	5
Rbp6	1.61E-10	1.90262144036739	0.182	0.057	1.92E-06	5
kmr	1.79E-10	1.06054635440413	0.136	0.021	2.13E-06	5
sog	2.01E-10	1.35303971044389	0.187	0.039	2.40E-06	5
cpo.2	3.42E-10	0.735925896734456	0.833	0.679	4.08E-06	5
CG8312.1	5.79E-10	1.00421569721361	0.616	0.414	6.91E-06	5
Fas1	7.27E-10	0.926020007831707	0.182	0.039	8.67E-06	5
GstT4	1.40E-09	1.13129328634988	0.202	0.051	1.68E-05	5
CG42327	1.51E-09	1.14865501177131	0.141	0.024	1.81E-05	5
zormin	1.86E-09	1.01624489271776	0.136	0.024	2.22E-05	5
CG11147	2.09E-09	1.06382487846654	0.126	0.018	2.49E-05	5
cv-2.1	2.35E-09	1.73346368688969	0.207	0.065	2.80E-05	5
chas	2.49E-09	1.02496475089672	0.111	0.011	2.97E-05	5
bbg	3.82E-09	1.27222791170672	0.121	0.021	4.56E-05	5
scrib.1	4.60E-09	0.921579175089883	0.48	0.28	5.49E-05	5
CG42673	4.67E-09	1.3489478933044	0.111	0.015	5.57E-05	5
Nrg.4	6.95E-09	0.703995135436859	0.293	0.116	8.29E-05	5
Msp300.2	1.38E-08	0.923032503573533	0.697	0.55	0.0001641539376	5
nrm	1.41E-08	1.02507775912871	0.101	0.013	0.0001677190799	5
Pura	1.55E-08	1.06190429025536	0.106	0.014	0.0001844364312	5
CenG1A.1	2.10E-08	0.993542867516391	0.293	0.145	0.0002508349435	5
Ddc	2.23E-08	0.940642613726841	0.106	0.014	0.0002654680498	5
EbpIII	2.58E-08	1.13477101386183	0.177	0.07	0.0003079517653	5
fng	3.50E-08	1.08392565215095	0.101	0.016	0.0004179704056	5
CG7378	3.83E-08	1.13054345674624	0.116	0.019	0.0004573850372	5
csw	3.92E-08	0.971280148716596	0.394	0.234	0.0004672643021	5
bab2	5.09E-08	1.26169726400605	0.116	0.027	0.0006077742149	5
SPoCk	5.57E-08	1.06820032724577	0.172	0.057	0.0006646789551	5
sima	6.38E-08	0.56878772050336	0.859	0.78	0.0007614399332	5
Gp150	7.72E-08	0.853500306127669	0.187	0.061	0.0009209720893	5
emp	8.53E-08	0.966751703806653	0.131	0.033	0.0010177683073	5
pum.1	2.00E-07	-0.339908235627545	0.99	0.995	0.0023841494372	5
fus	2.07E-07	0.747376235958421	0.141	0.035	0.0024678234363	5
Egfr	2.23E-07	0.983594980620053	0.182	0.053	0.0026619753153	5
Hex-A.1	2.50E-07	0.864695725806822	0.439	0.261	0.0029840535537	5
T48	2.70E-07	1.04252013367841	0.167	0.046	0.0032247196061	5
how.1	2.98E-07	1.01506279328951	0.434	0.257	0.0035580934741	5
plx	3.26E-07	0.924243454002575	0.121	0.026	0.0038909561647	5
dally	4.99E-07	1.339826317757	0.136	0.04	0.0059501412085	5
sm.1	5.99E-07	0.984188743308983	0.359	0.222	0.0071502738178	5
Bx	7.94E-07	0.994245487066472	0.157	0.043	0.0094674994953	5

rols	1.23E-06	0.998404470637188	0.101	0.022	0.0146541894907	5
jing.2	1.33E-06	0.856601260617102	0.343	0.172	0.0158857377857	5
msn.1	2.20E-06	-0.527843197171642	0.813	0.895	0.0262766454244	5
tna.3	2.48E-06	0.501800058466302	0.374	0.196	0.0295546582699	5
Eaat1	3.07E-06	0.831789714620402	0.111	0.028	0.0366469381999	5
ex	3.10E-06	0.87311325544345	0.172	0.067	0.0369955043365	5
ps	3.69E-06	0.338216163601067	0.98	0.913	0.0440240181697	5
Cip4.4	1.53E-79	2.31198871856296	0.89	0.481	1.83E-75	6
luna.3	4.60E-61	1.63596995942019	0.983	0.779	5.49E-57	6
spir.3	1.25E-60	2.17208729571211	0.919	0.388	1.50E-56	6
Myo31DF.4	2.54E-53	2.69465049881466	0.692	0.154	3.02E-49	6
mamo.1	4.08E-42	-1.76135404578201	0.488	0.901	4.86E-38	6
Myc.2	7.18E-42	1.94282314129141	0.767	0.423	8.56E-38	6
cher.3	1.42E-41	2.68603383823239	0.465	0.052	1.70E-37	6
Fas3.5	6.39E-41	3.15326390179933	0.576	0.169	7.63E-37	6
Act5C.3	1.60E-40	2.02419150423245	0.733	0.312	1.91E-36	6
AnxB9.3	4.91E-40	2.10125504630921	0.721	0.268	5.86E-36	6
MCU.3	1.11E-38	2.5828817702538	0.442	0.053	1.32E-34	6
Dscam1.4	3.02E-34	2.00732519231755	0.628	0.206	3.61E-30	6
Ppn.2	5.51E-32	-1.17441880742761	0.884	0.977	6.57E-28	6
RhoGAP71E.3	1.19E-31	1.53262892583706	0.814	0.517	1.42E-27	6
fog.3	7.24E-31	-1.79985692715253	0.262	0.697	8.63E-27	6
Col4a1.2	1.37E-30	-1.10323254474797	0.797	0.943	1.63E-26	6
Pgant9.1	1.64E-30	-1.67633167990383	0.349	0.756	1.96E-26	6
Spn.3	2.15E-30	-1.82906010953569	0.302	0.726	2.56E-26	6
Btk29A.4	3.77E-30	-1.62763920794425	0.453	0.82	4.50E-26	6
Naam.2	1.50E-29	2.08395250615486	0.587	0.203	1.79E-25	6
CG6891.1	7.78E-29	2.0691803096194	0.355	0.048	9.28E-25	6
Mmp2.4	4.24E-27	1.65204249855055	0.779	0.415	5.06E-23	6
CG12991.1	7.25E-27	2.09273240844404	0.343	0.043	8.65E-23	6
Pxn.3	8.63E-27	-2.36255249697619	0.198	0.592	1.03E-22	6
GEFmeso.3	1.65E-26	1.43038263412882	0.75	0.39	1.97E-22	6
MYPT-75D.2	2.89E-26	-2.13412405421835	0.18	0.592	3.45E-22	6
mys.2	5.01E-26	1.49754566770972	0.698	0.355	5.97E-22	6
CG3726.1	5.75E-26	-1.56155991236659	0.279	0.693	6.86E-22	6
CG15673	6.29E-26	2.01098184381879	0.32	0.034	7.50E-22	6
Pvr.3	9.35E-26	-1.06957931417026	0.663	0.909	1.12E-21	6
stac	2.67E-25	1.97701377162183	0.331	0.044	3.18E-21	6
aqz.1	2.80E-25	-1.23077430112767	0.738	0.92	3.34E-21	6
Men-b.3	3.26E-25	2.00983157980392	0.378	0.063	3.89E-21	6
CG5399	7.03E-25	2.20457619941179	0.337	0.044	8.38E-21	6
px.2	7.41E-25	-1.31097838211605	0.541	0.81	8.84E-21	6
mtd.2	8.33E-25	-1.3940929916382	0.517	0.794	9.93E-21	6
Sema2a.3	1.38E-24	-2.40216320438423	0.11	0.496	1.65E-20	6
rhea.3	1.61E-24	1.53507733825612	0.64	0.331	1.92E-20	6
Ae2.2	2.62E-24	1.95715960126434	0.494	0.158	3.13E-20	6
Pax.2	1.85E-23	1.70452412548743	0.541	0.185	2.20E-19	6
CG31145.2	1.06E-22	-1.3577974254814	0.488	0.782	1.27E-18	6
Fim.3	1.16E-22	1.52397488441846	0.68	0.322	1.39E-18	6
loco.2	1.81E-22	2.00786692876478	0.39	0.086	2.15E-18	6
CG43867.2	1.92E-22	2.01791885541131	0.448	0.123	2.28E-18	6
Xrp1.2	2.33E-22	1.33892815733283	0.919	0.678	2.78E-18	6
schlank.2	4.32E-22	1.85106970801662	0.407	0.097	5.15E-18	6
Prosap.1	1.21E-21	-0.590106749399883	0.808	0.966	1.45E-17	6
Inos.2	2.62E-21	-1.81966996155248	0.186	0.566	3.12E-17	6
wge.3	6.65E-21	1.59008951617564	0.512	0.172	7.94E-17	6
pyr	9.66E-21	2.28195967453643	0.262	0.033	1.15E-16	6
sr.1	1.49E-20	-1.66502434976002	0.25	0.576	1.78E-16	6
cic.1	2.03E-20	-1.06147808866176	0.884	0.966	2.43E-16	6
vir-1.3	3.73E-20	1.91632832946651	0.581	0.266	4.45E-16	6

lola	5.86E-20	-0.797333821213819	0.843	0.956	6.99E-16	6
CG40006.1	6.00E-20	-1.2571068056644	0.308	0.663	7.15E-16	6
vkg.2	7.86E-20	-1.16982168559847	0.57	0.845	9.38E-16	6
CG5004.3	7.98E-20	1.70909410469832	0.331	0.062	9.52E-16	6
Hml.4	1.05E-19	-1.45927693905627	0.355	0.694	1.25E-15	6
TotM	4.15E-19	2.9518444511814	0.227	0.025	4.95E-15	6
fax.3	5.99E-19	1.14100383530658	0.843	0.581	7.14E-15	6
betaTub60D.4	6.20E-19	1.70081276705519	0.529	0.215	7.40E-15	6
Cam.2	9.25E-19	1.36539357832915	0.733	0.478	1.10E-14	6
scb.2	1.26E-18	1.66172342799268	0.413	0.112	1.51E-14	6
Socs36E.2	1.53E-18	1.80849600870425	0.448	0.211	1.83E-14	6
Gadd45.2	3.38E-18	1.89971915480147	0.395	0.108	4.03E-14	6
cdi.2	1.20E-17	1.35350464011676	0.576	0.26	1.43E-13	6
gce.2	1.57E-17	-1.45165032479568	0.262	0.583	1.87E-13	6
CD98hc.1	1.65E-17	1.5349776431715	0.297	0.06	1.97E-13	6
Sr-CI.2	1.76E-17	-1.43840448792984	0.297	0.619	2.10E-13	6
Rtnl1.2	3.83E-17	1.57605777026156	0.349	0.087	4.57E-13	6
kek1.1	5.08E-17	1.92637855746803	0.471	0.212	6.06E-13	6
CG9328.1	5.47E-17	-1.64372029177854	0.192	0.522	6.52E-13	6
CG17760.1	8.51E-17	1.81732871386931	0.297	0.064	1.01E-12	6
Eb1.2	1.05E-16	1.28131507250307	0.57	0.288	1.25E-12	6
CG32486.3	1.11E-16	-1.36635439139745	0.273	0.579	1.32E-12	6
CG42674.4	2.54E-16	1.70258931803086	0.331	0.09	3.04E-12	6
Abl.2	2.63E-16	1.12286753047879	0.826	0.673	3.14E-12	6
CG1572	4.95E-16	1.46661323136707	0.291	0.057	5.90E-12	6
Ac76E.2	6.88E-16	1.48226324358952	0.424	0.144	8.20E-12	6
Hsp83.2	1.14E-15	1.56603524309602	0.663	0.369	1.36E-11	6
bbc.2	1.37E-15	1.46141217035561	0.471	0.19	1.63E-11	6
Nrg.5	1.90E-15	1.94366852178558	0.337	0.113	2.27E-11	6
regucalcin.5	2.46E-15	-1.50306496262481	0.221	0.534	2.94E-11	6
Myo61F	3.44E-15	1.51123450393555	0.244	0.046	4.11E-11	6
alphaTub84B.2	4.24E-15	1.50119271241632	0.488	0.201	5.06E-11	6
CG12163.2	6.89E-15	-1.27420256182726	0.297	0.6	8.22E-11	6
chic.1	7.51E-15	1.04239638758348	0.64	0.328	8.96E-11	6
Frl.1	1.19E-14	1.19388632214147	0.587	0.367	1.42E-10	6
foxo.1	1.45E-14	-1.22076450661154	0.297	0.589	1.73E-10	6
tai.2	2.10E-14	-0.82765349913163	0.692	0.839	2.51E-10	6
CG6006.2	3.83E-14	1.62438819312218	0.349	0.125	4.57E-10	6
srp.1	3.88E-14	-0.585436406685323	0.797	0.93	4.63E-10	6
Shrm.1	5.35E-14	0.941584015093946	0.227	0.049	6.38E-10	6
lectin-28C.3	6.08E-14	-1.21322479239875	0.384	0.666	7.25E-10	6
Imp.3	6.94E-14	0.980014071026558	0.709	0.414	8.28E-10	6
Arc1.2	7.76E-14	2.23968702925476	0.285	0.083	9.26E-10	6
Galphai.2	9.20E-14	1.24871211791309	0.488	0.227	1.10E-09	6
GlcAT-P.2	1.07E-13	-1.19967610883128	0.262	0.57	1.28E-09	6
Ten-m.3	1.66E-13	-0.507922568570978	0.994	0.996	1.98E-09	6
CG7120.3	2.05E-13	-1.40931442959463	0.209	0.497	2.45E-09	6
capu.2	4.10E-13	1.48943507004663	0.413	0.169	4.89E-09	6
CG31523.2	4.10E-13	1.32204176482925	0.413	0.148	4.89E-09	6
zfh1.2	4.21E-13	-0.637997511963193	0.773	0.933	5.03E-09	6
LamC	4.81E-13	1.20315191498071	0.244	0.049	5.74E-09	6
fz2.1	1.02E-12	-1.19766802922975	0.273	0.555	1.21E-08	6
RhoGAP18B.1	1.13E-12	1.16387178865409	0.599	0.362	1.35E-08	6
KrT95D.3	1.25E-12	1.34682621380297	0.506	0.279	1.49E-08	6
Sema5c.2	1.67E-12	-1.42558168462876	0.285	0.544	1.99E-08	6
CG10543.1	2.13E-12	-0.976747992736242	0.57	0.76	2.54E-08	6
Pkn.2	2.18E-12	-1.17153445421483	0.297	0.558	2.60E-08	6
LRR.1	2.62E-12	0.978015628413988	0.738	0.482	3.13E-08	6
psq.2	3.00E-12	-0.738036198687732	0.657	0.843	3.57E-08	6
Pde9.1	3.06E-12	-1.2427955349979	0.395	0.623	3.66E-08	6

CG5953.4	3.70E-12	1.24816073949874	0.709	0.459	4.41E-08	6
pan.2	4.26E-12	-0.889092524443599	0.669	0.744	5.08E-08	6
spin.2	5.06E-12	0.934308541371079	0.663	0.371	6.03E-08	6
rudhira.2	5.43E-12	-1.09358580619466	0.343	0.607	6.48E-08	6
CG10126	5.56E-12	1.17433421880221	0.227	0.047	6.63E-08	6
Fit1.1	6.46E-12	1.38301097629534	0.273	0.077	7.71E-08	6
l(3)L1231.2	7.55E-12	-0.938199202422839	0.552	0.753	9.00E-08	6
mew.2	7.55E-12	-0.687276393139681	0.686	0.859	9.00E-08	6
norpA.1	8.78E-12	0.954879910667433	0.692	0.411	1.05E-07	6
Lk6.2	9.20E-12	-0.960188823848751	0.593	0.742	1.10E-07	6
CG32091.3	1.89E-11	-0.937135715286904	0.483	0.696	2.25E-07	6
Glut4EF.4	2.04E-11	-0.843889224389244	0.797	0.906	2.43E-07	6
hid.3	2.05E-11	-1.50151063536696	0.157	0.403	2.44E-07	6
sdk.3	2.87E-11	1.11294805081317	0.61	0.378	3.43E-07	6
Snoo	3.23E-11	-0.977819890542773	0.419	0.647	3.85E-07	6
CG15145	3.42E-11	1.44434563315132	0.203	0.037	4.08E-07	6
r-l	3.73E-11	1.06207001940108	0.128	0.009	4.45E-07	6
CCT2	3.81E-11	1.05557520221604	0.221	0.049	4.54E-07	6
pain	3.85E-11	1.43077660206681	0.203	0.038	4.59E-07	6
Mmp1	4.10E-11	1.52666470148001	0.186	0.032	4.89E-07	6
GstD3	4.55E-11	1.54814016820779	0.227	0.055	5.43E-07	6
CG5346.1	4.92E-11	0.886308908770917	0.215	0.053	5.87E-07	6
jim.3	5.12E-11	-1.21888525048532	0.262	0.483	6.11E-07	6
gpp.1	5.75E-11	-0.747446151316425	0.599	0.789	6.86E-07	6
Baldspot.1	1.05E-10	1.20201744082829	0.343	0.117	1.25E-06	6
puc.2	1.22E-10	0.888059260941814	0.721	0.524	1.45E-06	6
Doa.2	1.23E-10	1.08518873663863	0.628	0.448	1.46E-06	6
Smr.1	1.55E-10	-0.659198327101183	0.738	0.873	1.84E-06	6
pum.2	1.68E-10	-0.36025514212366	0.977	0.997	2.00E-06	6
coro	1.83E-10	1.26955194839556	0.238	0.063	2.19E-06	6
l(2)41Ab.1	2.24E-10	-1.03651271038035	0.471	0.689	2.67E-06	6
CG9253	2.59E-10	0.781440442517916	0.14	0.02	3.09E-06	6
dl.3	2.79E-10	1.3751584786526	0.314	0.104	3.32E-06	6
msk	2.83E-10	0.967967209373978	0.227	0.055	3.37E-06	6
CG44325.2	2.96E-10	1.10253307940663	0.419	0.171	3.53E-06	6
gogo.2	3.05E-10	-1.63951746740808	0.041	0.227	3.64E-06	6
Hsp27.1	3.23E-10	3.00793670197076	0.192	0.105	3.85E-06	6
CG31955	5.03E-10	0.972652872573711	0.134	0.016	6.00E-06	6
vari.2	5.78E-10	1.18441838949792	0.395	0.157	6.89E-06	6
GstD1.2	6.63E-10	1.41457209848181	0.407	0.263	7.91E-06	6
Act42A.3	8.13E-10	1.07975495123389	0.372	0.144	9.70E-06	6
Nop60B	1.02E-09	1.10454028417371	0.192	0.041	1.21E-05	6
fru	1.04E-09	1.09314243268886	0.203	0.049	1.24E-05	6
RhoL	1.11E-09	1.08123132453086	0.302	0.105	1.32E-05	6
CG3961.2	1.47E-09	-1.19445945195259	0.163	0.404	1.75E-05	6
CG13384.2	1.52E-09	1.03799635603812	0.407	0.194	1.82E-05	6
CG17646.2	2.82E-09	1.09595189132738	0.529	0.333	3.36E-05	6
ced-6.2	2.91E-09	-0.988867650270317	0.256	0.512	3.48E-05	6
Traf4.1	3.04E-09	-1.35064693265473	0.093	0.299	3.62E-05	6
EDTP.3	3.05E-09	-1.41868085762647	0.058	0.229	3.63E-05	6
Ets21C	3.34E-09	1.27834444413248	0.267	0.087	3.98E-05	6
Drp1	3.53E-09	0.754899834677647	0.151	0.03	4.21E-05	6
sqd.2	4.79E-09	0.755851178780526	0.738	0.558	5.72E-05	6
CG6770	4.84E-09	-0.926763455073823	0.43	0.657	5.77E-05	6
Lac.1	4.99E-09	1.08987774192787	0.238	0.07	5.95E-05	6
CG15144	5.30E-09	1.26505138881892	0.169	0.036	6.33E-05	6
Rel.1	5.64E-09	1.33777971129797	0.343	0.137	6.73E-05	6
CG5853	5.72E-09	1.3589951077597	0.151	0.031	6.83E-05	6
Xbp1	5.87E-09	0.653104571003728	0.419	0.203	7.00E-05	6
rl.1	6.30E-09	-0.448138402088961	0.919	0.973	7.51E-05	6

stv.2	6.47E-09	1.35469778574948	0.43	0.211	7.71E-05	6
NimB4.2	6.50E-09	-1.02263661699685	0.186	0.424	7.75E-05	6
CG9005.2	6.51E-09	-1.12421323625062	0.203	0.411	7.77E-05	6
Gclm.1	6.62E-09	1.23490484896526	0.285	0.102	7.89E-05	6
Atf3.2	7.08E-09	1.10644303722544	0.39	0.177	8.45E-05	6
Arpc2	7.91E-09	0.888447528329963	0.233	0.072	9.44E-05	6
spz	9.34E-09	1.13137588663489	0.157	0.029	0.0001114753968	6
Nmda1.1	9.91E-09	1.09968784777786	0.267	0.089	0.0001181625748	6
CG9003.3	1.13E-08	-1.11483417795882	0.157	0.355	0.0001349747715	6
Itgbn	1.15E-08	1.06394160050899	0.145	0.023	0.0001373091505	6
mam.1	1.18E-08	-1.1742877152006	0.203	0.424	0.0001411138565	6
ifc	1.20E-08	0.956946699318374	0.128	0.021	0.0001426330869	6
sgg.3	1.28E-08	-0.658744110159949	0.733	0.82	0.0001529380711	6
RasGAP1.1	1.41E-08	1.05090593895826	0.483	0.275	0.0001678519639	6
eIF2beta.1	1.44E-08	1.09051202082516	0.331	0.135	0.0001711956682	6
sbb	1.49E-08	-0.668665945144109	0.645	0.81	0.0001782377996	6
gish.1	1.54E-08	0.676625864775172	0.703	0.47	0.0001836018418	6
CG15143	1.60E-08	1.36152819537636	0.174	0.045	0.0001912904038	6
cindr.1	1.67E-08	0.897480618828072	0.535	0.295	0.0001988324379	6
prage.4	1.91E-08	0.921117986936419	0.494	0.262	0.0002281079015	6
Dmtn.1	1.93E-08	-0.989248918309783	0.151	0.359	0.000229753947	6
CG13117	1.94E-08	0.933874234444629	0.151	0.027	0.0002319355554	6
scyl.1	1.97E-08	-0.906231673196236	0.355	0.538	0.0002348015666	6
Nhe3	2.00E-08	1.0485249557112	0.267	0.088	0.0002388126895	6
h.1	2.04E-08	1.01204801029021	0.57	0.354	0.0002437204564	6
SNF4Agamma.1	2.25E-08	0.729876454003278	0.831	0.707	0.0002684872169	6
PAPLA1.1	2.48E-08	1.18848633765775	0.378	0.191	0.000296380527	6
Tm1.1	2.63E-08	0.848254832373959	0.564	0.359	0.00031382048	6
CG13185	2.85E-08	0.921840327293174	0.174	0.042	0.0003400172584	6
Drs.2	3.24E-08	1.90278556337941	0.192	0.106	0.000386247447	6
CG31122.1	3.25E-08	-1.24222135517111	0.029	0.182	0.0003882636238	6
Sur-8	3.29E-08	1.06795486295845	0.169	0.039	0.0003928669631	6
DOR.3	3.44E-08	-1.17762317432909	0.116	0.321	0.00040999718	6
CG11791.1	3.62E-08	1.02532949701687	0.39	0.18	0.000431449078	6
Tsp42Ed.1	3.73E-08	1.12230877486534	0.326	0.135	0.0004446323161	6
14-3-3zeta.1	3.96E-08	0.774063728450436	0.558	0.339	0.0004725051875	6
Ntf-2	4.69E-08	0.805071185626779	0.203	0.06	0.0005595962723	6
CG6231	4.84E-08	0.897085499602829	0.122	0.018	0.0005776250161	6
Ser.3	4.84E-08	-1.12748360664341	0.18	0.39	0.0005778822499	6
Rac2	4.94E-08	0.863544484900055	0.558	0.32	0.0005898193803	6
Dhap-at	5.09E-08	0.998684564365427	0.134	0.023	0.0006071410703	6
CG42668.2	5.16E-08	0.864456919217003	0.413	0.201	0.0006158729031	6
SPARC.3	5.51E-08	-0.796006599277504	0.326	0.548	0.0006577145248	6
plum.1	6.17E-08	1.39404565017161	0.267	0.115	0.0007355599662	6
Hsp23	6.27E-08	2.37919227511529	0.134	0.044	0.000748454293	6
pigs.4	6.51E-08	0.780671352217022	0.674	0.57	0.0007768454131	6
Npc2a.1	7.03E-08	1.08268247156722	0.273	0.096	0.0008384760594	6
Irc.1	7.11E-08	0.907132597341323	0.314	0.126	0.0008481486749	6
Hsc70-4.3	8.85E-08	0.94174873376235	0.465	0.268	0.001055152139	6
CG32425	1.00E-07	1.00242179519678	0.343	0.152	0.0011980933708	6
CG42588	1.18E-07	0.97187713669675	0.203	0.061	0.0014026571393	6
Pmp70	1.43E-07	1.08504570506049	0.157	0.037	0.0017041449661	6
Ziz.3	1.55E-07	-1.17132714071104	0.157	0.359	0.0018458734266	6
CG10311	1.58E-07	1.1122830798907	0.209	0.06	0.0018838090979	6
Ist1.2	1.67E-07	0.902985569487313	0.314	0.133	0.0019906273933	6
CG5059.3	1.68E-07	-1.05314675213976	0.221	0.366	0.00200745907	6
CG17739	1.93E-07	0.796795549685898	0.105	0.012	0.0023046110741	6
bves.2	2.03E-07	0.980992539785384	0.413	0.208	0.0024201761563	6
Diap1.2	2.06E-07	0.746469570803903	0.57	0.449	0.0024563250137	6
Mvl.2	2.26E-07	0.904109026960333	0.535	0.311	0.0027009720641	6

tsr.2	2.30E-07	0.661033065054304	0.262	0.102	0.0027432731129	6
Tomosyn	2.31E-07	0.649250432491459	0.587	0.378	0.0027592052806	6
kay.2	2.59E-07	1.03935901001286	0.57	0.393	0.0030842637053	6
PDZ-GEF.2	2.78E-07	-0.988606202479816	0.105	0.294	0.0033108298913	6
Vinc.1	2.93E-07	0.833651885443027	0.244	0.093	0.0034936555333	6
Fib	3.18E-07	0.858008716030872	0.105	0.015	0.0037901132644	6
egh.4	3.25E-07	0.645327664165607	0.61	0.394	0.0038823002883	6
Spn88Ea	3.37E-07	1.00687760054555	0.157	0.04	0.0040207598926	6
Hers.1	3.52E-07	-0.762655299930226	0.43	0.621	0.0042025233794	6
pod1.1	4.44E-07	0.922917057013304	0.395	0.194	0.0052927137874	6
Pdp1.3	4.79E-07	0.586667325307724	0.767	0.575	0.0057146278606	6
PRAS40.4	5.19E-07	-1.03700660253226	0.18	0.375	0.0061920067144	6
Hel89B.1	5.87E-07	0.853220259708341	0.512	0.299	0.007001700095	6
Dyrk2.3	6.08E-07	-0.787089649816142	0.39	0.589	0.0072514191435	6
alc.2	6.30E-07	-1.01264153857695	0.116	0.304	0.0075134089615	6
Sirup.1	7.25E-07	-1.09164260434845	0.087	0.259	0.008648754074	6
pnt.5	7.27E-07	-0.449388474703229	0.82	0.909	0.0086768649655	6
Chd64.3	8.45E-07	0.78894972651013	0.64	0.481	0.0100817447514	6
dnc.1	8.65E-07	-1.00745367847732	0.308	0.501	0.0103214472403	6
ATP8A.2	9.64E-07	1.00578180663746	0.308	0.145	0.0114937948649	6
RhoU	9.76E-07	1.25667981914152	0.169	0.049	0.0116373333338	6
CARPB	9.89E-07	0.701568923690421	0.116	0.023	0.011799642625	6
cib.1	1.04E-06	1.04859613120517	0.262	0.117	0.0124258770072	6
CG10365.1	1.09E-06	-1.12321255846465	0.035	0.136	0.0129661552405	6
CG6357.1	1.10E-06	1.00153229271809	0.238	0.082	0.0130888137453	6
CG12576.3	1.13E-06	-1.02444291130937	0.122	0.295	0.0135393604268	6
Esyt2.1	1.14E-06	0.971846906344913	0.401	0.206	0.0135883869029	6
CG5151.3	1.21E-06	-0.505950109909109	0.651	0.817	0.0143815303137	6
Corin.1	1.23E-06	-1.0602705900531	0.105	0.257	0.0146961597142	6
GlcT	1.24E-06	0.872637798667457	0.128	0.028	0.0148026254096	6
Moe.2	1.35E-06	0.648957806109882	0.657	0.445	0.0161228297459	6
slmb.1	1.44E-06	0.825444143932416	0.244	0.103	0.017235533005	6
Ac13E.1	1.45E-06	-0.73883741724591	0.291	0.459	0.017330069202	6
Thor.3	1.61E-06	-1.17357370474416	0.244	0.424	0.0192643402447	6
Msp300.3	1.77E-06	0.84412639020748	0.669	0.557	0.0210765620161	6
caz.1	1.80E-06	0.790651412248991	0.302	0.137	0.0214368319007	6
NKAIN	1.80E-06	0.931814277569261	0.355	0.175	0.0214583110592	6
NimB1.1	1.92E-06	-0.997034374847771	0.163	0.325	0.0228826279617	6
NFAT.1	2.02E-06	-0.73771856277641	0.395	0.524	0.0241038628278	6
mask	2.04E-06	0.810105921286839	0.541	0.402	0.0243131520109	6
eIF4A.2	2.41E-06	0.759245638787478	0.419	0.228	0.0287087698588	6
DIP-epsilon.1	2.44E-06	-1.07781471338521	0.105	0.276	0.0290910019341	6
Sarm.3	2.47E-06	0.70423940760115	0.709	0.608	0.0294967161649	6
ZnT63C.1	2.74E-06	0.836560867411036	0.372	0.188	0.0326515607728	6
RapGAP1.2	2.74E-06	-0.61019222358821	0.57	0.727	0.0326800691778	6
apt	2.76E-06	0.987565766846471	0.14	0.039	0.0329501787225	6
sd.1	2.85E-06	0.755443489856978	0.413	0.218	0.0340434853569	6
Tsp42Ee.1	2.86E-06	0.947586884198967	0.256	0.112	0.0340813765448	6
CG6051.1	2.91E-06	0.712888412321887	0.552	0.351	0.0347335724291	6
Tre1.1	2.98E-06	0.934720157698602	0.244	0.095	0.0355387071671	6
Timp	2.99E-06	1.1374204573151	0.128	0.031	0.0357224207929	6
eEF1alpha1.3	3.08E-06	0.579930479534842	0.68	0.499	0.0366846312332	6
srl	3.10E-06	0.944552010068692	0.116	0.023	0.0370032462332	6
mnb.4	3.11E-06	-0.805067431905526	0.285	0.41	0.037088499174	6
Had2.3	3.22E-06	-1.01789974188668	0.169	0.346	0.0384167353239	6
Sf3b3	3.25E-06	0.784888101610481	0.157	0.044	0.0388077292727	6
Ubi-p63E.1	3.30E-06	1.00466472115045	0.541	0.389	0.0393084844582	6
Crtc.3	3.42E-06	-0.7924112663749	0.372	0.555	0.0407673637586	6
CG31637.1	3.53E-06	-0.916162561236163	0.349	0.514	0.0421645775038	6
CG7029	3.66E-06	0.828729548143321	0.36	0.221	0.0436694646957	6

CG32066.1	3.69E-06	0.669457658764474	0.686	0.555	0.0439724749931	6
Tpr2.1	3.71E-06	0.965332832196116	0.413	0.238	0.0442564522243	6
Hsp26.1	4.03E-06	2.49333766445601	0.238	0.119	0.0480411169032	6
Arpc3B	4.12E-06	0.617568183695864	0.11	0.027	0.0491679757638	6
CG31145.3	4.60E-13	0.911557957133326	1	0.731	5.49E-09	7
Vha100-2.4	1.31E-10	0.95837242489987	0.565	0.206	1.57E-06	7
cwo.3	1.83E-10	-1.20529264649442	0.594	0.63	2.18E-06	7
blot.1	2.89E-10	-1.20359700595315	0.551	0.532	3.45E-06	7
DOR.4	3.12E-10	0.373873765426292	0.58	0.28	3.72E-06	7
CrebA.5	5.13E-10	0.276923634880653	0.536	0.242	6.12E-06	7
CaMKI.1	5.75E-10	-0.257045617265422	0.493	0.297	6.86E-06	7
RpL10Ab.3	1.30E-09	-1.4540940001325	0.145	0.266	1.55E-05	7
Cals.2	1.85E-09	0.471293938251133	0.522	0.234	2.21E-05	7
Pp1alpha-96A	2.92E-09	-0.522246443854827	0.203	0.143	3.48E-05	7
eEF2.4	4.57E-09	-0.798242043366142	0.362	0.312	5.46E-05	7
mtd.3	5.57E-09	0.756477849435458	0.942	0.749	6.65E-05	7
DIP-epsilon.2	6.79E-09	0.600439783891092	0.536	0.239	8.10E-05	7
app.3	6.88E-09	0.613235389285844	0.725	0.371	8.20E-05	7
Caper	9.68E-09	-0.378670942389034	0.362	0.275	0.0001154671556	7
Best1.1	1.38E-08	0.639011940381928	0.551	0.25	0.0001646993902	7
sug	1.44E-08	0.706420190266811	0.188	0.031	0.0001718024242	7
CG3777.3	1.72E-08	1.00933238657718	0.536	0.208	0.0002051001212	7
l(1)G0196.3	2.74E-08	0.612972944891488	0.725	0.387	0.0003263155509	7
pum.3	2.95E-08	0.470488238021447	1	0.994	0.0003517155225	7
eIF4A.3	3.00E-08	-0.945090427077968	0.246	0.253	0.0003583672329	7
Pxn.4	3.11E-08	0.715547703671833	0.87	0.525	0.0003712573447	7
CG43236.2	3.44E-08	1.08210729450477	0.406	0.124	0.0004099419717	7
Had2.4	4.27E-08	0.911002663988832	0.652	0.307	0.000509637681	7
CG5151.4	4.58E-08	0.748702068433371	0.957	0.788	0.0005466598434	7
CG3961.3	4.96E-08	0.722330294615636	0.71	0.355	0.000591609605	7
Pdk.4	5.58E-08	-1.74310650887849	0.203	0.44	0.0006650875403	7
Ten-m.4	5.72E-08	0.529774136530953	1	0.995	0.0006823783686	7
Prps.3	6.20E-08	-1.82797393795983	0.159	0.361	0.0007396003642	7
RpL4.2	6.84E-08	-1.15781844400715	0.145	0.202	0.000815429863	7
CG14153.1	7.00E-08	0.876663029320994	0.304	0.083	0.0008351354935	7
hppy.2	7.56E-08	0.43783519828308	0.884	0.568	0.0009020610575	7
Adar.1	7.83E-08	0.502206500519088	0.464	0.213	0.000934347717	7
l(3)80Fg.2	9.48E-08	0.768664561558645	0.899	0.594	0.0011314379622	7
Rbp1-like.2	9.60E-08	0.79369863722389	0.522	0.225	0.001144975294	7
wrd.1	1.03E-07	0.325438449250979	0.391	0.182	0.0012299759808	7
PGRP-LC.3	1.10E-07	0.662945426331171	0.638	0.324	0.0013063168984	7
Ten-a.1	1.12E-07	-1.30706633245325	0.159	0.219	0.0013405637204	7
RpL21.4	1.13E-07	-1.16535141570248	0.217	0.278	0.0013435519574	7
Idgf2	1.17E-07	0.258676856284519	0.348	0.168	0.0013987235539	7
jim.4	1.19E-07	-0.282603348091005	0.594	0.448	0.001420888878	7
CG42694.1	1.21E-07	0.596757707580433	0.261	0.093	0.0014406877226	7
Lpin.4	1.37E-07	-2.01366341441665	0.101	0.32	0.0016337163458	7
Nc73EF.3	1.49E-07	-0.632095106996303	0.203	0.177	0.0017767678347	7
Cat	1.52E-07	-0.534170314133718	0.174	0.128	0.0018084396106	7
ninaE.1	1.53E-07	-1.26998163559212	0.217	0.242	0.0018198981461	7
CG3164.2	1.59E-07	0.726581053048084	0.507	0.222	0.0018932572516	7
Culd	1.89E-07	-0.420608898584119	0.145	0.1	0.0022565741876	7
CG4259	2.08E-07	1.16816457278795	0.391	0.118	0.0024806932133	7
Pcf11.1	2.21E-07	-0.282414064711854	0.391	0.28	0.0026390830157	7
larp.1	2.23E-07	-0.74485514286592	0.275	0.276	0.0026567933728	7
Sema2a.4	2.29E-07	0.816868916053676	0.768	0.43	0.0027265976497	7
RpL3.4	2.46E-07	-1.54618825153499	0.101	0.27	0.0029311610793	7
Indy.1	2.53E-07	0.556254699178224	0.435	0.189	0.0030185939223	7
Pde9.2	2.62E-07	0.322826352427115	0.87	0.58	0.0031252087724	7
CG15695.4	2.64E-07	0.469790039689265	0.246	0.083	0.0031545135729	7

ush.4	2.68E-07	0.678539580068329	0.942	0.711	0.0032005272155	7
Ank	2.75E-07	-0.459548672582807	0.406	0.354	0.0032762906827	7
bves.3	3.18E-07	0.471703924486226	0.449	0.222	0.0037980640508	7
Btk29A.5	4.05E-07	0.693016379213187	0.957	0.764	0.0048269190161	7
Mad	4.41E-07	0.399012438521696	0.435	0.215	0.0052659413854	7
ClC-a.1	4.48E-07	0.805839498545189	0.391	0.144	0.0053415198289	7
CG31122.2	4.50E-07	0.831901166810735	0.391	0.151	0.0053643058183	7
Sema5c.3	4.99E-07	1.03093441708664	0.754	0.498	0.005954593275	7
egh.5	5.26E-07	0.690901476049363	0.739	0.405	0.0062732159984	7
fl(2)d	5.64E-07	0.301770330844545	0.377	0.18	0.0067315625849	7
rhea.4	5.96E-07	-0.513394217976425	0.435	0.367	0.0071047075759	7
eEF1alpha1.4	6.15E-07	-0.926147961044881	0.507	0.523	0.0073343458765	7
Rga.1	6.33E-07	0.535222136414592	0.333	0.143	0.0075537747918	7
RhoGEF2	6.57E-07	0.512636648683072	0.681	0.381	0.0078391743431	7
CG31211.2	6.72E-07	0.402083544718687	0.319	0.147	0.0080128158009	7
Thd1.2	6.73E-07	0.376344259183325	0.609	0.358	0.0080324231488	7
eEF1beta.1	8.42E-07	-0.720617881227189	0.116	0.127	0.0100474585325	7
CG17124.2	1.01E-06	0.636757480660783	0.739	0.411	0.011993631654	7
pAbp.4	1.07E-06	-0.832879953681083	0.42	0.492	0.0127380036101	7
blw.1	1.14E-06	-0.672633093994622	0.13	0.135	0.0136437823992	7
CG9328.2	1.24E-06	0.817300542268463	0.783	0.464	0.0148215544462	7
CG41099	1.30E-06	0.511486232590042	0.348	0.152	0.0154706958349	7
NimB2.2	1.31E-06	-0.586356536815866	0.261	0.24	0.0156633390999	7
upSET	1.48E-06	0.465643371444513	0.725	0.44	0.0176245619939	7
Srrm234	1.50E-06	0.307476159606345	0.377	0.195	0.0179107632695	7
uex.4	1.60E-06	0.820612547969088	0.826	0.539	0.0191120495775	7
Cyp6w1	1.62E-06	0.305983695608118	0.188	0.064	0.0193103069751	7
drongo.1	1.62E-06	0.506436526568405	0.783	0.48	0.0193168122744	7
RpS30.3	1.71E-06	-0.81322498332096	0.232	0.235	0.0204376826262	7
UQCR-Q.1	1.81E-06	-0.35588601080733	0.145	0.088	0.0216044787892	7
GstE12.1	1.93E-06	0.272313060679344	0.232	0.08	0.0229944045445	7
Atf6.1	2.01E-06	0.713607522753656	0.594	0.294	0.0239566543264	7
Saf-B.2	2.08E-06	0.301613490623656	0.29	0.139	0.0248530854155	7
l(3)L1231.3	2.10E-06	0.34339073664455	0.957	0.715	0.0250730171053	7
Bacc.2	2.76E-06	-0.468186681407827	0.464	0.388	0.0329535233675	7
RpL23.2	2.77E-06	-0.980105584340238	0.275	0.334	0.0330971273664	7
InR.5	2.86E-06	-0.993041751223259	0.812	0.856	0.0341723327058	7
sta.3	3.05E-06	-0.76032598778818	0.246	0.277	0.0364234815012	7
CG9171.4	3.31E-06	0.799132226887671	0.652	0.339	0.039435066285	7
Evi5.1	3.34E-06	0.460184042728668	0.42	0.208	0.0398968678346	7
Syp.3	3.35E-06	0.570230478880741	0.971	0.844	0.0399561607133	7
SCaMC.3	3.54E-06	-1.65167699853991	0.087	0.297	0.0421877918162	7
crq.1	3.63E-06	0.709927603401177	0.725	0.42	0.0432987098795	7
CG3726.2	3.66E-06	0.385607868650641	0.899	0.627	0.0436598630247	7
RpL7.2	3.72E-06	-0.96430137559859	0.188	0.247	0.0443343326672	7
Hml.5	3.74E-06	0.730232787454471	0.899	0.638	0.0445913167333	7
RpS15.3	3.75E-06	-1.45327867343981	0.072	0.328	0.044748804669	7
CG11360.2	3.76E-06	0.764327916027372	0.319	0.111	0.0448111000039	7
CG31635.1	4.00E-06	0.596939043280344	0.609	0.324	0.0477147606795	7
sesB.2	4.10E-06	-1.17693505359118	0.13	0.212	0.0488851152861	7
RpS27.3	4.18E-06	-1.55988439970122	0.13	0.322	0.0499050285859	7
rl.2	4.19E-06	0.443673766331298	1	0.964	0.0499629376875	7
CG13743	2.30E-36	5.05377176338013	0.518	0.019	2.75E-32	8
PPO2	3.98E-35	5.40881120107843	0.536	0.024	4.74E-31	8
robo2	6.91E-35	3.92189664925887	0.643	0.033	8.25E-31	8
lz	2.65E-32	3.84345127799603	0.482	0.006	3.16E-28	8
Pde1c	6.51E-32	6.36811396414423	0.464	0.062	7.77E-28	8
klu	1.52E-30	4.12494679341857	0.536	0.024	1.82E-26	8
N.3	1.58E-29	2.83026898190371	0.786	0.288	1.88E-25	8
peb	9.30E-28	3.80577857845701	0.482	0.018	1.11E-23	8

Ten-m.5	1.41E-27	-1.35353870907328	0.929	0.998	1.68E-23	8
PPO1	6.49E-27	4.11993023473892	0.446	0.015	7.74E-23	8
E(spl)mbeta-HLH	2.94E-26	2.82568935716919	0.518	0.024	3.51E-22	8
Tet.2	1.78E-24	3.05185387503231	0.482	0.196	2.13E-20	8
ct.3	2.76E-23	1.8080753775039	0.786	0.764	3.30E-19	8
mtgo.1	2.18E-20	-1.53217269579425	0.804	0.97	2.60E-16	8
tna.5	2.96E-20	2.6674408523898	0.536	0.208	3.54E-16	8
CG43187	3.49E-15	2.05199570356668	0.214	0.001	4.16E-11	8
caps.5	3.61E-15	2.64364062884188	0.357	0.093	4.31E-11	8
E(spl)malpha-BFM	1.20E-14	2.37533758586283	0.321	0.02	1.43E-10	8
Jupiter.2	1.55E-13	-1.74186372497464	0.536	0.854	1.85E-09	8
CG31431	2.51E-13	2.41214480202999	0.375	0.047	2.99E-09	8
Ppn.3	2.08E-12	-1.16908074712517	0.768	0.974	2.48E-08	8
cpo.4	7.67E-12	1.32649256398665	0.893	0.693	9.15E-08	8
Mctp	1.14E-11	2.28728579604902	0.232	0.012	1.36E-07	8
Men.3	1.93E-11	2.32064744399492	0.554	0.216	2.31E-07	8
CG9932.1	4.58E-11	-1.19900304196207	0.768	0.94	5.46E-07	8
zfh2	1.18E-10	2.5245189074594	0.25	0.036	1.41E-06	8
CG13252	1.30E-10	1.49809198448044	0.214	0.01	1.56E-06	8
Cirl.1	1.77E-10	1.49294080599716	0.607	0.405	2.11E-06	8
Ndae1	3.08E-10	2.2196801701454	0.375	0.1	3.68E-06	8
ATP8B.1	6.13E-10	1.9079872129239	0.357	0.06	7.31E-06	8
CG5828	4.44E-09	1.55189300320081	0.179	0.008	5.29E-05	8
Prosap.3	5.32E-09	-1.21506602073192	0.821	0.952	6.34E-05	8
kst.2	6.26E-09	2.01110878600526	0.518	0.18	7.47E-05	8
Trim9	1.07E-08	1.84180501280649	0.179	0.011	0.000128167431	8
drpr.3	3.65E-08	-1.26428837074838	0.482	0.765	0.0004352140573	8
Pde9.3	1.10E-07	1.15360444602179	0.821	0.585	0.0013151266027	8
bru2.1	1.44E-07	1.32549359890955	0.304	0.063	0.0017237210128	8
fkh	1.51E-07	1.20026033303061	0.143	0.008	0.001801488964	8
Rtnl1.4	1.76E-07	1.25231527238536	0.411	0.108	0.0020997416743	8
CG32264.6	1.95E-07	1.33680739234895	0.696	0.435	0.0023225739843	8
sm.3	2.33E-07	1.41793499676652	0.536	0.229	0.0027800020257	8
CAP	2.50E-07	1.63227154964222	0.304	0.064	0.002982202647	8
Ctr1A.1	2.51E-07	1.81889673981981	0.286	0.1	0.0029948194254	8
Elk	3.28E-07	1.34267628608433	0.143	0.005	0.0039176836388	8
Col4a1.3	3.35E-07	-0.815942915037313	0.714	0.933	0.0039966566129	8
fok.4	3.54E-07	1.78448595835372	0.411	0.176	0.004218029435	8
AstA-R1	3.97E-07	5.40642392662272	0.143	0.012	0.0047345886719	8
Sema1b.2	3.99E-07	-1.58154195035238	0.304	0.556	0.0047544953258	8
kek5.2	4.35E-07	1.24595408178074	0.589	0.38	0.0051875001262	8
Fili	4.38E-07	1.44978513442364	0.161	0.011	0.0052190154668	8
CG9518	4.39E-07	2.39107892517803	0.125	0.023	0.0052324866861	8
SKIP	4.63E-07	2.50883160354613	0.214	0.03	0.0055209293855	8
Pvr.4	4.76E-07	-1.05534953458516	0.732	0.884	0.0056745409296	8
aqz.2	4.85E-07	1.0642167461772	0.964	0.894	0.0057904028181	8
CG9743	5.16E-07	1.69460272110426	0.214	0.026	0.0061505064768	8
sty.4	6.52E-07	-1.09834380185359	0.643	0.859	0.0077804242662	8
CG8468	7.65E-07	1.60639432674133	0.196	0.029	0.0091290078883	8
CAH2	7.83E-07	1.06453641537061	0.143	0.008	0.0093396158214	8
LpR2.4	8.22E-07	-0.982033725003838	0.768	0.908	0.009806557902	8
Mvl.4	9.90E-07	-1.88262202250617	0.054	0.352	0.011812759761	8
CG43693	1.01E-06	1.27362067860464	0.196	0.023	0.0120948565142	8
cv-c.6	1.20E-06	0.844524068124958	0.982	0.919	0.0143115226677	8
Egfr.1	1.27E-06	1.73048232354399	0.286	0.063	0.0151678805072	8
Dl	2.42E-06	1.68166242573306	0.125	0.006	0.0288663830346	8
Had2.5	2.69E-06	-1.85941820916523	0.054	0.336	0.0320568581272	8
nudC	3.09E-06	1.14376620991359	0.196	0.028	0.0369000302672	8
Ncc69	3.27E-06	1.65321262049189	0.161	0.013	0.0389765696669	8
CG31145.4	3.49E-06	-1.11832179995781	0.5	0.755	0.0415871515885	8

Mmp2.5	3.50E-06	-2.06963393096392	0.179	0.473	0.0417573787593	8

ntity

List of *Drosophila* lines used in this study	Source	ID
w^{1118};HmlΔ -Gal4,UAS-2xeGFP	Gift from Marc S. Dionne	N/A
w^{1118};UAS-tefu-IR	Vienna Drosophila Research Center	VDRC ID: 108074
w^{1118};UAS-mei41-IR	Vienna Drosophila Research Center	VDRC ID: 11251
w^{1118};UAS-nbs-IR	Vienna Drosophila Research Center	VDRC ID:110366
w^{1118};UAS-mei41-IR;UAS-tefu-IR	made for this study	N/A
w^{1118};UAS-bsk-DN	Vienna Drosophila Research Center	VDRC ID: 104569
w^{1118};;HmlΔ-DsRed.nuc	Gift from Katie J. Woodcock	N/A
w^{1118};UAS-upd3-IR	Vienna Drosophila Research Center	VDRC ID: 106869
w^{1118};HmlΔ -Gal4,UAS-2xeGFP;tubGal80/tm6csb´	Gift from Katie J. Woodcock	N/A
w^{1118};UAS-hep[act]/CyO; Dr/tm6csb'	Gift from Anne-Kathrin Classen	N/A
w^{1118};UAS-upd3/Sm6a	Gift from Katie J. Woodcock	N/A
w[*] upd3[Δ]	Bloomington Drosophila Stock Center	BDSC ID: 55728
w´upd3Δ; UAS-upd3/Sm6a	made for this study	N/A
w^{1118};tub-Gal80^{ts}/Sm6a;crq-Gal4/TM6 c, Sb'	Gift from Marc S. Dionne	N/A
w1118;;UAS-rpr/TM6 c, Sb1	Bloomington Drosophila Stock Center	BDSC ID: 5824
w1118;UAS-CD8-mCherry	Bloomington Drosophila Stock Center	BDSC ID: 27391

List of RTqPCR primers used in this study	Source
Primer: Rpl1_for 5'-TCCACCTTGAAGAAGGGCTA-3'	Designed for this study
Primer: Rpl1_rev 5'-TTGCGGATCTCCTCAGACTT-3'	Designed for this study
Primer: Upd1_for 5'-GCACACTGATTTCGATACGG-3'	Designed for this study
Primer: Upd1_rev 5'-CTGCCGTGGTGCTGTTTT-3'	Designed for this study
Primer: Upd2_for 5'-CGGAACATCACGATGAGCGAAT-3'	Designed for this study
Primer: Upd2_rev 5'-TCGGCAGGAACTTGTACTCG-3'	Designed for this study
Primer: Upd3_for 5'-ACTGGGAGAACACCTGCAAT-3'	Designed for this study
Primer: Upd3_rev 5'-GCCCGTTTGGTTCTGTAGAT-3'	Designed for this study
Primer: Socs36E_for 5'-AAAAAGCCAGCAAACCAAAA-3'	Designed for this study
Primer: Socs36E_rev 5'-AGGTGATGACCCATTGGAAG-3'	Designed for this study
Primer: TotA_for 5'-CCAAAATGAATTCTTCAACTGC-3'	Designed for this study
Primer: TotA_rev 5'-GAATAGCCCATGCATAGAGGAC-3'	Designed for this study
Primer: Puc_for 5'-CGTCATCATCAACGGCAAT-3'	Designed for this study
Primer: Puc_rev 5'-AGGCGGGGTGTGTTTCTAT-3'	Designed for this study
Primer: Ilp-2_for 5'-ATCCCGTGATTCCACCACAAG-3'	Designed for this study
Primer: Ilp-2_rev 5'-GCGGTTCCGATATCGAGTTA-3'	Designed for this study
Primer: Ilp-3_for 5'- CAACGCAATGACCAAGAGAA-3'	Designed for this study
Primer: Ilp-3_rev 5'-TGAGCATCTGAACCGAACT-3'	Designed for this study
Primer: Ilp-5_for 5'-GCCTTGATGGACATGCTGA-3'	Designed for this study
Primer: Ilp-5_rev 5'-AGCTATCCAAATCCGCCA-3'	Designed for this study
Primer: Thor_for 5'- CAGGAAGGTTGTCATCTCGGA-3'	Designed for this study
Primer: Thor_rev 5'-GGAGTGGTGGAGTAGAGGGTT-3'	Designed for this study
Primer: Pepck_for 5'-GGATAAGGTGGACGTGAAG-3'	Designed for this study
Primer: Pepck_rev 5'-ACCTCCTGCGACCAGAACT-3'	Designed for this study
Primer: InR_for 5'-GCACCATTATAACCGGAACC-3'	Designed for this study

Primer: InR_rev 5’-TTAATTCATCCATGACGTGAGC-3’	Designed for this study
Primer: Def_for 5’-TTCTCGTGGCTATCGCTTTT-3’	Designed for this study
Primer: Def_rev 5’-GGAGAGTAGGTCGCATGTGG-3’	Designed for this study
Primer: AttA_for 5’-CACAATGTGGTGGGTCAGG	Designed for this study
Primer: AttA_rev 5’-GGCACCATGACCACCATT	Designed for this study
Primer: DiptA_for 5’-ACCGCAGTACCCACTCAATC	Designed for this study
Primer: DiptA_rev 5’-CCCAAGTGCTGTCCATATCC	Designed for this study
Primer: Mtk_for 5’-TCTTGGAGCGATTTTTCTGG	Designed for this study
Primer: Mtk_rev 5’-TCTGCCAGCACTGATGTAGC	Designed for this study
Primer: Dro_for 5’-CCATCGAGGATCACCTGACT	Designed for this study
Primer: Dro_rev 5’-CTTTAGGCGGGCAGAATG	Designed for this study
Primer: Drs_for 5’-GTACTTGTTCGCCCTCTTCG	Designed for this study
Primer: Drs_rev 5’-CTTGCACACACGACGACAG	Designed for this study
Primer: daw_for 5’-CAGTCGGTGAATGTGCAAGA	Designed for this study
Primer: daw_rev 5’-GAGGTGGCTCAGCTCGTG	Designed for this study
Primer: dpp_for 5’-GCTGATTGGATACATAATTCTCAGG	Designed for this study
Primer: dpp_rev 5’-TTTGAAAAGTCGCCAGCAC	Designed for this study
Primer: eiger_for 5’-CGACGAGTTCCAAAAGGAGT	Designed for this study
Primer: eiger_rev 5’-GTCGTCGTCCTCCTCATC	Designed for this study